INVESTIGATION OF UNDERGROUND MINE PILLAR DESIGN PROCEDURES

By

YVES POTVIN

B.Sc., LAVAL University, QUEBEC 1981

A THESIS SUBMITTED IN PARTIAL FULFILLMENT OF

THE REQUIREMENTS FOR THE DEGREE OF

MASTER OF Applied SCIENCE

in

THE FACULTY OF GRADUATE STUDIES

Mining and Mineral Process Engineering

We accept this thesis as conforming

to the required standard

THE UNIVERSITY OF BRITISH COLUMBIA

March 1985

© Yves Potvin, 1985

22

In presenting this thesis in partial fulfilment of the requirements for an advanced degree at the University of British Columbia, I agree that the Library shall make it freely available for reference and study. I further agree that permission for extensive copying of this thesis for scholarly purposes may be granted by the head of my department or by his or her representatives. It is understood that copying or publication of this thesis for financial gain shall not be allowed without my written permission.

Department of Mining and Mineral Process Engineering

The University of British Columbia
1956 Main Mall
Vancouver, Canada
V6T 1Y3

Date MArcH 25th 1985

ABSTRACT

The principal functions of underground mine pillars are to stabilize openings and to carry the load of overlying rôck strata. They are often (partially or completely) recovered at a later stage when their stabilizing effect is no longer required.

For economic reasons, an optimum-sized pillar is the smallest one satisfying safety requirements.

Thus the pillar design problem consists of determining the pillar's minimum dimensions as the load approaches the ultimate pillar strength.

Because the pillar's strength and the load acting upon it are both functions of many interrelated factors, which may vary as mining progresses, the determination of pillar dimensions is a complex task.

Furthermore, the multiplicity of pillar shapes, sizes, rock material and functions add to the designers' problem.

Consequently, pillar design programs are still generally performed as a trial-and-error process.

In order, to improve the present pillar design practices :

(1) -AApillar classification is proposed to standardize the design procedure

(2) The principal design methods, divided into four groups, are summarized and their applicability
is is defined

(3) A five-phase design procedure with design charts is developed

(4) The design procedure is applied in analysing two case histories

TABLE OF CONTENTS

LIST OF FIGURES

LIST OF TABLES

ACKNOWLEDGEMENTS

The author first wishes to thank Noranda Research Mining Division Group, who have made this project feasible by financing the research, providing an impressive amount of information and for their outstanding cooperation. The involvement of the following Noranda mines and the assistance of their employees was also appreciated:

- Brunswick Mining and Smelting
- Heath Steele Mine
- Geco Division
- Goldstream Mine.

As well, special acknowledgements to Dr. H.D.S. Miller for his supervision of the research project, the pertinent advice given, and for his stimulating approach towards rock mechanics.

The author wishes to thank the following scholarship funds for financial support:

- Cy and Emerald Keyes
- Frederick Armand McDiarmid
- George E. Winkler

In addition, thanks to the members of the Department of Mining and Mineral Process Engineering for their helpful attitude, to W. M. Cumming for proof reading, and finally to Jacques and Jeannine Potvin for their continuous encouragement and support.

CHAPTER 1

Introduction

The principal functions of underground mine pillars are to stabilize openings, and to carry the load of overlying strata. They are often (partially or completely) recovered at a later stage when their stabilizing effect is no longer necessary.

For economic reasons, an optimum-sized pillar is the smallest one that satisfies safety requirements.

Thus, the pillar design problem consists of determining the pillar's minimum dimension as the load reaches the ultimate pillar strength.

Because the pillar's strength, and load acting upon it are both functions of many interrelated factors, which vary as mining progresses, pillar dimensioning is a difficult task.

Furthermore, the multiplicity of pillar shapes, sizes, rock material and applications add to the designers' confusion.

Consequently, pillar design programs are still generally a trial-and-error process.

In September 1982, a research project was undertaken, under the supervision of Dr. H. D. S. Miller, with the collaboration and financial support of Noranda Research, Mining Division, to develop a comprehensive pillar design procedure. The project's first year was entirely dedicated to a complete review of the pillar design methods available.

This is reproduced in appendix A.

Another of the project tasks was to investigate the current pillar design procedures and the role of rock mechanics techniques in mine pillar design.

To achieve this goal, a questionnaire was mailed to seven Noranda underground operations. The information was completed by visiting four mines in New Brunswick, Quebec, Ontario and British Columbia.

Table 1 shows that a fair amount of rock mechanic studies had been com-

TABLE 1 Rock Mechanic Studies in Noranda Underground Mines

			Goldstream	Mattabi	Matagami	Mines Gaspe	Geco	Brunswick (BM & S)	Heath Steele
1. ROCK STRENGTH PARAMETER	Unit Weight	γ	x			x	x	x	x
	Elastic Mod	E				x	x	x	x
	Poisson's Ratio	ν				x	x	x	x
2. STRESS INVESTIGATIONS	In-Situ Measurement					x		x	
	Photo-Elastic Model						x		
	Computer Modelling					x		x	
3. LABORATORY TEST	Compress. Strength	σ_c	x	x		x	x	x	x
	Tensile Strength	σ_t				x	x		
	Triaxial Strength	$\frac{\sigma_1}{\sigma_3}$				x	x		
	Shear Strength	τ				x			
	Failure Criterion					x			
4. ROCK MASS CLASSIFICATION	R Q D		x			x	x		x
	N G I		x			x	x		x
	C S I R					x	x		x
	Laubscher					x			
	Structural Mapping		x			x	x		x
5. MONITORING	Multi-Wire Extensom.				x	x	x	x	x
	Boroscope Observ.					x			
	Compression Pad					x			
	Closure Station		x						
	Levelling Survey Station				x				
	Piezometer				x				

pleted. However, it must be emphasized that these experiments are related to the operations' size and age, as well as the stability problems encountered.

Table 2 confirms that the mines rely mainly upon previous experience for design, leaving the more sophisticated methods to mining consultants.

Table 2

Pillar and Opening Designing Methods
Used by Noranda Underground Mines

	Experience Methods Group 1		Empirical Methods Group 2		Analytical Methods Group 3		Computer Methods Group 4	
	Pillars	Openings	Pillars	Openings	Pillars	Openings	Pillars	Openings
Goldstream	M	M	M	M				
Mattabi	M	M						
Matagami	M	M						
Mines Gaspe	M	M		C	C		C	C
Brunswick	M	M					C	C
Heath Steele	M	M	M					
Geco	M	M						

Note: M - The mine's staff performed the design.
C - Consultant performed the design.

In order to improve the actual pillar design practices:

- a pillar classification system is proposed to standardize the design procedure
- the principal design methods are summarized and their applicability is defined

- a five-phase design procedure with design charts is developed
- the procedure is applied in analysing two case histories.

CHAPTER 2

The Classification and Definition of Pillars

2.1 Pillar Classification

The literature provides no standard definition for the term, "underground pillar." If one attempts to elaborate a general definition, it should be borne in mind that the pillar may or may not be mineralized, may be permanent or temporary, but in any event reference must be made to the notion of stability and security.

Regardless of which mining method is used, every mine must leave pillars to stabilize underground structures. However, because of the variable ground conditions, stress, and the multiple pillar applications related to mining methods and orebody geometry, no two pillars are identical.

In the documents reviewed, more than twenty names describing various kinds of pillars were encountered. This wide variety of pillars makes the elaboration of a standard design procedure a difficult task.

The pillar shape, the load acting on the pillar, and the strength of the pillar meterial are the three most important factors to be considered when designing a pillar.

A simple classification (for pillar design purposes) is suggested, regrouping under the same "category" pillars of similar shape which are submitted to similar loading situations. In this manner, every pillar in each category can be designed using identical equations and a given methodology.

Because the behaviour of hard rock differs greatly from that of soft rock, each category is broken into two sub-categories: (a) hard rock pillars, and (b) soft rock pillars.

Note: The width, height and length of the pillars may vary greatly within a category, but the general shape must be similar.

2.2 Category 1. "Plate Pillars"

2.2.1 Description

Figure 1 shows that "Plate Pillars" are submitted to a biaxial horizontal stress field. The top and the bottom of the pillars are not loaded. However, this is not true in the case of surface pillars, which must bear the vertical load due to surficial overburden. The designer should be aware of this fact when dimensioning a surface pillar.

No cases of soft rock "Plate Pillars" (Category 1B) were found in the literature. This is due principally to the soft rock mining methods which rarely require plate pillars.

2.2.2 Definitions

Category 1A: Hard Rock

- Crown Pillars, Roof Pillars, Level Pillars, Strike Pillars, Horizontal Pillars:

These are horizontal slices of varying thickness, left above the excavated area to provide support. They are generally recovered after their support function is no longer required. The term "crown pillar" is often used to define the shallowest horizontal pillar carrying the overburden load (surface pillar).

- Sill Pillars:

Sill pillars are very similar to crown pillars but they are situated underneath the stopes at each sublevel.

2.3 Category 2. "Separation Pillars"

2.3.1 Description

Separation pillars (Category 2) are subjected to a vertical and horizontal load. They are open on their longitudinal side (Figure 2). It

CATEGORY I
"plate pillar"

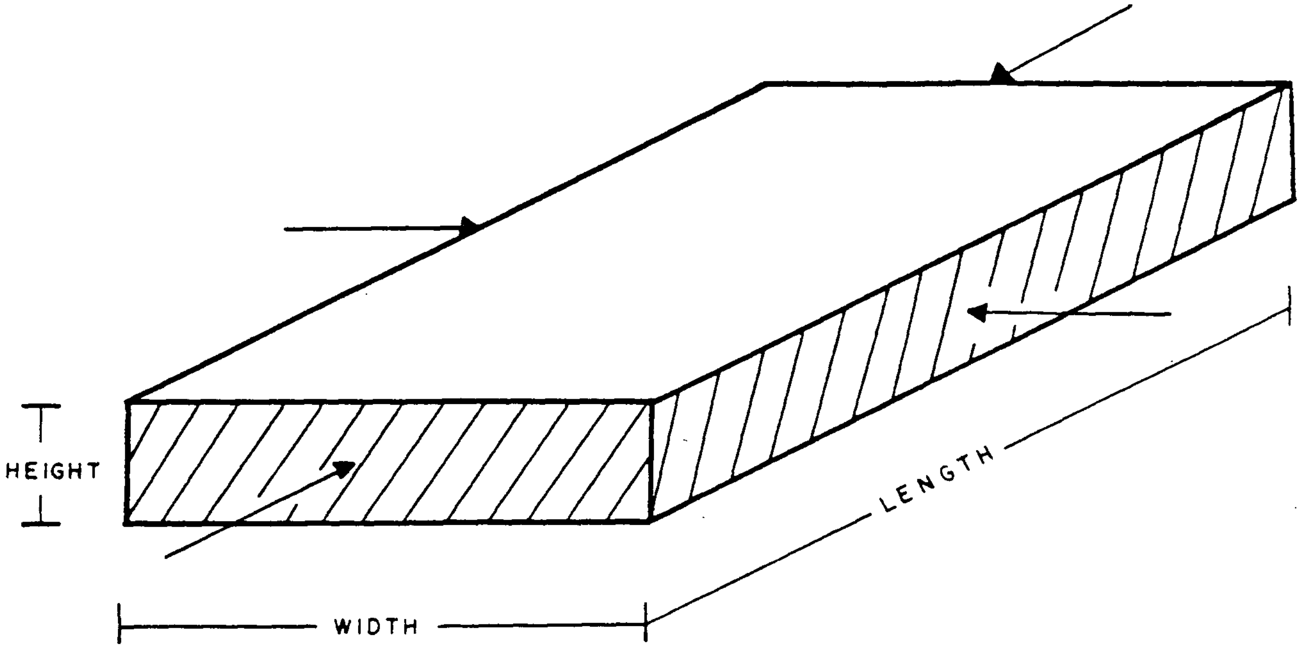

category I a. (hard rock)

CROWN PILLARS
ROOF PILLARS
LEVEL PILLARS
STRIKE PILLARS
HORIZONTAL P.
SILL PILLARS
SURFACE PILLARS

category I b. (soft rock)

FIGURE 1 Pillar Category 1 " Plate Pillars"

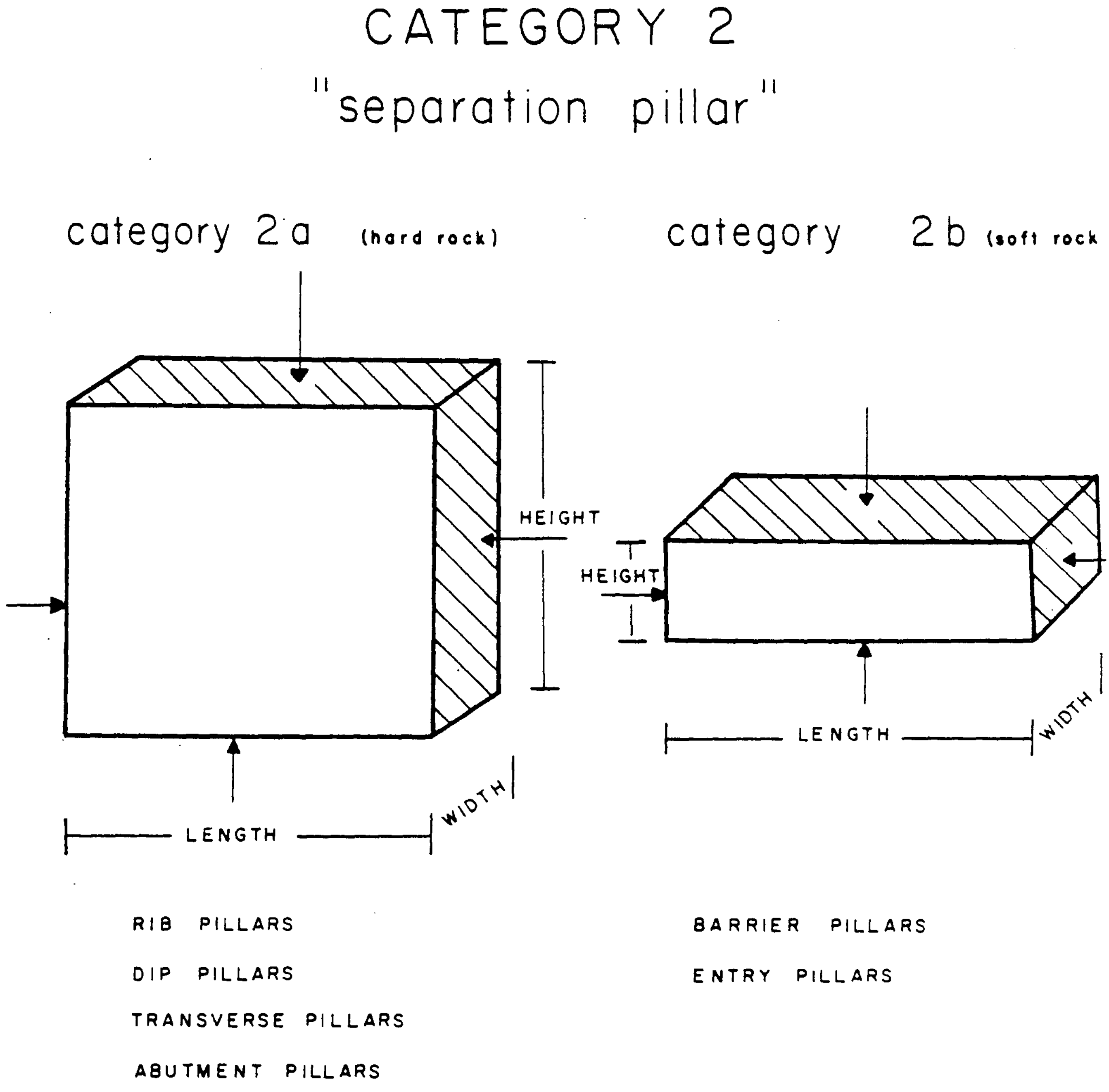

FIGURE 2 Pillar Category 2 "Separation Pillars"

should be noted that the hard rock (Category 2A) and soft rock separation pillars (Category 2B) do not possess identical characteristic shapes, since soft rock pillars are usually lower and wider (Figure 2).

In the case of a very long separation pillar (compared to the other dimensions) the horizontal stress may have a negligible effect and the problem may be considered to be two dimensional.

2.3.2 Definitions

Category 2A: Hard Rock

- Rib Pillars, Dip Pillars, Transverse Pillars:

A rib pillar is a separating wall between two stopes. The length of the rib is usually in the orebody dip direction and is continuous. The rib pillars transfer the vertical load from the roof to the floor, stabilizing the rock overlying the stoped area. They may be recovered at a later stage of mining.

Category 2B: Soft Rock

- Barrier Pillars:

Barrier pillars are used to isolate coal mine panels. They are usually permanent pillars which control roof stability and play a major role in ventilation.

- Entry Pillars:

These pillars refer to the longwall mining method. They provide a protection to the panel entries and are recovered during the panel's final exploitation stage.

2.4 Category 3. "Stub Pillars"

2.4.1 Description

The shape of "stub pillars" (Category 3) may be square or rectangular (Figure 3). They are open on the four vertical sides and are subjected to a uniaxial compressive stress field.

2.4.2 Definitions

Category 3A: Hard Rock

- Centre Pillars:

These pillars have the same function as rib pillars, but are situated in the middle of the stopes. They reduce the span of openings and help to carry the roof load. Contrary to the rib pillars which are continuous, the centre pillars are transected by cross-cuts or drifts.

- (Room and Pillar) Pillars, Stub Pillars:

The stub pillars may refer to a uniform room and pillar panel or simply be left randomly wherever stabilization is needed. Their length, width, height, shape and composition vary according to the site and requirements. They support the vertical load of overlying rock, and may be permanent or recoverable.

- Post Pillars, Yielding Pillars:

These pillars refer to the "post pillar" mining method. They provide temporary support to the immediate roof. As mining progresses from the bottom up, the post pillars start to yield and finally collapse "gently" at the bottom, where they are confined by backfill.

Category 3B: Soft Rock

- Panel Pillars:

These temporary pillars are uniformly distributed within a longwall panel. They support the panel's immediate roof and will be removed at a

CATEGORY 3
"stub pillars"

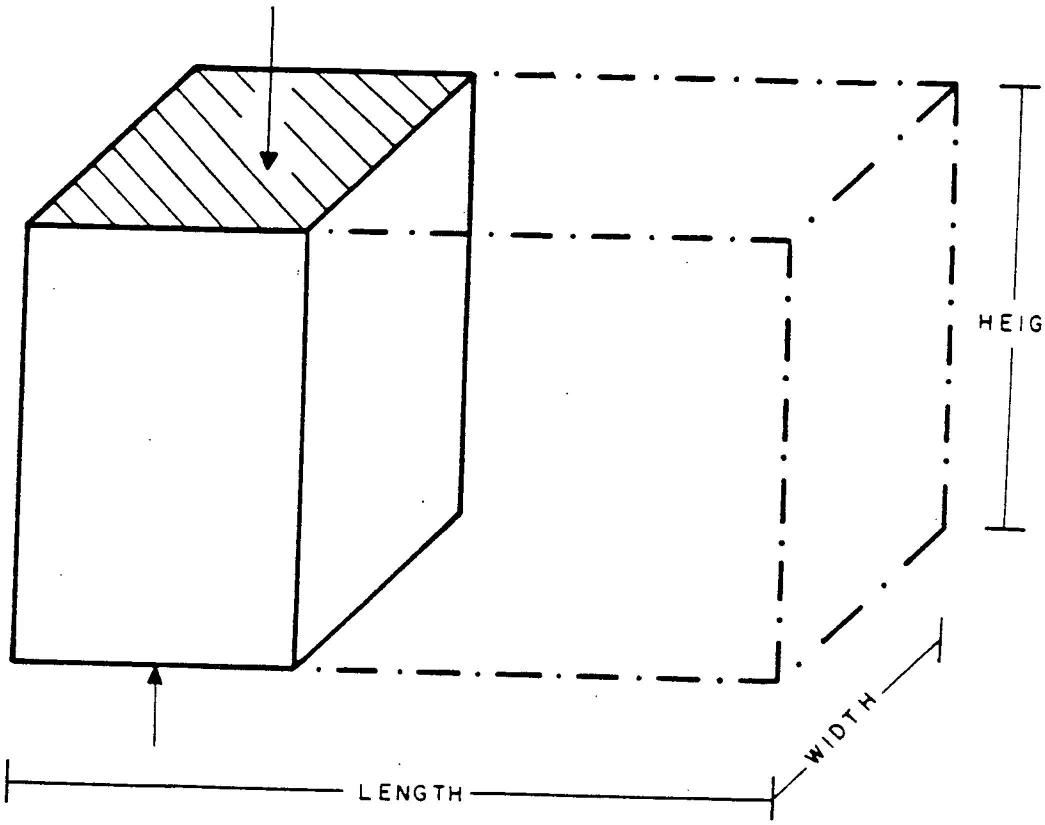

category 3a (hard rock)

CENTER PILLARS

(ROOM & PILLAR) PILLARS

POST PILLARS

category 3b (soft rock)

PANEL PILLARS

SPLIT PILLARS

REMNANT PILLARS

CHAIN PILLARS

FIGURE 3 Pillar Category 3 "Stub Pillars" later stage.

- Split Pillars:

During longwall pillar recovery, the panel pillars are cut into two split pillars.

- Remnant Pillars:

Remnant pillars are the residual portion of split pillars. As mining retreats, they either collapse or are completely recovered.

- Chain Pillars:

These pillars play the same role as barrier pillars, but they are composed of a series of aligned small pillars instead of a long, massive, continuous pillar. This provides the highest extraction ratio. The pillars may be designed to yield, permitting the roof to deform.

2.5 Category 4. "Inclined Pillars"

2.5.1 Description

Inclined pillars do not have a particular shape or are not submitted to a particular loading situation. However, because they do not fit into the three preceding categories, and they require special consideration for design because of their inclination, inclined pillars form the fourth category of the pillar classification (Figure 4).

2.6 Discussion

The author is aware that pillars in the forementioned categories are illustrated with idealized shapes, which is not the case for real underground pillars. In addition, it should be realized that the load acting on a pillar is a function of several factors:

- Virgin stress
- Stress induced by mining

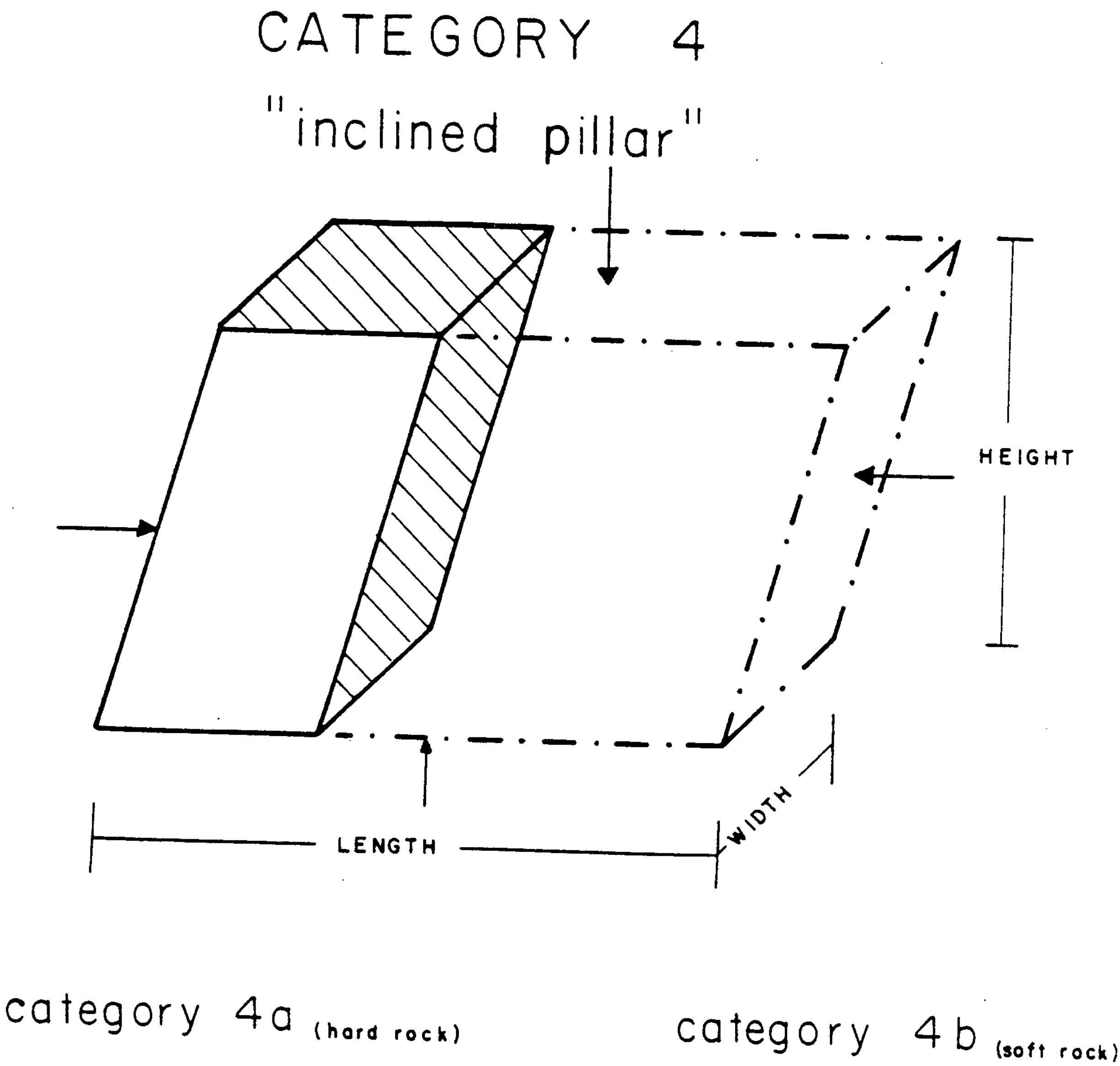

FIGURE 4 Pillar Category 4 "Inclined Pillars"

- Geological features
- Pillar shape and orientation
- Openings and general mine structures
- Ground water.

However, it is believed that every pillar may fall into one of the above four categories, even though the classification oversimplifies the loading mechanism and the pillar geometry.

Finally, because shaft pillars are fundamentally different from other pillars, they are not included in this classification. Nevertheless, the following definition is proposed:

Shaft Pillars:

These are permanent pillars providing protection to the mine shaft system. The shaft and the shaft pillar may be vertical or inclined. Shaft pillars become larger with increased depth, and their shapes are variable. Because the shaft is a vital component in underground mines, these pillars are designed with a high safety factor.

Table 3 summarizes the pillar classification. The design methodology and dimensioning formulas applicable to each category will be developed in the following chapters.

Most of the previous pillar definitions were taken from "Roche Mines Associates" (1984)[1] as well as Figures 5, 6, and 7 reproduced in Appendix C, which illustrate the different kinds of pillar.

TABLE 3

PILLAR CLASSIFICATION SUMMARY

Category 1 Plate Pillars		Category 2 Separation Pillars		Category 3 Stub Pillars		Category 4 Inclined Pillars	
A Hard Rock	B Soft Rock	A Hard Rock	B Soft Rock	A Hard Rock	B Soft Rock	A Hard Rock	B Soft Rock
Crown	-	Rib	Barrier	Centre	Panel	Inclined	Inclined
Roof		Dip	Entry	Stub	Split		
Level		Transverse		"Pillar" (R+P)	Remnant		
Strike		Abutment			Chain		
Horizontal				Post			
Sill							
Surface							
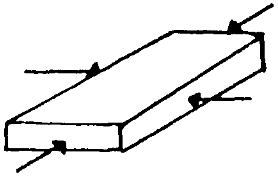		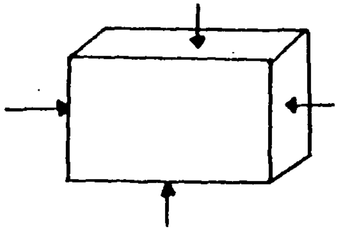		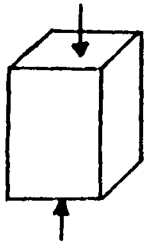		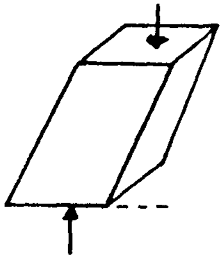	

CHAPTER 3

Review of Pillar Design Methods

3.1 Introduction

The principle for designing any underground structure is simple:

$$\frac{\text{strength}}{\text{stress}} > 1$$

Thus, a pillar will remain stable if the load applied is less than its long term load bearing capability. Difficulties arise in estimating the pillar's ultimate strength as well as the precise load acting upon it.

Pillar strength:

Because of the rock material's complexity and variability, the evaluation of rock mass strength is perplexing. Furthermore, the true strength of a pillar can only be calculated after considering the strength of the pillar material together with:

- The probability of including a weakness zone in the pillar
- The deformation and triaxial strength of the pillar material
- The geometry of the pillar
- The pillar as part of the general rock structure.

Also, environmental factors may cause a time dependent alteration of the pillar strength.

Pillar load:

As mentioned in Chapter 2, the load acting on a pillar is a function of:

- The virgin stress
- The stress induced by mining
- Geological features
- Pillar shape and orientations
- Openings and general mine structure
- Ground water.

Hence, the stress level induced in pillars (pillar load), changes as mining progresses.

Although several techniques can be used to measure in situ stress, these are expensive, and the results are not always reliable.

Because there are so many factors involved in the complex mechanism of pillar loading (and deformation) as well as pillar strength, the designer must depend upon numerous methods to account for these factors.

The following summarizes the most important designing methods. They are divided into four groups, according to their level of sophistication.

Group 1 - Experience Methods

Group 2 - Empirical Methods

Group 3 - Theoretical Methods

Group 4 - Computer Methods.

It should be noted that every method, if used correctly, is capable of producing adequately sized pillars with respect to safety.

3.2 Group 1. Experience Methods

This is by far the most widely used and the least sophisticated method. Based on observations, history, and on the designer's "feeling" for the rock, it also relates to similar work completed in corresponding geological situations. A conservative dimensioning is first laid out and modifications may have to be made according to the requirements and performance of the designed structure.

No specific experience method is proposed, but it is strongly recommended that detailed active files be kept on information concerning the mine stability: failures, slabbing, squeezing, caving, convergence, et cetera.

This will improve the future experience design and may lead to an empirical approach.

3.3 Group 2. Empirical Methods

An empirical method is the quantification of experience into designing formulas or curves. Because most of these methods do not take into account many important factors, one should be aware of the conditions in which they were developed.

While the majority of empirical pillar design methods considers strength and stress separately, some do incorporate strength and stress into a dimensioning formula.

The following is a review of the most important empirical methods. A brief description, the formula(s) and the parameters are given. As well (referring to Chapter 2's pillar classification), the pillar categories which can be designed by each method are indicated.

3.3.1 Empirical Strength Formulas.

Empirical pillar strength formulas essentially involve extrapolating the results of laboratory tests on rock specimens, to full-size mine pillars.

A) Size Effect Formula (Appendix A. Section 3.1)

$$\sigma_p = \sigma_c \quad [A + B(\frac{W}{h})]$$

where: σ_p = Pillar strength (psi)

σ_c = Uniaxial compressive strength of a cube of pillar material

W = Pillar width

h = Pillar height

A, B = Constants given in units of pillar strength (Table 4).

Description:

Rocks have a natural strength anisotropy which is predominantly due to the presence of discontinuities (i.e. joints, cleats, blast fractures, et cetera) but can also be attributed to variations in rock fabric (i.e. foliation, bedding planes, et cetera) and mineralogy. As rock samples of a constant shape increase in size, the strength of the specimen decreases. Table 4 gives the constants proposed by different authors to model this behaviour.

TABLE 4

CONSTANTS A AND B USED IN THE "SIZE EFFECT FORMULA"

SOURCE	FORMULA	W/H
Bunting (1911)	$0.700 + 0.300 \frac{w}{h}$	0.5 - 1.0
Obert et al (1960)	$0.778 + 0.222 \frac{w}{h}$	0.5 - 2.0
Bieniawski (1968)	$0.556 + 0.444 \frac{w}{h}$	1.0 - 3.1
Van Heerden (1973)	$0.704 + 0.296 \frac{w}{h}$	1.14 - 3.4
Sorensen & Pariseau (1978)	$0.693 + 0.307 \frac{w}{h}$	0.5 - 2.0

- Applicable to pillar categories: 3. Stub Pillars
  4. Inclined Pillars.

B) <u>Shape Effect Formula</u> (Appendix A, Section 3.2)

$$\sigma_p = K \frac{W^a}{h^b}$$

where: σ_p = Pillar strength (psi)

K = Constant related to the pillar material

W = Pillar width

h = Pillar height

a, b = Dimensionless constants

Description:

The shape effect denotes a difference in the unit strength for pillars of different shape but equal cross-section. A change in mode of failure is one apparent cause of shape effect. Slender pillars tend to fail by means of a limited number of fractures. For wide pillars the probability of developing a single continuous fracture plane is less. Thus, failure of the pillar results from crushing of the pillar material, thereby increasing pillar strength. The triaxial state of stress in a squat pillar's inner core also contributes to an increase in pillar strength. Table 5 gives the constants a and b proposed by different authors to model this behaviour.

TABLE 5

CONSTANTS a AND b USED IN THE "SHAPE EFFECT FORMULA"

SOURCE	FORMULA	a	b
Streat (1954)	$kh^{-1.00}w^{0.5}$	0.5	1.00
Holland-Gaddy (1962)	$kh^{-1.00}w^{0.5}$	0.5	1.00
Greenwald et al (1939)	$kh^{-0.83}w^{0.5}$	0.5	0.833
Hedley & Grant (1972)	$kh^{-0.75}w^{0.5}$	0.5	0.75
Salamon & Munro (1967)	$kh^{-0.66}w^{0.46}$	0.46	0.66
Bieniawski (1968)	$kh^{-0.55}w^{0.16}$	0.16	0.55
Morrison et al	$kh^{-0.5}\ w^{0.5}$	0.5	0.5
Zern (1926)	$kh^{-0.5}\ w^{0.5}$	0.5	0.5
Hazen & Artler (1976)	$kh^{-0.5}\ w^{0.5}$	0.5	0.5
Holland (1956)	$kh^{-0.5}\ w^{0.5}$	0.5	0.5

- Applicable to pillar categories: 3. Stub Pillars

  4. Inclined Pillars

C) <u>Salamon "Modified" Shape Effect Formula</u> (Appendix A, Section 3.3.4)

$$\sigma_p = K \frac{We^a}{h^b}, \quad \text{where } We = \sqrt{W_1 . W_2}$$

where: σ_p = Pillar strength (psi)

K = Constant related to the pillar material compressive strength

W_1, W_2 = Cross-section sides of the pillars

We = The equivalent width for a rectangular pillar

h = Pillar height

a, b = Dimensionless constants

Description:

The results of underground tests (Wagner, 1974)[2] on coal pillars have shown that pillars of rectangular cross-sections are about 40% stronger than square pillars of the same width and height. A reasonably good estimate of the strength of rectangular pillars can be obtained by substituting the square root of the cross-sectional area of the pillar for W, in the shape effect formula.

- Applicable to pillar categories: 3. Stub Pillars
  4. Inclined Pillars

D) <u>Sheorey and Singh "Modified" Shape Effect Formula</u> (Appendix A, Section 3.3.4)

$$\sigma_p = \frac{K\left[\frac{W_1+W_2}{2}\right]^a}{h^b}$$

where: σ_p = Pillar strength (psi)

K = Constant related to the axial compressive strength of the pillar material

W_1, W_2 = Cross-section sides of the pillar

h = Pillar height

a,b = Dimensionless constants (Table 5)

Description:

This method as the Salamon modified formula uses the concept of an equivalent width. However, Sheorey and Singh recommend using the average value of the rectangular cross-section sides as equivalent width.

- Applicable to pillar categories: 3. Stub Pillars

  4. Inclined Pillars

E) Hoek and Brown Curves (Appendix A, Section 3.3.7)

$$\sigma_1 = \sigma_3 + \sqrt{m\sigma_c\sigma_3 + s\sigma_c^2}$$

where: σ_1 = Major principal stress at failure

σ_3 = Minor principal stress at failure

σ_c = The uniaxial compressive strength of intact rock material

m and s are constants which depend upon the properties of the rock and upon the extent to which it has been broken before being subjected to the stresses σ_1 and σ_3.

Description:

The Hoek and Brown[3] curves were developed based on the assumption that the overall strength of a pillar is approximately equal to the average strength across the centre of the pillar. Figure 8 shows the results of a series of calculations using stress distribution from computer modelling, together with Hoek's failure criterion. Once the rock mass quality is defined, one may determine the pillar strength for different pillar dimensions.

- Applicable to pillar categories: 2. Separation Pillars

  3. Stub Pillars

  4. Inclined Pillars.

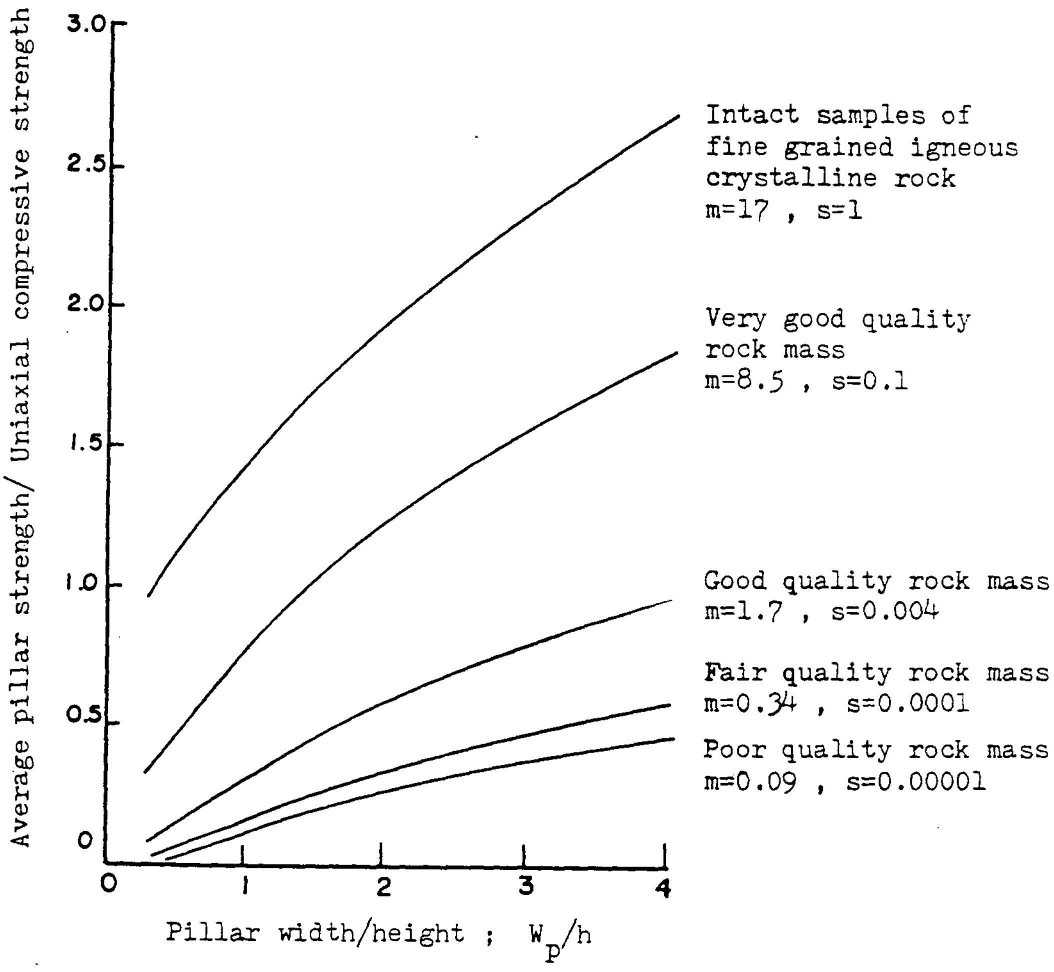

FIGURE 8 Influence of Pillar Width to Height ratio on Average Pillar Strength. After Hoek and Brown (1980)[3]

3.3.2 Empirical Stress Formulas

A) The Extraction Ratio Formula or Tributary Area (Appendix A, Section 1.3.4)

$$\sigma_p = \frac{\gamma H \ (W+B)(L+B)}{W \times L}$$

where: σ_p = Pillar load

γ = Unit weight of the rock

H = Depth below surface

B = Width of the opening

L = Pillar length

W = Pillar width.

Description:

If a large area is mined out with a reasonably uniform pattern of pillars, it can be said that nearly the whole weight of the overburden will be carried by the pillars in equal proportions. Figure 9, Hoek and Brown (1980)[3] gives the extraction ratio formula for different pillar shapes. It should be noted that the tributary area theory represents the upper limit of the average pillar stress. (Overestimates the load on pillars by about 40%). Bieniawski (1983)[4]. The tributary area does not take into account the arching effect, or any other mechanical behaviour of the overlying strata.

- Applicable to pillar categories: 2. Separation Pillars
  3. Stub Pillars.

B) Chain Pillar Formula (Appendix A, Section 1.3.8)
Swilski (1983)[5]

$$\sigma_p = \frac{1}{\gamma H} \cdot \frac{2W_p . L_p}{(L_p+S)(W_F+2W_p+3S)}$$

where: σ_p = Pillar load (psi)

γ = Unit weight of the rock

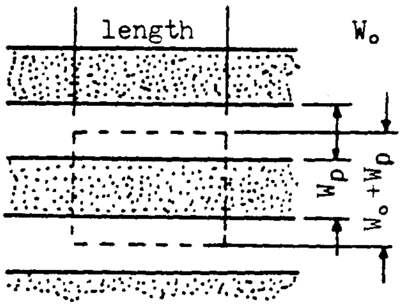

RIB PILLARS

$\sigma_p = \gamma z \, (1 + W_o/W_p)$

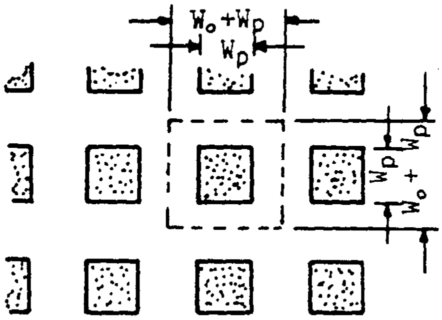

SQUARE PILLARS

$\sigma_p = \gamma z \, (1 + W_o/W_p)^2$

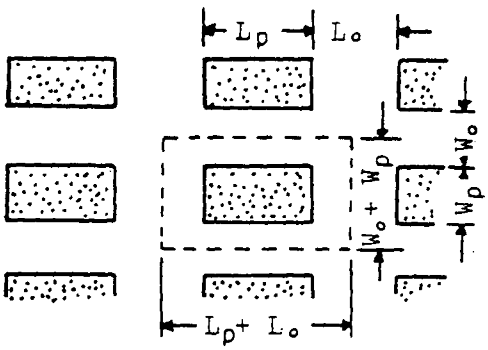

RECTANGULAR PILLARS

$\sigma_p = \gamma z \, (1 + W_o/W_p)\,(1 + L_o/L_p)$

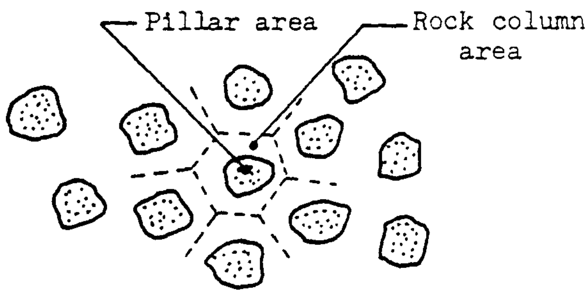

IRREGULAR PILLARS

$$\sigma_p = \gamma z \, \frac{\text{Rock column area}}{\text{Pillar area}}$$

FIGURE 9 Average Vertical Pillar Stresses in Typical Pillar Layouts. Illustrations are all plan views. After Hoek and Brown (1980)[3]

H = Depth below surface

W_p = Pillar width

L_p = Pillar length

S = Spacing between chain pillars

W_F = Width of the face.

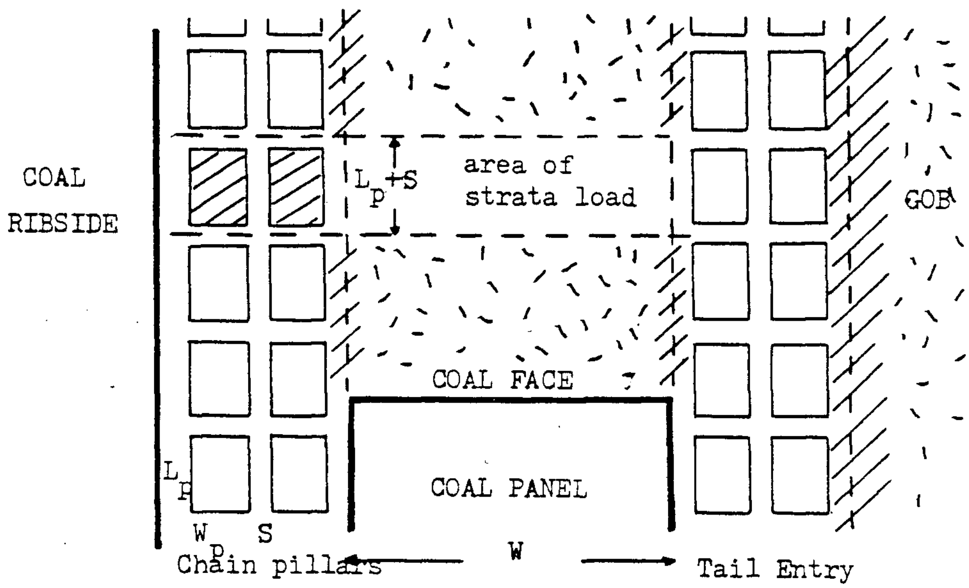

FIGURE 10. Determination of Load on Chain Pillars by the "first panel" Load Concept. After Szwilski (1983)[5]

Description:

The chain pillar formula is based on the extraction ratio formula but it considers the extra load acting on the chain pillars by the cantilever action of the immediate roof. However, this simplified procedure ignores the effect of the gob support, creating a pressure arch from the compacted gob to the nearest solid coal panel.

- Applicable to pillar category: 3B - Chain Pillars.

C) <u>Subsidence Formula</u> (Appendix A, Section 10.3) Whittaker and Singh (1981)[6]

$$\sigma_p = \frac{9.81\gamma}{1000\ p^2} \quad (P + W)\ .\ D - 1/4W^2 + \cot\phi\ .P$$

For $W/D < 2 \tan\phi$

and $$\sigma_p = 9.81\ \gamma \quad P(P.D + D^2\tan\phi)$$

For $W/D > 2 \tan\phi$

where: σ_p = Pillar load (psi)

γ = Average density of the overburden

ϕ = Angle of shear of roof strata at edge of longwall extraction and measured to vertical

P = Width of barrier pillar

W = Width of longwall extraction

D = Depth below surface.

Description:

The subsidence theory has been applied to the barrier pillar situation to ascertain the extent of strata pressure arching across a longwall extraction to produce loading of the adjacent barrier pillars.

Basically, this approach assumes that the goaf area behind the longwall is loaded by a triangular roof mass which shears at an angle ϕ to the vertical. The loading developed by the mass of roof strata outside the triangular region is presumed to be transferred to the barrier pillars.

- Applicable to pillar category: 2B - Barrier Pillars

3.3.3 Empirical Dimensioning Formulas.

Other empirical formulas do not consider stress and strength separately. Pillar dimensioning formulas are often used to design coal barrier pillars.

A) Mines' Inspector Formula (Appendix A, Section 10.2) Ashley (1930)[3]

$$W = 20 + 4T + 0.1D$$

where: W = Width of pillar (feet)

T = Bed Thickness (feet)

D = Thickness of the overburden (feet)

Description:

The Ashley formula was developed from experiments in the Pennsylvania coal fields. It is based on the conservative assumption that an arch of height equal to half the panel width will stabilize. Simple hand calculations based on the above assumption result in pillar sizes with width to height ratios of approximately three to five depending upon depth, pillar height and panel width.

- Applicable to pillar category: 2B - Barrier Pillars

B) Holland Formula (Appendix A, Section 10.2)

$$D = 15T \quad \text{or} \quad = \frac{\log 2W_2}{K \log e}$$

where: D = Width of Barrier Pillar (feet)

T = Thickness of pillar (feet)

W_2 = The estimated convergence on the high stress side of the pillar (mm). (W_2 may be estimated with Fig. 11)

K = Constant
= 0.09 if caving following mining is permitted
= 0.08 if strip packs are built
= 0.07 if hydraulic stowage is carried out.

Description:

The Holland formula is based on the convergence studies by Belinski and Borecki (1964)[8]. Compared with Ashley's formula, it gives a more realistic pillar width and considers pillar thickness, as well as other pertinent factors. Holland's formula, however, is incomplete in that it disregards the properties of the pillar rock. Consequently, this method should be applied only in conditions similar to those in which Holland experimented. (Figure 11)

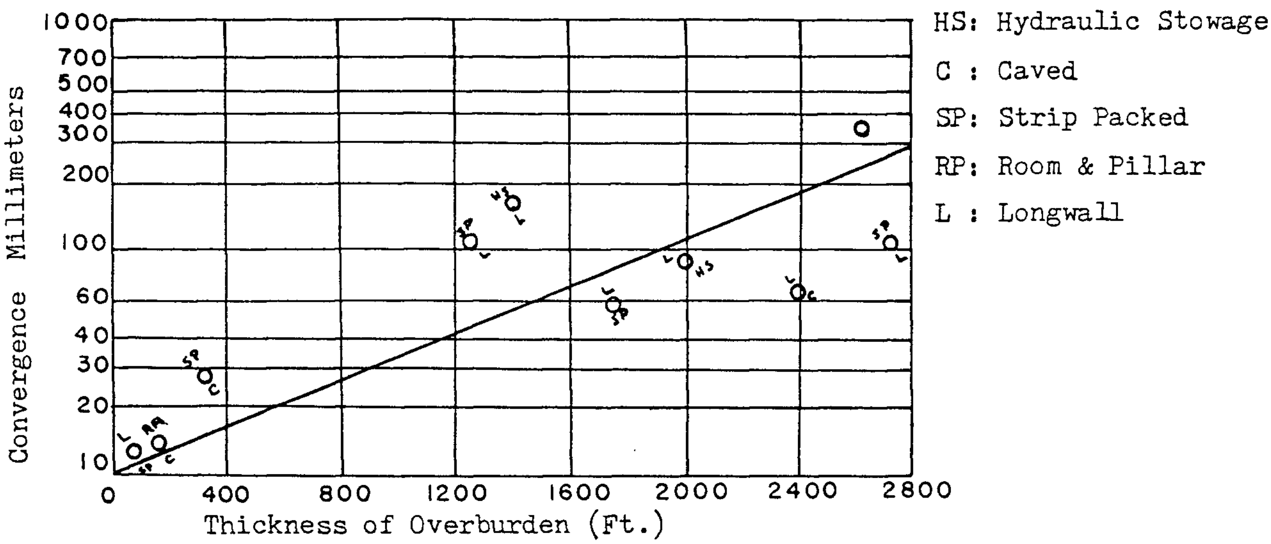

FIGURE 11 Observed Value of W_2 for Coal seams 7 ft. Thick and Having a Crushing Strength in the 3 in. Cube of 3000 psi. $\pm$ 10%

- Applicable to pillar category: 2b - Barrier Pillars.

C) Morrison, Corlett and Rice. (Appendix A, Section 10.2)

$$W = \frac{1}{8} D \quad \text{for } D < 4000 \text{ feet}$$

where: W = Width of pillar (feet)

D = Depth below surface (feet)

Description:

The two previous formulas were developed specifically for coal. The Morrison, Corlett and Rice formula gives satisfactory results in most kinds of rock. Nonetheless, it oversimplifies the problem and should be used as a guide or preliminary estimation only.

- Applicable to pillar categories: 2a) - Abutment Pillars
  b) Barrier Pillars

Note Not applicable to Rib Entry and Dip Pillars.

D) Barrier Pillar Formula (Appendix A, Section 10.2)

$$W = \frac{1}{10} D + 15$$

where: W = Width of pillar (feet)

D = Depth below surface (feet)

Description:

This formula is cited in the literature as a traditional rule of thumb approach to designing barrier pillars. Again it is oversimplified and should be used as a rough estimation only.

- Applicable to pillar category: 2B - Barrier Pillars

3.4 Group 3. Theoretical Methods

The theoretical methods attempt to evaluate mathematically the principal factors affecting the stress and strength of pillars. A more realistic model is then proposed. However, the behaviours of pillars are very complicated and to be consistent with the theory, the methods need a fair number of input parameters. Collecting data in a mining environment (especially at the early stage of a mine's life) is not an easy task, and often the techniques are too expensive or not adequately advanced to provide accurate data. Because the theoretical methods are complex and difficult to apply, the results are often not reliable. They are useful in further comprehending the mechanism involved in pillar design.

3.4.1 Theoretical Strength Formulas

At least four theoretical methods have been reviewed in the literature research:

	Appendix A
- Coates	(Section 3.3.3)
- Grobbelaar	(Section 3.5.1)
- Wilson	(Section 3.5.2)
- Panek	(Section 3.5.3)

It was noted that only Wilson's method has been used by designers, and a brief description of this method is given below.

A) Confined Core Method (Wilson)

$$\frac{Y}{h} = \frac{1}{(\tan \beta)^{0.50}(\tan \beta - 1)} \cdot \ln \frac{\sigma_V}{\sigma_o}$$

where: γ = The depth of yield zone from the ribside (feet)

h = Seam height (feet)

σ_V = The maximum pillar stress (psi) (situated at the yield zone/confined core interface)

σ_o = Unconfined compressive strength (psi)

$$\tan \beta = \text{Triaxial stress coefficient} = \frac{1 + \sin \phi}{1 - \sin \phi}$$

ϕ is the angle of internal friction of the coal.

Description:

This concept recognizes that a "yield" or "fracture" zone develops around the periphery of a pillar which confines a central elastic core. Because of this confinement the inner core is subjected to triaxial stress conditions.

The limit of the average core stress is reasoned to be equal to the pillar peak abutment stress, which is located at the yield zone/confined core interface. Based on this assumption, pillar strengths can be calculated.

- Applicable to pillar category: 2B. Barrier Pillars

3.4.2 Theoretical Stress Formula

Five theoretical methods to evaluate the stress acting on a pillar have been reviewed in the literature research.

	Appendix A
- Beam and Plate Theory	(Section 1.3.5)
- Wall deflection theory	(Section 1.3.6)
- Photoelastic data	(Section 1.3.7)
- Pariseau	(Section 9.2)
- Hedley	(Section 9.3)

The wall deflection formula and the photoelastic technique were relatively popular in the past but they are no longer widely used. Thus they will not be reviewed.Although they played an important role in the early development of rock mechanics, they can now be replaced by more efficient techniques.

A) Beam and Plate Theory Method

Description:

A number of equations were derived from Civil engineering beam theory. Some of them may be used to design pillars if they realistically describe the in situ underground situation. A complete understanding of the theory as well as the implications of the input parameters are essential.

- Applicable to pillar categories: 1. Plate Pillars
  2. Separation Pillars

B) Pariseau Inclined Pillar Formulas

$$S_p = \frac{\gamma h \, \dfrac{(1 + K_o) + (1 - K_o) \cos 2\alpha}{2}}{1 - R}$$

$$\tau_p = \frac{\gamma h \, \dfrac{(1 - K_o) \sin 2\alpha)}{2}}{1 - R}$$

where: S_p = Average pillar stress in the normal direction

τ_p = Average pillar shear stress

γ = Unit weight of the rock

h = Depth below surface

K_o = Ratio of horizontal over vertical virgin stress

R = Extraction ratio

α = Inclination of the seam

Description:

Pariseau proposed an extension of the applicability of the extraction ratio (or tributary area) formula to inclined seams of arbitrary dip. The shear forces caused by the seam's inclination is accounted for.

- Applicable to pillar category: 4. Inclined Pillars

C) Hedley's Modified Formula for Inclined Pillars

$$\sigma_p = \frac{\gamma h \cos^2\alpha + \sigma_H \sin^2\alpha}{1 - R}$$

where: σ_p = Average pillar stress in the normal direction

γ = Unit weight of the rock

h = Depth below surface

R = Extraction ratio

σ_H = Horizontal virgin stress

α = Inclination of the orebody

Description:

The pre-mining stress field and extraction ratio are the two principal factors affecting pillar stress. For inclined workings Hedley stated that the normal stress acting on the seam is a combination of the components of vertical stress and horizontal stress. This combination is used in the extraction ratio formula to determine the average pillar stress.

- Applicable to pillar category: 4. Inclined Pillars

3.5 Group 4. Computer Methods

The computer methods are versatile and may be adapted to every pillar category. Also, the use of digital computers in underground mine design is, from the mathematical point of view, the most precise method.

However, the accuracy of the results is related directly to the quality of the input data. Table 6 gives the characteristic input data required by computer models.

Numerous computer programs are used by rock mechanic specialists. The methods are summarized in Table 7 and are divided into two groups:

- integral methods

- derivative methods

At present, very few Canadian mines have their own computer models. Mine designers generally prefer to rely on consultants' expertise for these sophisticated methods. More information on "BITEM", the boundary element program used in this study is available in APPENDIX D.

TABLE 6

CHARACTERISTIC INPUT DATA FOR COMPUTER METHODS

1. Rock(s) Strength Parameters:
   - Uniaxial compressive strength (σ_c)
   - Unit weight (γ)

2. Virgin Stress:
   - Vertical Stress (σ_V)
   - Horizontal stress (σ_H)

3. General Mine Geology

4. General Structure and Geometry of the Mine

5. Rock Deformation Indices
   - A. Elastic: - Elastic Modulus (E)
     - Poisson's Ratio (ν)
   - B. Plastic - Creep Constants
     - Viscosity constants

6. Others
   - m and s Indices (Hoek criteria)
   - Friction angle.

TABLE 7

SUMMARY OF COMPUTER METHODS

Integral Methods

- Boundary elements - 2 dimensional
  - 3 dimensional
- Displacement discontinuities - 2 dimensional
  - 3 dimensional

Derivative Methods

- Finite elements - 2 dimensional
  - 3 dimensional
- Finite difference - 2 dimensional
  - 3 dimensional

Hybrid Methods

- Mixed Boundary and Finite elements Programs have been developed recently.

Finally, a summary is given below of the principal design methods reviewed in this chapter.

Further information on these methods, formulas and curves are available in the literature review, Appendix A.

GROUP 1. EXPERIENCE METHODS

GROUP 2. EMPIRICAL METHODS

STRENGTH	PILLAR CATEGORY	STRESS	PILLAR CATEGORY	DIMENSIONING	PILLAR CATEGORY
a) Size Effect	(3,4)	a) Extraction ratio (tributary area)	(2,3)	a) Ashley	(2b)
b) Shape Effect	(3,4)	b) Chain Pillar	(3b)	b) Holland	(2b)
c) Salamon Modified	(3b,4)	c) Subsidence	(2b)	c) Morrison, Corlett, Rice	(Abutment Pillar)
d) Sheorey, Singh	(3b,4)			d) Barrier Pillar	(2b)
e) Hoek curves	(2,3,4)				

GROUP 3. THEORETICAL METHODS

STRENGTH	PILLAR CATEGORY	STRESS	PILLAR CATEGORY
a) Wilson	(2b)	a) Beam Theory	(1,2)
* Grobbelaar		b) Pariseau	(4)
* Coates		c) Hedley	(4)
* Panek		* Photoelastic analysis	
		* Wall deflection (Coates)	

GROUP 4. COMPUTER METHODS

* Are no longer widely used.

CHAPTER 4

PILLAR DESIGN PROCEDURE

4.1 Philosophy of Pillar Design

Hoek and Brown (1980)[3] have described the philosophy of underground structure design as follows:

> *"The basic aim of any underground structure design should be to utilize the rock itself as the principal structural material, creating as little disturbance as possible during the excavation process and adding as little as possible in the way of concrete or steel support. The extent to which this design aim can be met depends upon the geological conditions existing on site and the extent of the designer's awareness and consideration of these conditions.*
>
> *"A good engineering design is one of balance and one in which all factors interact. Designers must consider even those elements which cannot be quantified."*

A good pillar design is one properly sized for both safety and efficiency. An optimum sized pillar might be defined as the smallest one that satisfies safety requirements.

4.2 Design Procedure

Many pillar design methods, formulas and curves have been reviewed in Chapter three, but none of these is completely independent.

In the following five phase design procedure, the designer uses several methods which become more sophisticated as experience with the rock material is gained. Also, design charts are included to help select suitable methods for each type of pillar.

4.2.1 Phase 1. Experience Design.

Initially a fair amount of uncertainty exists concerning the mechanical behaviour of rock on a large scale, and on the location, attitude, and properties of faults or joints.

Hence, at this stage, only a conservative preliminary design is possible, using the designer's experience and the study of similar case histories.

Also during this phase, the collection of rock mechanics data should be undertaken to prepare for the following phases of design, which employ more sophisticated methods.

4.2.2 Phase 2. Pillar Structural Analysis

The second phase objective is to determine whether plane(s) of weakness (faults or major discontinuities) control the pillar's stability. These discontinuities affect the pillar strength because they reduce the resistance to sliding (shear failure). This can occur in two ways:

1. By a single plane and movement that takes place along the plane (Figure 12)
2. By intersecting planes (Figure 13).

The movement may be in the direction of the trend and plunge of their intersections, or along one of the single planes.

4.2.2.1 Pillar Transection Verification

For very simple cases, a scale drawing may be sufficient to determine whether the pillar failure may be structurally controlled. However, for more complicated situations a sterographic method will be required. Comprehensive instructions for using the stereographic technique is reproduced in Appendix VI of the literature review, J. A. Tousseuil[9].

Because the plane must intersect both sides of the pillar and be continuous over its entire length, pillars having a high width to height ratio are not likely to fail by sliding.

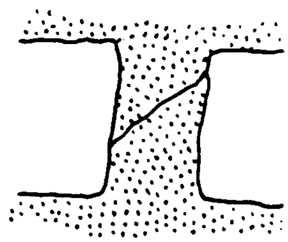

FIGURE 12 Pillar Transected by a Single Plane of Weakness. After Touseull [9]

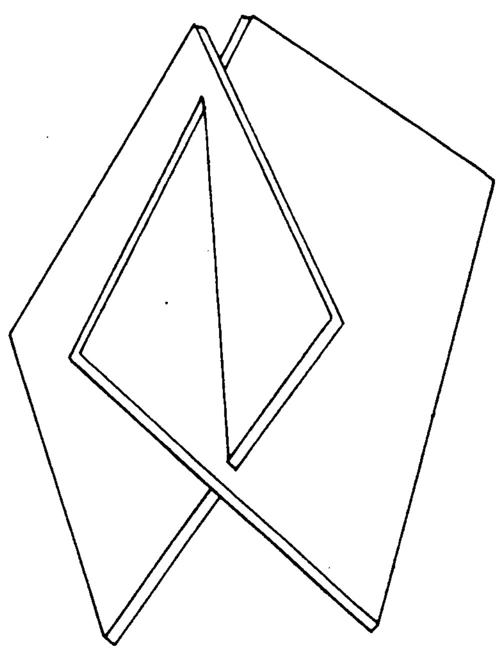

FIGURE 13 Intersecting Planes of Weakness. After Touseull [9]

4.2.2.2 <u>Shear Stability Analysis</u>

If transection occurred, Hoek and Brown (1980)[3] suggest evaluating the shear stability along a fault or major discontinuity using the following technique:

- estimate these parameters on several points along the fault

  σ_1 : major principal stress

  σ_3 : minor principal stress

  β : angle between the fault and σ_1

Assume that

$$\text{Shear Stress: } \tau = 1/2\ (\sigma_1 - \sigma_3) \sin 2\beta \qquad (1)$$

$$\text{Normal Stress: } \sigma = 1/2\ (\sigma_1+\sigma_3) - (\sigma_1-\sigma_3) \cos 2\beta \qquad (2)$$

and the shear strength τs of the fault is defined by:

$$\tau s = c + \sigma \text{ Tan } \phi \qquad (3)$$

where:

c is the cohesion

ϕ is the angle of friction

σ is the normal stress

- Equation 3 in Equation 2

$$\tau s = c + 1/2((\sigma_1+\sigma_3) - (\sigma_1-\sigma_3) \cos 2\beta) \tan \phi$$

- Then, a factor of safety ($\tau s/_\tau$) can be calculated along the fault and gives an indication of the potential for slip on the fault.

This analysis should be used in conjunction with a structural analysis to ensure that wedges which are free to fall or slide are not formed by the fault and other faults or joints.

4.2.3 Phase 3. Empirical Design

The rock mechanics data collection program should now be adequately advanced to provide the input parameters required by the empirical methods, which may be selected using the charts (Figures 14, 15, 16, 17).

If none of the empirical formulas reviewed are applicable to a particular situation, the designer may attempt to develop his own curves or formulas, adapted to his conditions by monitoring, many observations and good engineering judgement.

4.2.4 Phase 4. Theoretical Design

The real aim of theoretical design methods is to aid in understanding the complexity of the problem and to provide a mathematical model for rock behaviours. However, because it requires advanced mathematics as well as a considerable amount of input data, only a few theoretical methods have been adapted to mine design.

In any case, it is a valuable exercise to "play" with a theoretical method at this stage of design.

4.2.5 Phase 5. Computer Design

During this phase the pillar dimensions will be optimized. A computer model will be "adapted" to the mine's pillars. First, it should be used to analyze case histories in order to gain confidence in the model and to investigate the rock mass behaviour.

Finally, careful underground observations, monitoring and measurements should provide feedback on each computer design.

4.3 Design Charts

The charts (Figures 14 to 17) summarize the preceding five phase design procedure. A chart representing each pillar category ((1) Plate, (2) Separation, (3) Stub, (4) Inclined) indicates the methods, relationships and formulas that should be used in the five phase procedure.

FIGURE 14

PILLAR CATEGORY I
"plate pillars"

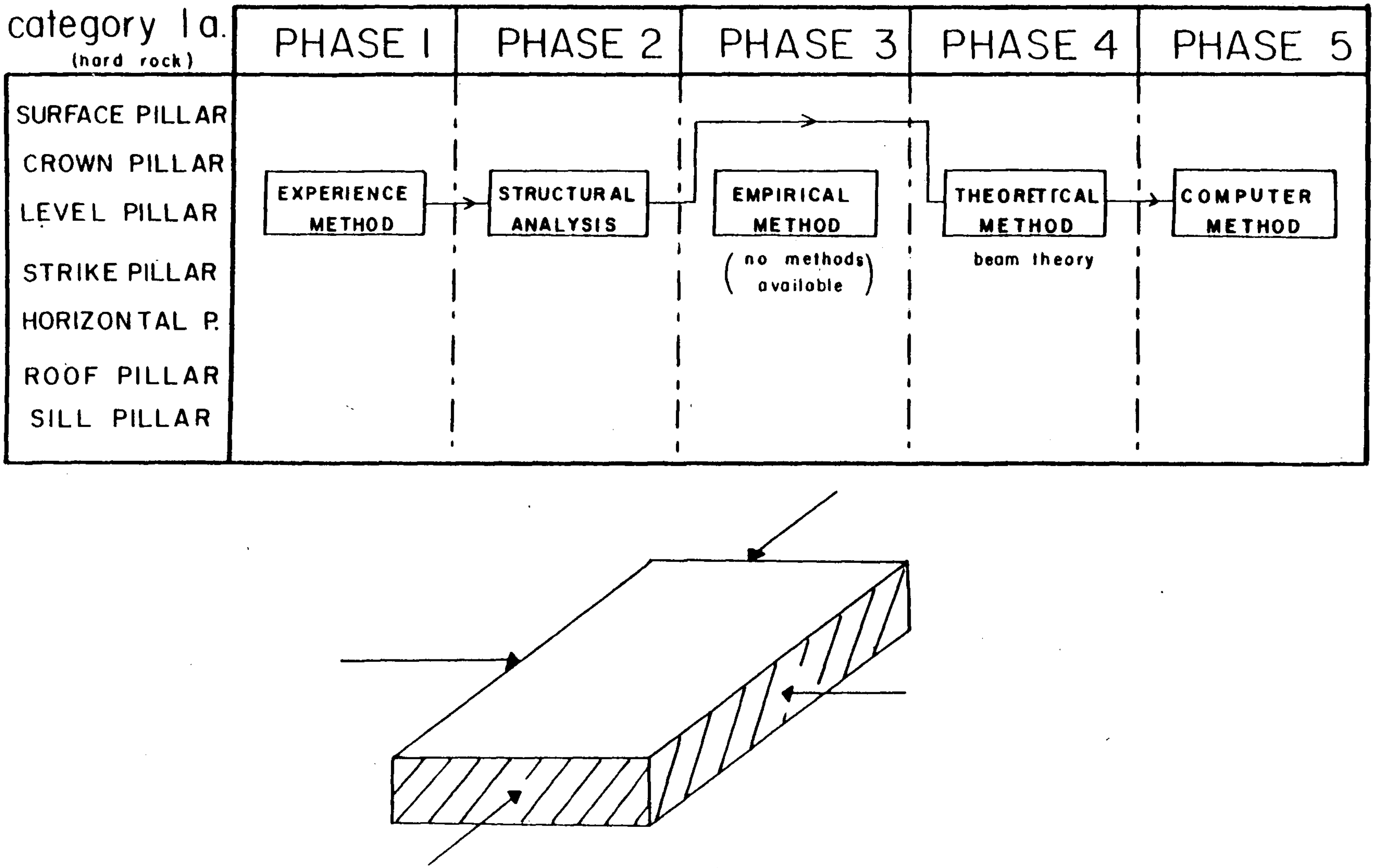

FIGURE 15

PILLAR CATEGORY 2

"separation pillars"

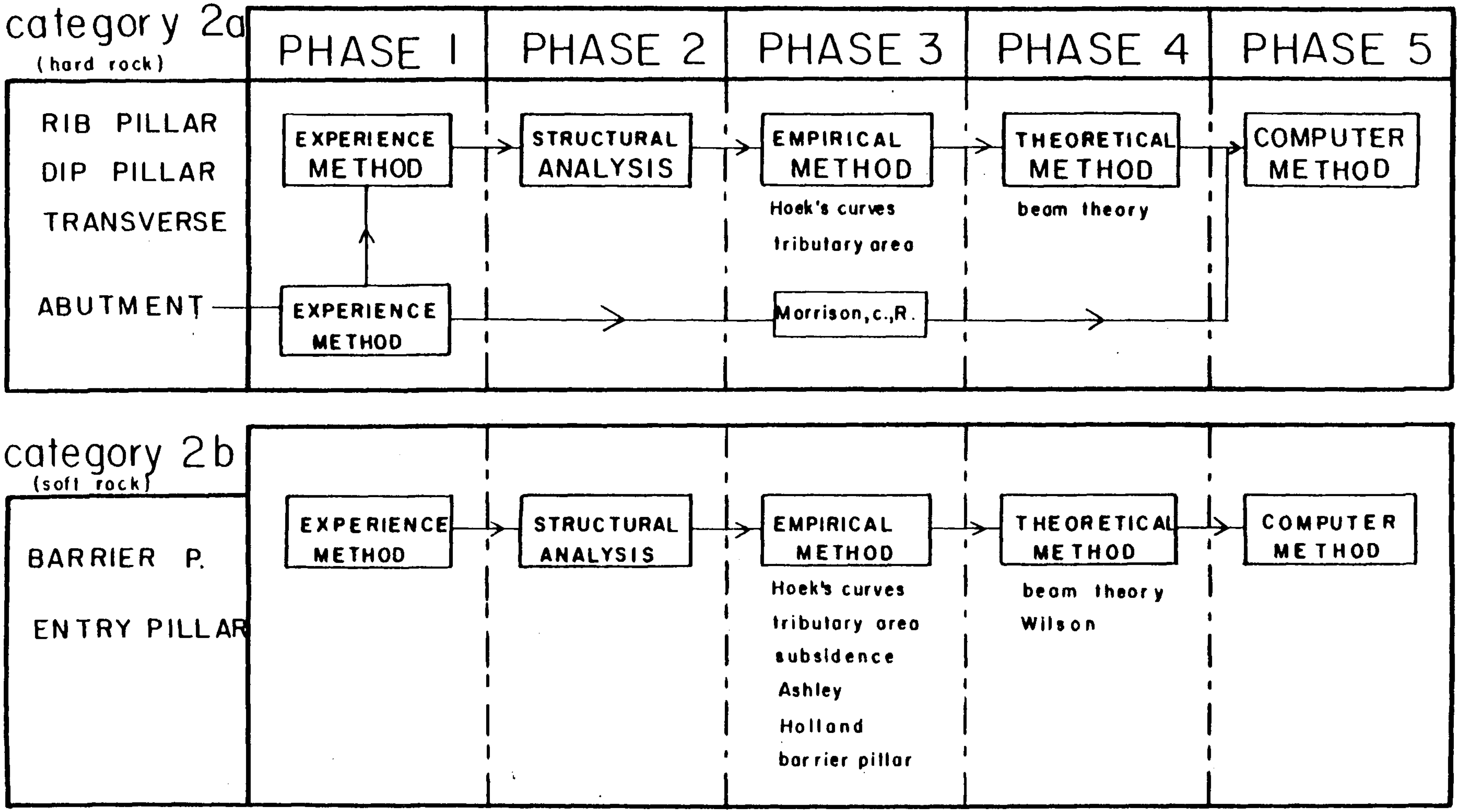

FIGURE 16

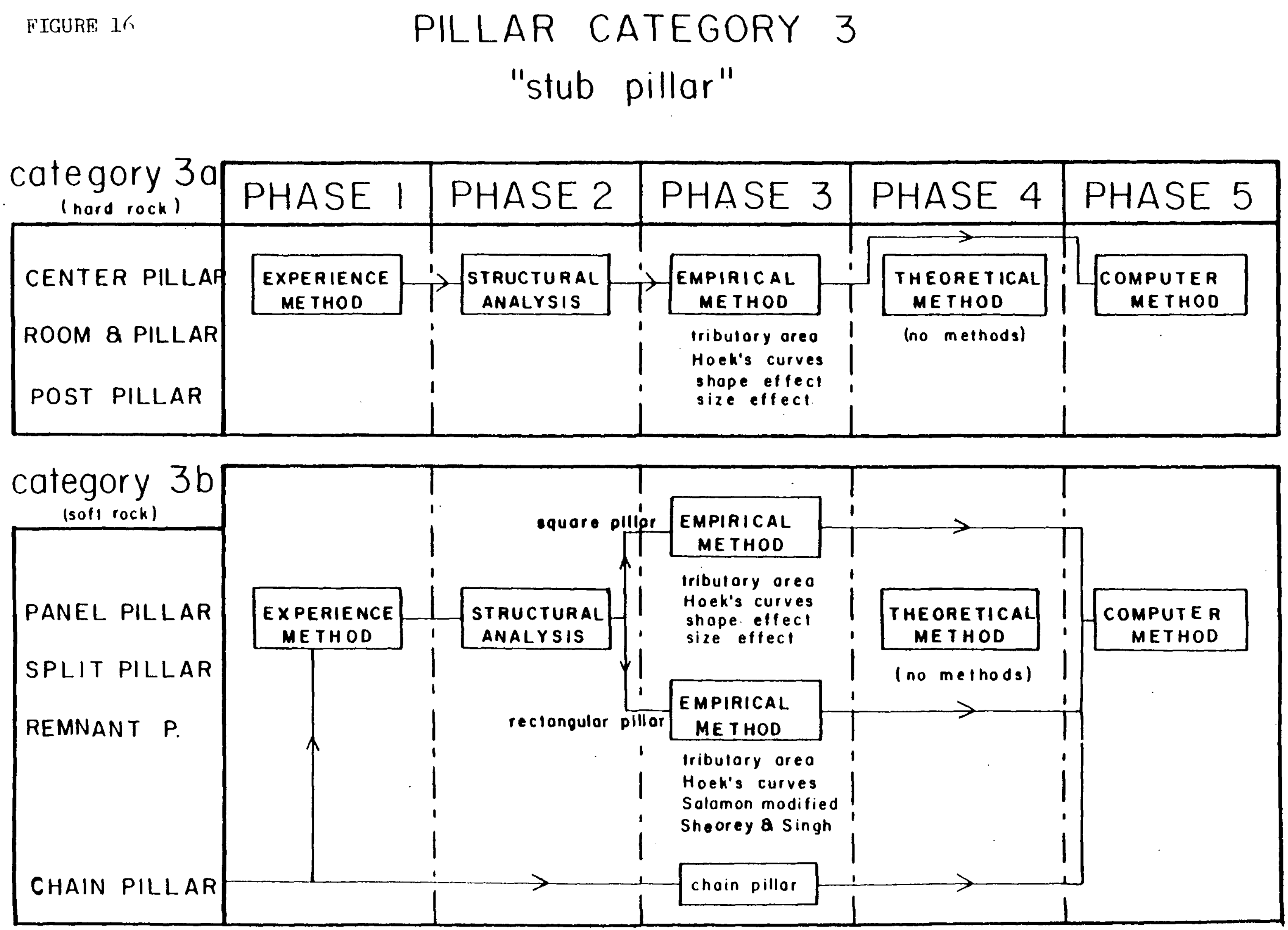

PILLAR CATEGORY 3
"stub pillar"
category 3a
(hard rock)
PHASE 1
PHASE 2
PHASE 3
PHASE 4
PHASE 5
CENTER PILLAR
ROOM & PILLAR
POST PILLAR
EXPERIENCE METHOD
STRUCTURAL ANALYSIS
EMPIRICAL METHOD
tributary area
Hoek's curves
shape effect
size effect
THEORETICAL METHOD
(no methods)
COMPUTER METHOD
category 3b
(soft rock)
PANEL PILLAR
SPLIT PILLAR
REMNANT P.
CHAIN PILLAR
EXPERIENCE METHOD
STRUCTURAL ANALYSIS
square pillar
EMPIRICAL METHOD
tributary area
Hoek's curves
shape effect
size effect
rectangular pillar
EMPIRICAL METHOD
tributary area
Hoek's curves
Salamon modified
Sheorey & Singh
chain pillar
THEORETICAL METHOD
(no methods)
COMPUTER METHOD

FIGURE 17

PILLAR CATEGORY 4

"inclined pillar"

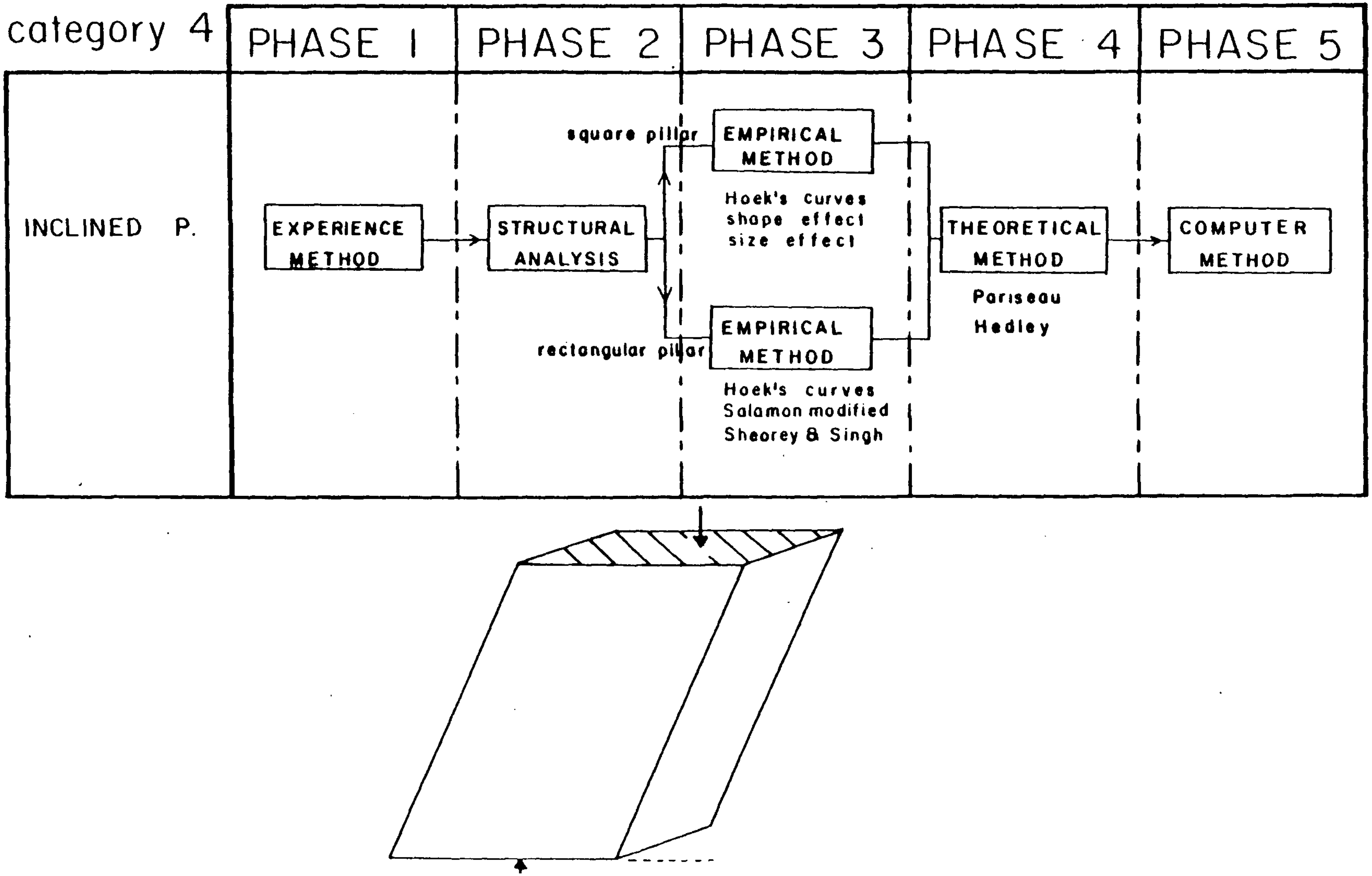

CHAPTER 5

HEATH STEELE CASE HISTORY ANALYSES

INTRODUCTION

During the summer of 1984, four Noranda underground mines were visited seeking pillar failure case histories. The Geco "B-Block", mined out in the early 60's, was selected because the failures were well documented by Bray (1967)[10]. The 77-92 and 77-94 rib pillar failures at Heath Steele were also chosen to take advantage of Allcot and Archibald (1981)[11] pillar design study.

The examination of case histories may generate pertinent and useful information for future designs. Geco (Chapter 6) and Heath Steele (Chapter 5) case histories are analyzed using the following procedure:

Review of General Information

1. Geology
   - 1.1 Regional geology
   - 1.2 Mine geology
   - 1.3 Structural geology
2. Mining method and underground structures dimensions.
3. Rock Mechanics Data
   - 3.1 Rock strength parameters
   - 3.2 Laboratory tests
   - 3.3 Rock Mass Classification
   - 3.4 Virgin stress

Review of Pillar Information

4. Pillar Characteristics
5. Mining sequence
6. Failure history and pillar geometry

Pillar Design Study

7.1 Phase 1 Experience method

7.2 Phase 2 Pillar structural analysis

7.3 Phase 3 Empirical methods

7.4 Phase 4 Theoretical methods

7.5 Phase 5 Computer methods

5.1 Geology (After Allcott and Archibald (1981)[11])

5.1.1 Regional Geology

The massive sulphide stratiform deposits of northern New Brunswick are hosted by the Tetagouche rock group. This rock group is highly folded, middle Ordovician in age and covers a circular area approximately 56 km. (35 miles) in diameter.

The Tetagouche rock group is broken into three lithological units: Sedimentary, Metabasalt, and Rhyolitic.

5.1.2 Mine Geology

The massive sulphide deposits lie within the rhyolite unit in close proximity to the quartz feldspar crystal tuff, which is also known as Augen Schist and Porphyry.

The stratigraphic rock units in the ore zone area top towards the north, which is indicated by the metal zoning in the sulphides and graded bedding in the sediments. These units listed from youngest to oldest are as follows: (Figure 18)

1. Banded Quartz Feldspar Crystal Tuff

   This rock unit is banded in places with 5-10 cm. bands, interlaid with varying grain size and proportions of quartz and feldspar phenocrysts.

7800 LEVEL

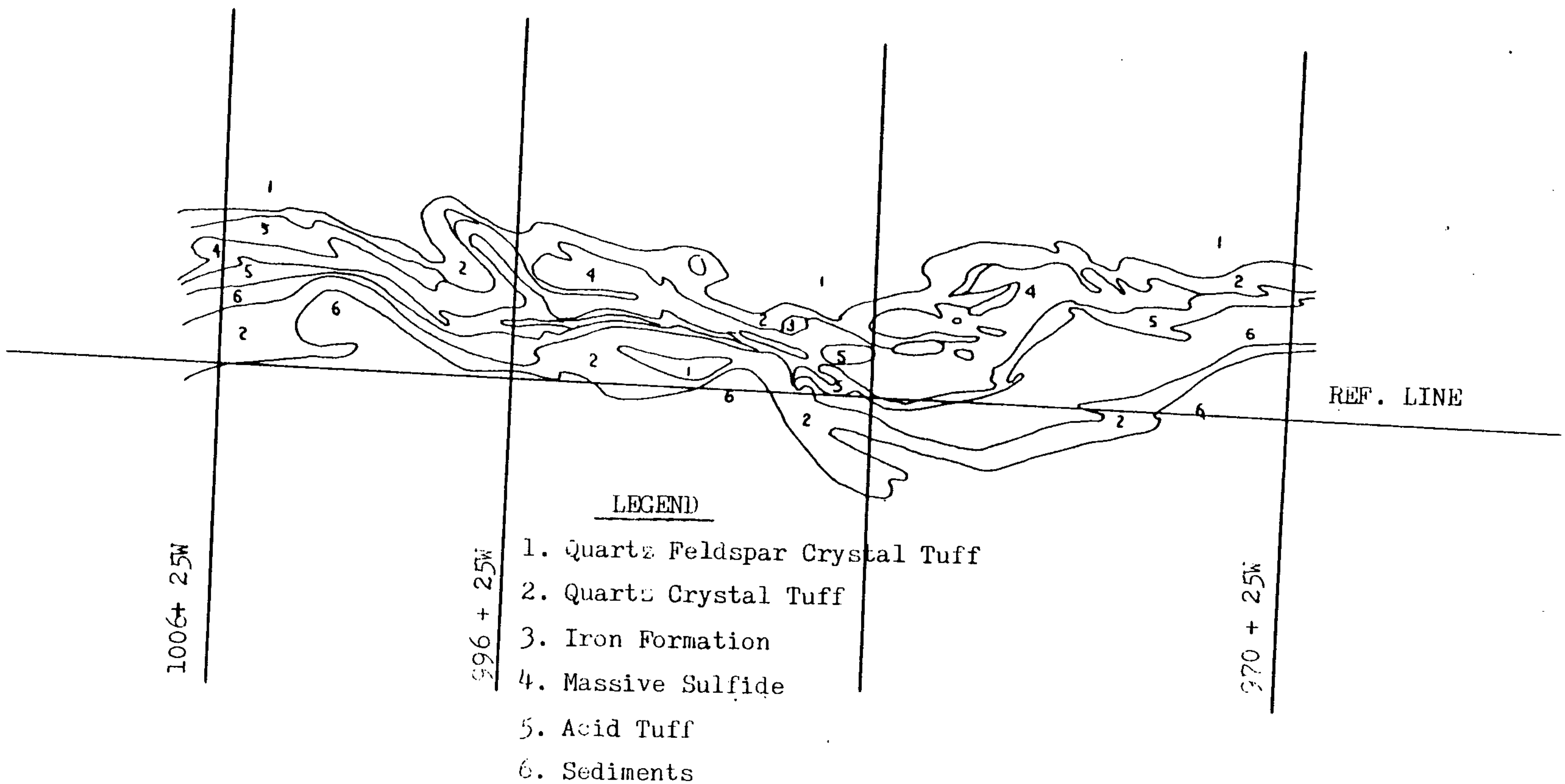

FIGURE 18 Heath Steele Geology

2. Banded Quartz Crystal Tuff

The quartz crystal tuff occurs as a 9 to 15 m. (30-50 ft.) thick bed on the hanging wall side of the massive sulphides. The porphyry is quite competent and fresh in appearance, with a compressive strength of 56.5 MPa (8200 psi). However, the fracturing tends to be blocky when exposed on the stope's wall.

3. Iron Formation

This zone is present as a discontinuous thin band along the upper margin of the massive sulphide formation. However, it also occurs in small patches along the footwall contact and within the sulphide zone. This is a competent bed, but is too thin and discontinuous to be relied upon as a stabilizing unit.

4. Massive Sulphides

The massive sulphides are very fine grained, with a compressive strength of 177 MPa (22,917 psi), and form the most competent rock unit in the mine. Very little sloughing occurs where the walls of the stopes consist of massive sulphides.

5. Acid Tuff

This is the least competent rock unit in the mine, and tends to be soft and sloughs readily when exposed on the walls of stopes. It forms a 1.5 to 21 m. (5-70 ft.) thick bed on the footwall of the sulphides and becomes discontinuous in places.

6. Clastic Sedimentary Rocks

The sedimentary rocks in the footwall below the acid tuff are intercalated with quartz feldspar crystal tuffs and form a band approximately 366 m. (1200 ft.) thick.

5.1.3 Structural Geology

The B Zone is a tabular shaped vertical or steep northerly dipping massive sulphide body, which strikes at N 73°E. The massive sulphides have a strike length of approximately 1150 m. (3,800 ft.), vary in thickness from a few centimeters to 75 meters (250 ft.) and have been traced to a depth of 1097 m. (3,600 ft.).

Folding is the primary structural control and although there is minor faulting, faults have had no major influence on the shape of displacement of the ore zone. The orebody has undergone five periods of folding which are numbered one to five in time sequence as they occurred. (Figure 19)

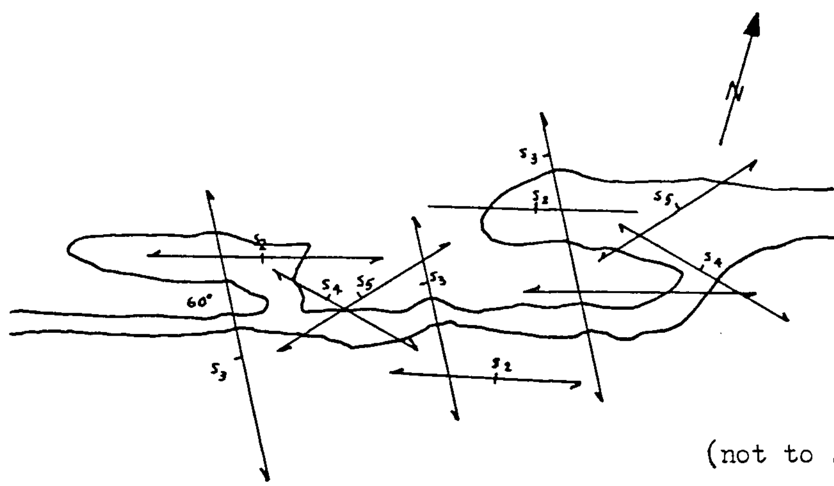

(not to scale)

FIGURE 19. Diagramatical Plan View of Heath Steele Orebody, Showing Orientation of Folding

S_1: The first period of folding left very little if any imprint on the massive sulphide. The only real evidence for this period of folding is a few flat lying relict cleavage planes in the host rocks.

S_2: The second period of folding had the greatest effect on the shape of the orebody. This period has shaped the orebody into a number of shaped isoclinal folds which plunge at approximately 60° in a S 73° W direction.

S_3: The third period of deformation produced open or tight concentric folds which plunged steeply northwest or southeast. This folding leads to some dilution problems in mining as the folds are difficult to define with the normal fifteen meters (50 ft.) spaced definition diamond drilling.

S_4: The fourth period of deformation resulted in a series of open, concentric folds, which plunged to the northwest and appeared as not more than gentle warps.

S_5: The fifth period of folding produced open folds which plunged 70° in a northeasterly direction. This period of deformation produced only rare folds in the mine area.

- JOINTING Golder Associates (1981)[12]

There are two major joint sets evident throughout the mine. Both are steeply dipping, with one set approximately parallel to the strike of the orebody and one approximately transverse to the strike. A third set of near horizontal joints appeared to be more prominent in the sulphides.

The joint set parallel to the strike indicated a spread in strike direction and is probably a combination of two joint sets.

Joints are usually planar or slightly undulating and spaced at about 1 m. to 3 m. (3.3 - 9.8 ft.).

5.2 Mining Method and Underground Structures Dimension

After Allcott and Archibald (1981)[11]

Mining of Heath Steele B Zone orebody proceeded with blast hole open stoping method, with later selected area filling. Extraction progressed from the upper levels to the lower levels and east to west with production maintained on two to three levels simultaneously. The production rate was

3000 tons per day from 1970 to 1976, increased to 3,500 tons per day in 1977, and finally reached 4,200 tons per day in 1982.

Mining of 8600 production level, 110 m. (360 ft.) below surface, was completed without any serious stability problems and a dilution factor of 10% was adequate compensation for overbreak or minor falls of waste. Five centimeters (2 inches) diameter blasthole rings were used, and underground ore haulage was by Track equipment. Stope dimensions were generally about 30 m. (100 ft.) on strike and up to 45 m. (150 ft.) high. Twelve meters (40 ft.) rib pillars were left to separate the stopes.

Mining advanced to the 8300 production level, at 200 m. (650 ft.) below surface, using the same method. Stope height was increased to 60 m. (200 ft.) and trackless load-haul-dump was introduced.

Although it had been easy to mine adjacent footwall and hanging wall stopes with an intervening 15 m. (50 ft.) pillar of low grade sulphides and the 10% dilution was still satisfactory, at this stage small scale sloughing started from the west side of 83-78 rib pillar. The cause was ascribed to the intersection of joints at the face of the pillar, but not to loading.

Mining started on 8050 production level, 275 m (900 ft.) from surface. It was decided to remove sill pillars under 8300 level so that the new stope heights would be increased to 140 m. (450 ft.). At this time the strike length was 45 m. (150 ft.) and the rib pillars were 15 m. (50 ft.) wide.

Real stability problems occurred when recovering rib pillars between primary stopes. In the first instance a rib pillar that was instantaneously blasted caused the adjacent rib pillar to burst and initiated a cave in the back extending over a 150 m. (500 ft.) strike length. After this, stope lengths were limited to 43 m. (140 ft.), and 85 m. (280 ft.) height. The rib pillar lengths were increased to 18 m. (60 ft.)

Ground problems were encountered with increasing frequency as the depth from surface increased.

The last procedure utilized backfilling the critical area and removing rib pillars only between filled stopes.

At level 7430 the stope dimensions were presumed to be 30 m. (100 ft.) long, 60 m. (200 ft.) high and separated by 30 m. (100 ft.) rib pillars.

5.3 Rock Mechanics Data

5.3.1 Rock Strength Parameters

- Density
  - Ore: γ = 4581 kg/m^3 (286 $\frac{lbs}{ft^3}$)
  - Waste: γ = 2883 kg/m^3 (179 $\frac{lbs}{ft^3}$)
- Elastic Modulus
  - F-W Chlorite Tuff E = 68,536 MPa (9.9 M. psi)
  - Ore Massive Sulphide E =119,284 MPa (17.3M. psi)
  - H-W Qtz. Porphyry E = 68,743 MPa (9.9 M. psi)
- Poisson's Ratio
  - F-W Chlorite Tuff ν = 0.25
  - Ore Massive Sulphide ν = 0.24
  - H-W Qtz. Porphyry ν = 0.19

5.3.2 Laboratory Testing

- Unconfined Compressive Strength
  - F-W Chlorite Tuff σ_c = 84 MPa (12,182 psi)
  - Ore Massive Sulphide σ_c= 176.5 MPa (25,598 psi)
  - H-W Qtz. Porphyry σ_c = 91 MPa (13,198 psi)

5.3.3 Rock Mass Classification

The footwall, hanging wall and orebody rocks were classified by Golder Associates (1981)[12] using the NGI system. Results are given below as well as an estimated CSIR rating for comparison purposes.

77-92 Cross-Cut Footwall - Chlorite Tuff

	NGI	
RQD	95	90
Jn	3	6
Jr	2	2
Ja	0.75	0.75
Jw	1.0	1.0
SRF	1.0	1.0
Q	84	40

	CSIR
Intact Strength	7
RQD	20
Spacing of Joints	25
Condition of Joints	6
Ground Water	10
	68

77-92 Cross-Cut Sulphides

	NGI	
RQD	85	95
Jn	6	6
Jr	1	1
Ja	0.75	0.75
Jw	1.0	1.0
SRF	1.0	1.0
Q	18.9	21

	CSIR
Intact Strength	12
RQD	17
Spacing Joints	25
Condition of Joints	6
Ground Water	7
	67

77-92 Cross-Cut Hangingwall Porphyry

	NGI	
RQD	95	95
Jn	6	3.0
Jr	2.0	1.0
Ja	0.75	0.75
Jw	1.0	1.0
SRF	1.0	1.0
	42	42

	CSIR
Intact Strength	7
RQD	20
Spacing of Joints	25
Condition of Joints	6
Ground Water	10
	68

5.3.4 Virgin Stress

No virgin stress measurements have been made at the mine. Measurements have been achieved at Brunswick Mining, which is located in the same rock formation about 50 km (30 miles) away. The results at 700 m. (2300 ft.) depth are as follows: (Figure 20)

- To determine the virgin stress at Heath Steele, the following assumption has to be made:

"The ratio of stresses (vertical and horizontals) at Brunswick is comparable with the ratio of stresses at Heath Steele".

Thus, the stress regime 300 m. (1000ft.) below surface at Heath Steele is:

$$\sigma_V = \sigma_3 = \gamma_{waste} \times \text{(depth below surface)}$$

$$= 2883 \text{ kg/m}^3 \times 305 \text{ m} = 8.79 \times 10^5 \text{ kg/m}^2$$

$$\sigma_3 = 8.79 \times 10^5 \text{ kg/m}^2 = 8.62 \text{ MPa} \quad (180 \text{ KPSF})^*$$

* Note: KPSF = kilo pounds per square foot

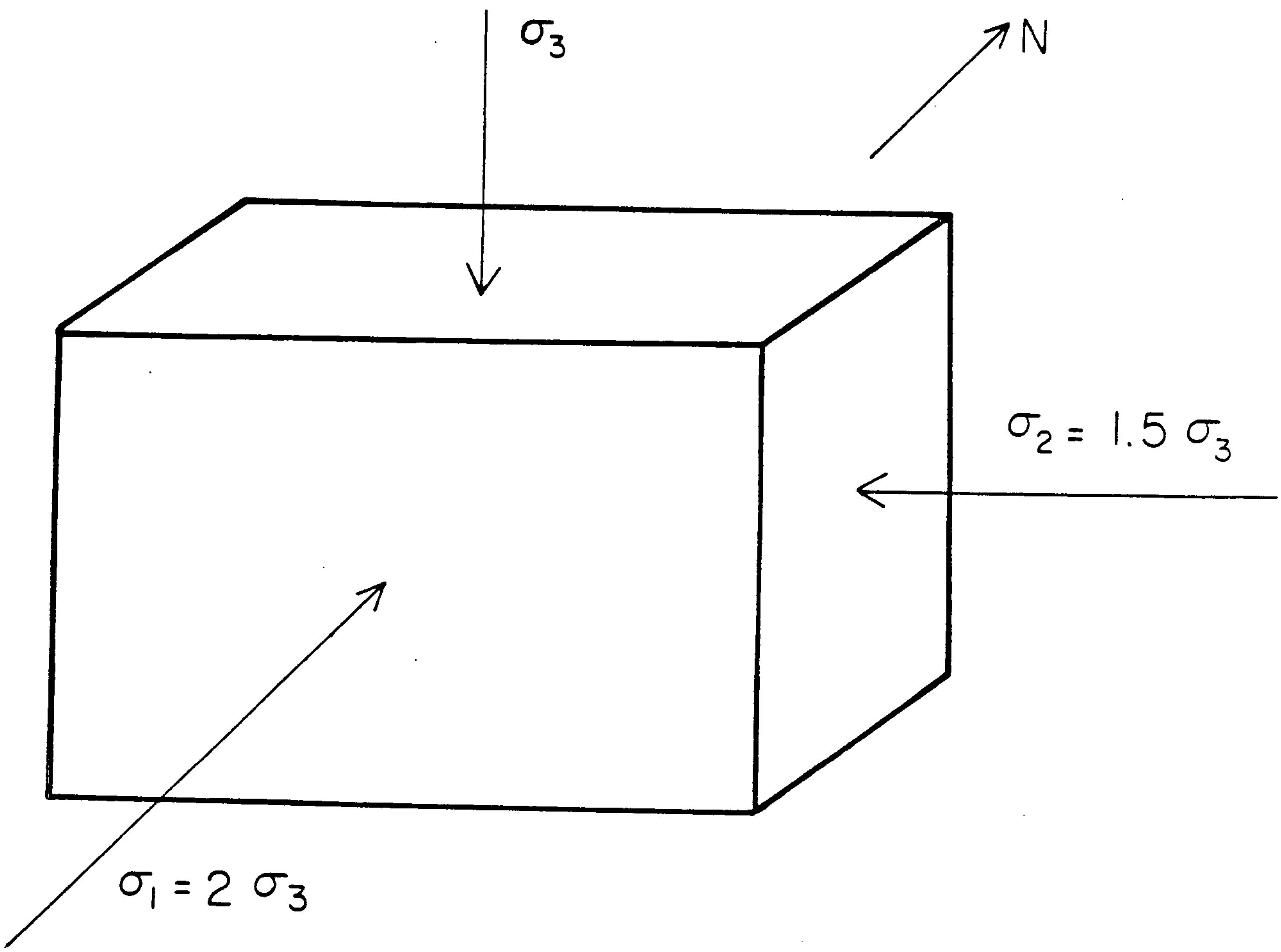

FIGURE 20 Virgin Stress at Heath Steele

$$\sigma_{H\ (\text{north-south})} = \sigma_1 = 2 \times \sigma_3 = 2 \times 8.62 \text{ MPa}$$

$$\sigma_1 = 17.24 \text{ MPa} \quad (360 \text{ KPSF})$$

$$\sigma_{H\ (\text{east-west})}\sigma_2 = 1.5 \times \sigma_3 = 1.5 \times 8.62 \text{ MPa}$$

$$\sigma_2 = 12.93 \text{ MPa} \quad (272 \text{ KPSF})$$

5.4 Pillar Characteristics

- Ribs:

  Originally 12 m. (40 ft.) x 61 m. (200 ft.) high x ore width

  Laterally 27 m. (90 ft.) x 76 m. (250 ft.) high x ore width

- Sills/Crowns:

  Production level up contains cones or trough usually extending up 15 meters (50 ft.) above level. Below level usually 15 to 23 meters (50 to 75 feet) depending on ore widths and local geometry.

- Pillar Support:

  Generally no systematic support is given. In specific problem areas some cable bolting has been used. In some small pillars in the room and pillar overcuts, some perimeter strapping has been done in isolated problem areas. Otherwise local support of development within pillar areas has been the use of standard rock bolts (5 or 8 ft.) 1.5 to 2.5 m. Early practice was to use mechanical bolts and straps or plates. Latterly resin anchored rebar pins are almost exclusively used.

5.5 Mining Sequence

The investigated area consists of four open stopes (77-95, 77-93, 77-91, 77-89) separated by three rib pillars (77-94, 77-92, 77-90). The depth varies from 245 m. (800 ft.) to 366 m. (1200 ft.) below surface, and a 300 m.

(1000 ft.) depth was assumed for calculation purposes.

Figure 21 is a longitudinal view of the stope/pillar panel layout, and Table 8 summarizes the mining sequence (from Blasting Record).

TABLE 8

MINING SEQUENCE OF THE PANEL

STOPE	START DATE	FINISH DATE
77-95	May, 1977	Nov. 1978
77-93	Dec. 1976	May, 1978
77-91	Apr. 1976	Apr. 1978
77-89	May, 1975	Dec. 1977
77-92 (Pillar Recovery)	Apr. 1978	Apr. 1978

5.6 Failure History and Pillar Geometry

- November 1977: 77-92 Rib Pillar

It was discovered that there was excessive wedge type sloughing from the walls of this pillar into the stopes on each side to the extent that it was considered not to be providing any support. Accordingly, it was decided to blast out this pillar and to stop further mining west in 77-93 stope to increase the 77-94 pillar.

- April 1978: The 77-92 rib was blasted, and recovered.
- September, 1978: 77-94 Rib Pillar

After the 77-92 rib was blasted, mining continued in 77-95 stope. On September 23/78, a blast in 77-95 stope appeared to have triggered a violent reaction in 77-94 rib causing seismicity and buckling of track rails in this pillar on both 7950 and 7800 levels.

- July 1980: 77-96 Rib Pillar. (supplementary information)

Activity in this rib on 7700 level developed in July 1980 and was

FIGURE 21 Schematic Longitudinal View of the Investigated Area at Heath Steele. (Mining method: Blast hole Open stoping)

Scale: 1 in. = 100 ft.

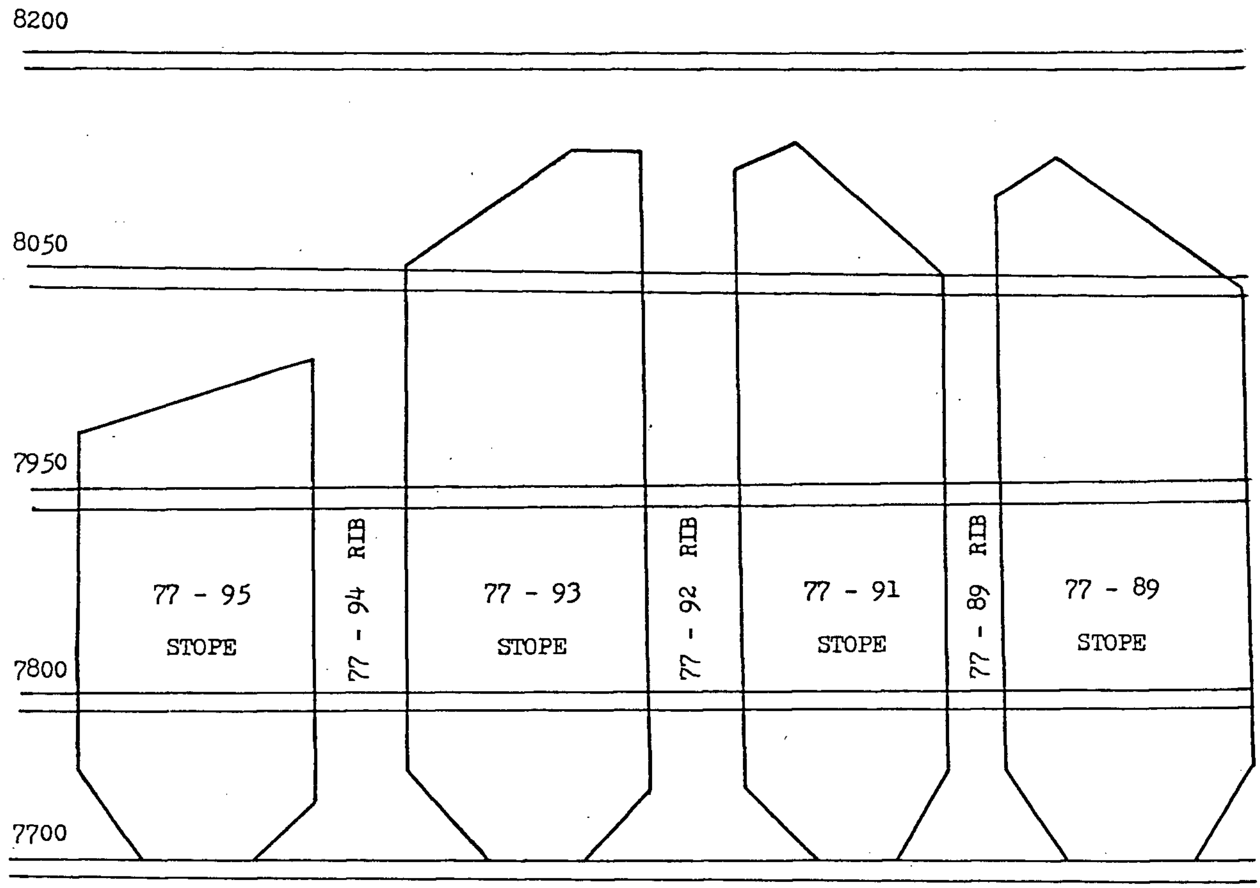

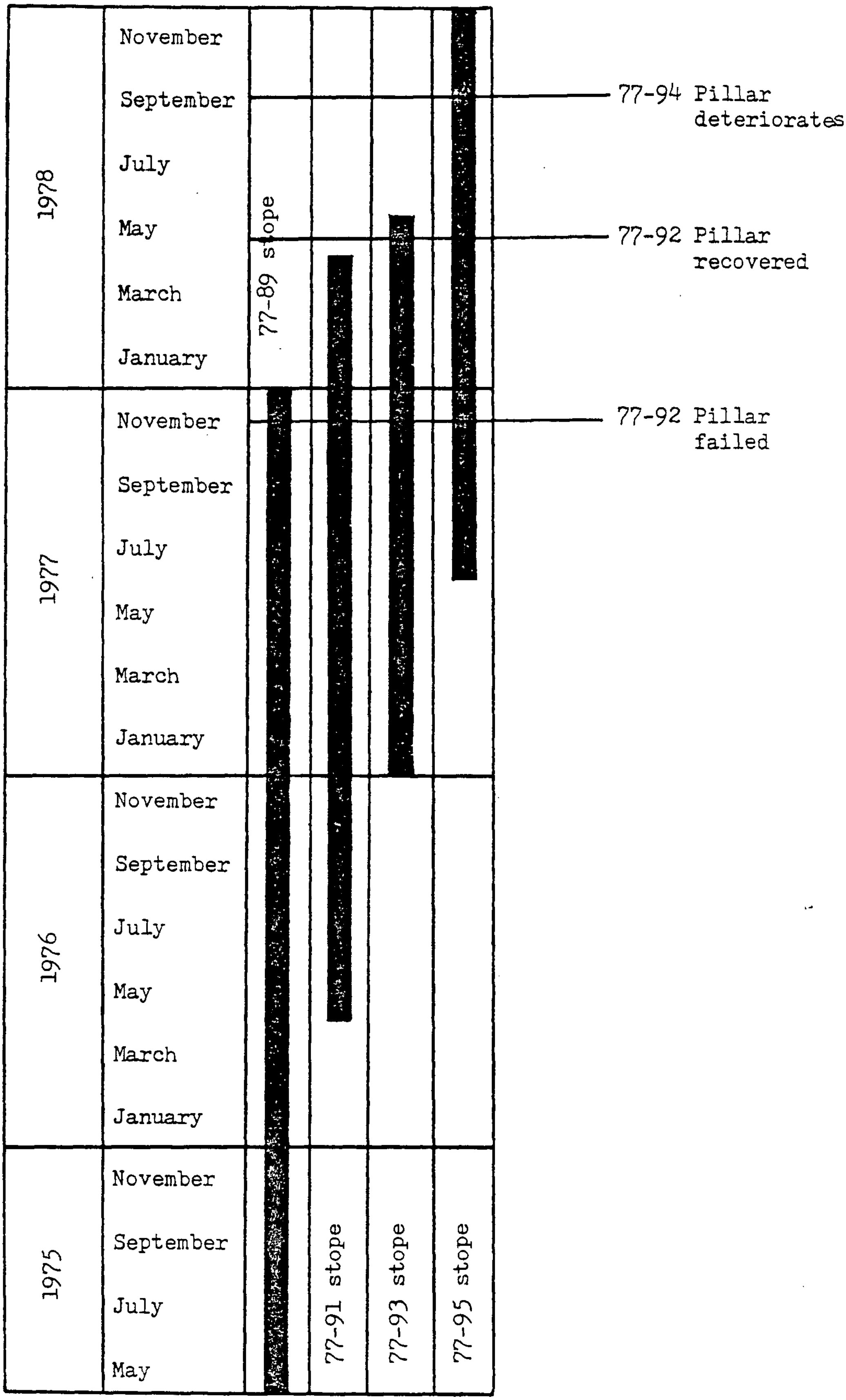

FIGURE 22 Extraction Flowchart of 77-89, 77-91, 77-93, and 77-95 Stopes

associated with the blasting of 74-97 stope.

From the Figure 22 Extraction Flowchart the stope and pillar geometries and dimensions were estimated:

a) when the 77-92 rib pillar failed in November 1977 (Figure 23, Table 9)

b) when the 77-94 pillar collapsed in September 1978 (Figure 24, Table 10).

The design study will concentrate on these two particular cases, and because the major principal stress is horizontal in the N-S axis direction, only the plan view needs to be considered.

TABLE 9

APPROXIMATE STOPE + PILLAR DIMENSIONS WHEN 77-92 PILLAR FAILED (NOVEMBER, 1977)

	Length	Width	Height
Stopes			
77-89	43m. (140 ft)	15m. (50 ft)	110m. (360 ft)
77-91	30m. (100 ft)	40m. (130 ft)	120m. (395 ft)
77-93	27m. (90 ft)	40m. (130 ft)	120m. (395 ft)
77-95	18m. (60 ft)	40m. (130 ft)	90m. (300 ft)
Pillars			
77-90	15m. (50 ft)	15m. (50 ft)	117m. (385 ft)
77-92	27m. (90 ft)	40m. (130 ft)	122m. (400 ft)
77-94	30m. (100 ft)	40m. (130 ft)	107m. (350 ft)

TABLE 10

APPROXIMATE STOPE AND PILLAR DIMENSIONS WHEN 77-94 PILLAR FAILED (SEPTEMBER, 1978)

	Length	Width	Height	
Stopes				
77-89	43m. (140 ft)	15m. (50 ft)	137m. (450 ft)	caved
77-91)) 77-93)	98m. (320 ft)	40m. (130 ft)	168m. (550 ft)	"
77-95	43m. (140 ft)	40m. (130 ft)	90m. (300 ft)	"
Pillars				
77-90	15m. (50 ft)	15m. (50 ft)	122m. (400 ft)	
77-92	---------------	F A I L E D	----------------------	
77-94	18m. (60 ft)	40m. (130 ft)	122m. (400 ft)	

5.7 Pillar Design Analysis

Every pillar involved in the Heath Steele case history may be classified as "separation pillars" (Category 2 of the pillar classification).

According to the design charts of Chapter three, the following designing methods should be used.

5.7.1 Phase 1. Experience Design

From the description of the mining method (Section 5.2), the most recent practice at Heath Steele was backfilling the critical area and recovering rib pillars only between primary filled stopes, which were estimated to be 30m. (100 ft) long, 60m. (200 ft) high and separated by 30m. (100 ft) rib pillars.

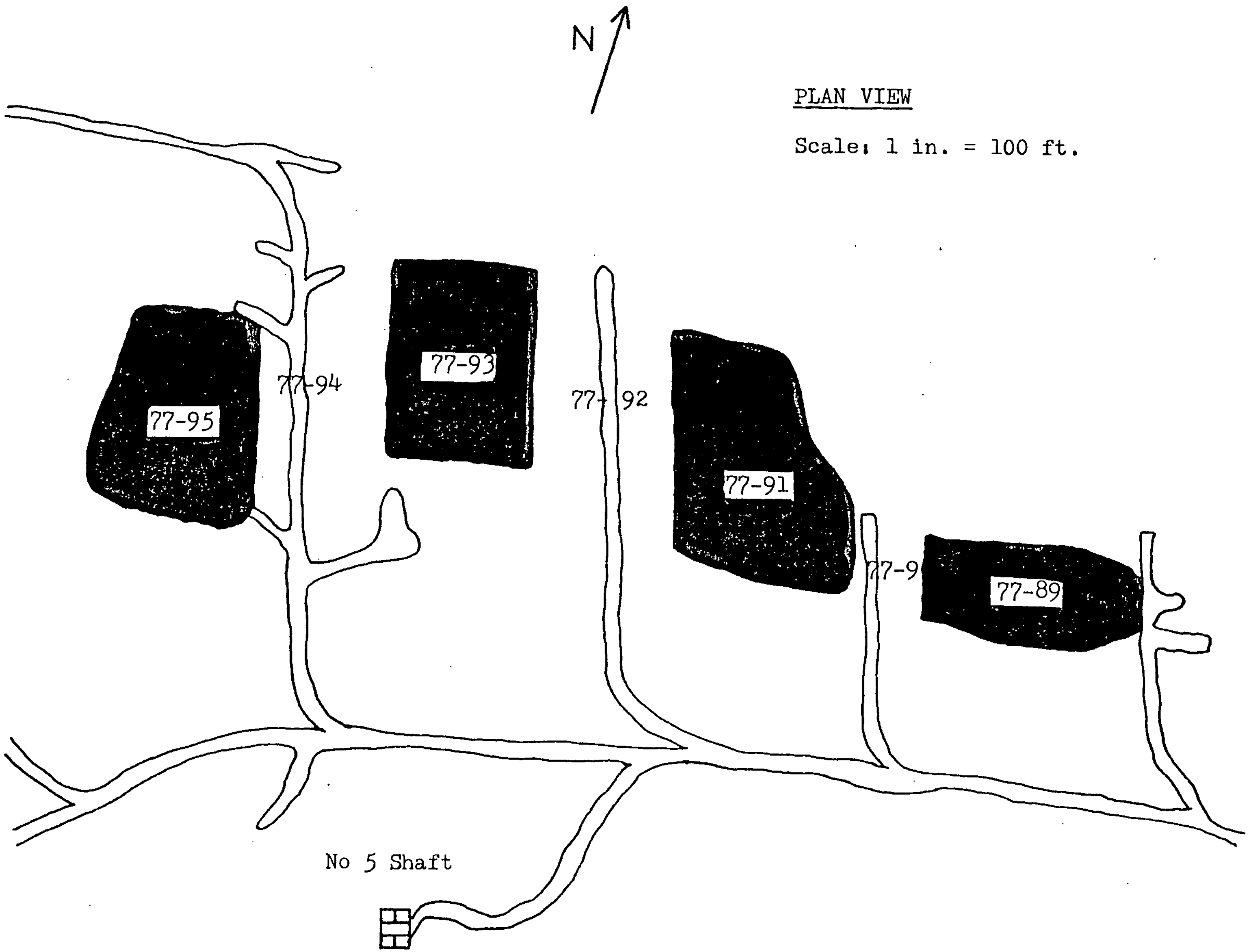

FIGURE 23 Estimated Layout When 77-92 Rib Pillar Failed

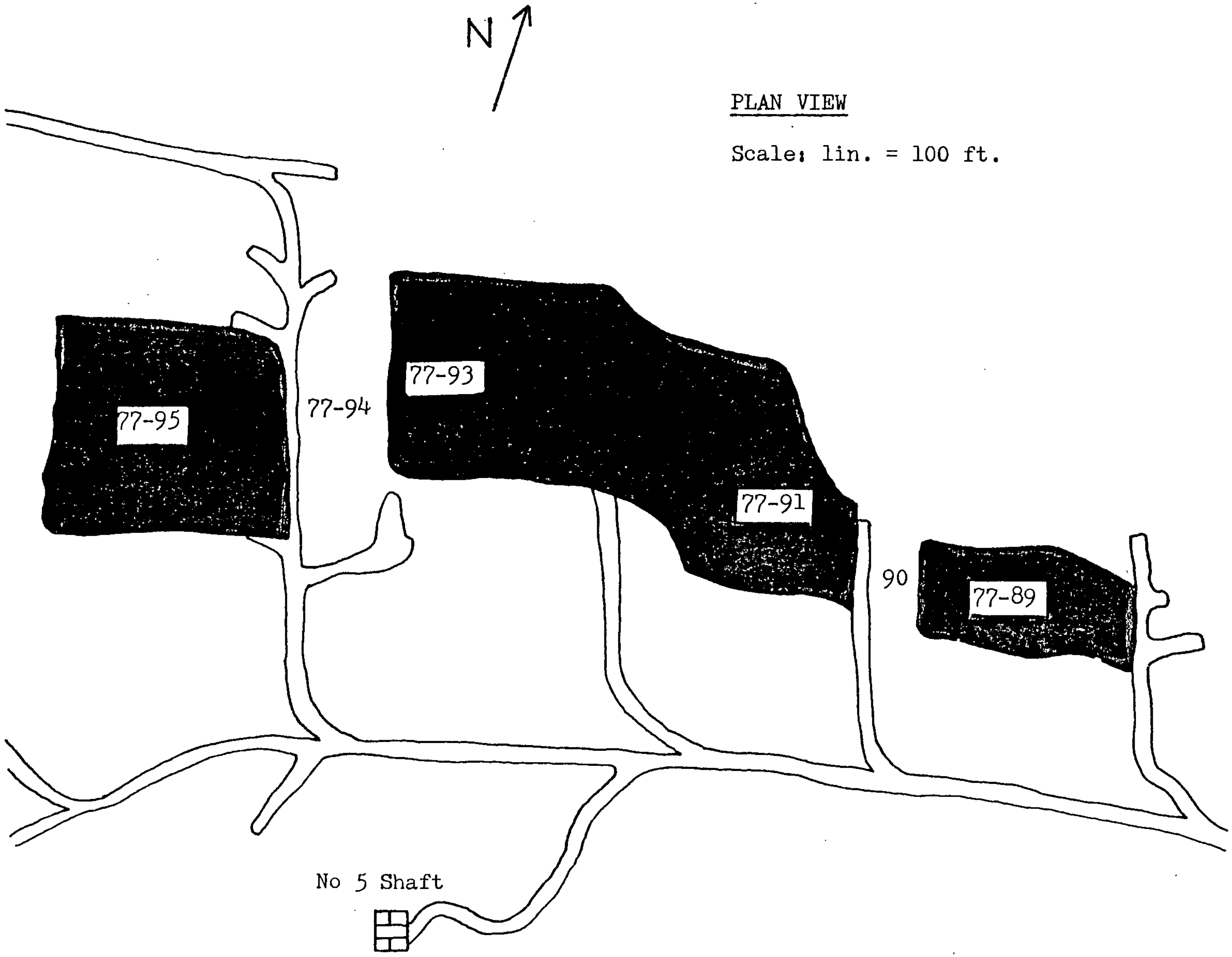

FIGURE 24 Estimated Layout When 77-94 Rib Pillar Failed

5.7.2 Phase 2. Pillar Structural Analysis After Allcott and Archibald (1981)[11]

The pillars consist of massive sulphides which have a compressive strength of 176.5 MPa (25598 psi), the strongest unit in the geological sequence.

The most important factor affecting the strength of the pillars is the fracture systems, more specifically S_3 and S_5.

The S_3 fractures strike at N 30°W, which is approximately 15° to the N-S axis of the rib pillars and the direction of the compressive forces acting on the pillars (Figure 25).

Note that pillars with a north-south axis of 30m. (100 ft) and east-west axis of 18m (60 ft) have the S_3 fractures supported on both hanging wall and footwall over a strike length of 10m (33 ft) (Figure 26). However, a pillar with a north-south axis of 60 m. (200 ft) and an east-west axis of 18m. (60 ft) has the S_3 fractures supported on both the hanging wall and footwall over a strike length of only 2m. (7 ft) (Figure 27).

In the present cases, the pillar lengths (N-S axis) never exceed 40m. (130 ft) (Tables 9 and 10). Thus, the S_3 fractures alone should not provoke sliding in the pillars.

The S_5 (N 40°E) fractures strike at about 60° to the north-south axis of the rib pillars and dip steeply to the northwest. (Figure 28). They are much less well developed than the S_5 fractures and are at a flatter angle to the direction of the compressive forces.

The intersection of the S_3 and S_5 fractures near the sides of the rib pillars sometimes result in spalling and deterioration of the pillars. (Figure 29).

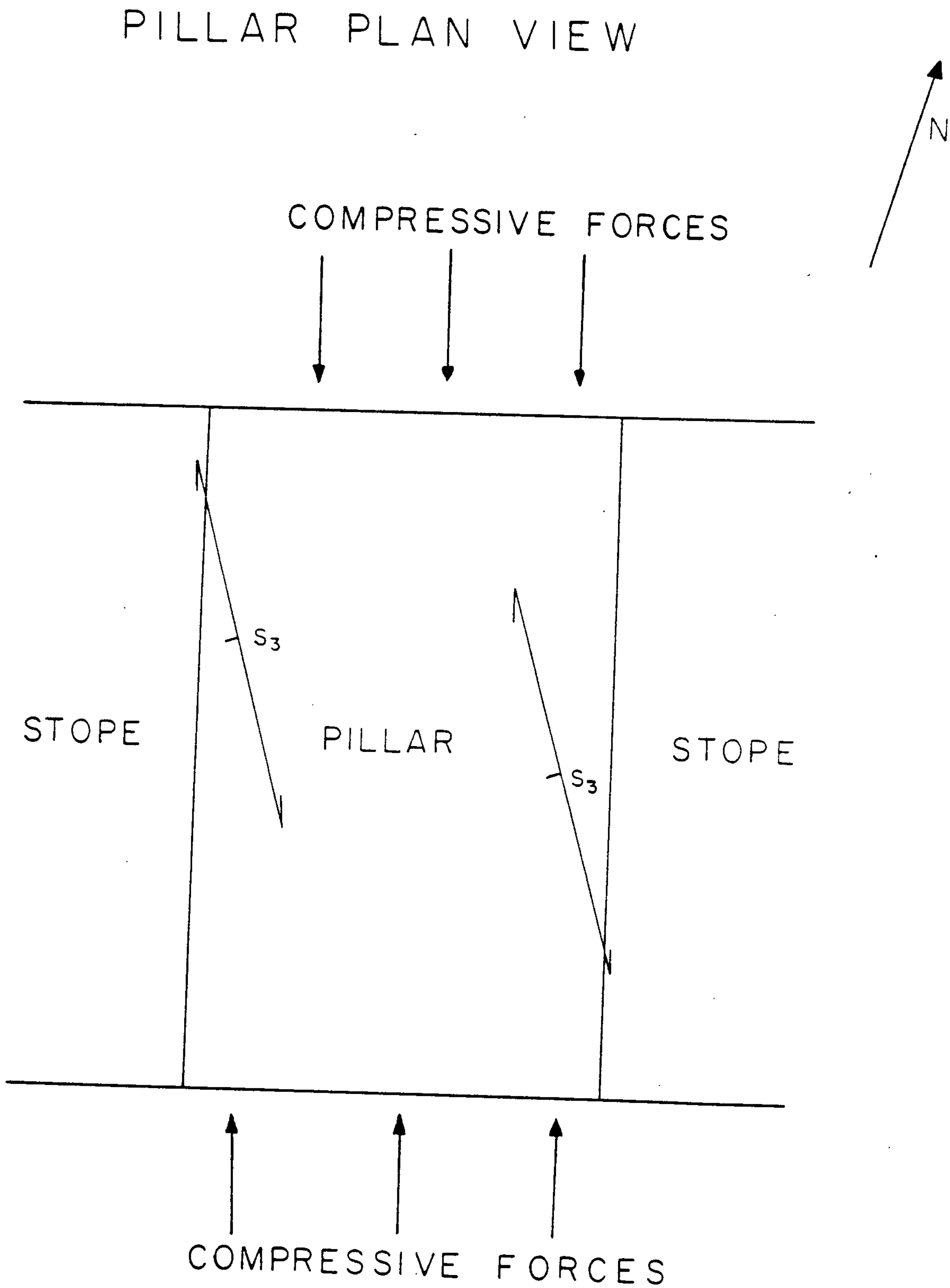

FIGURE 25. S_3 Fracture System

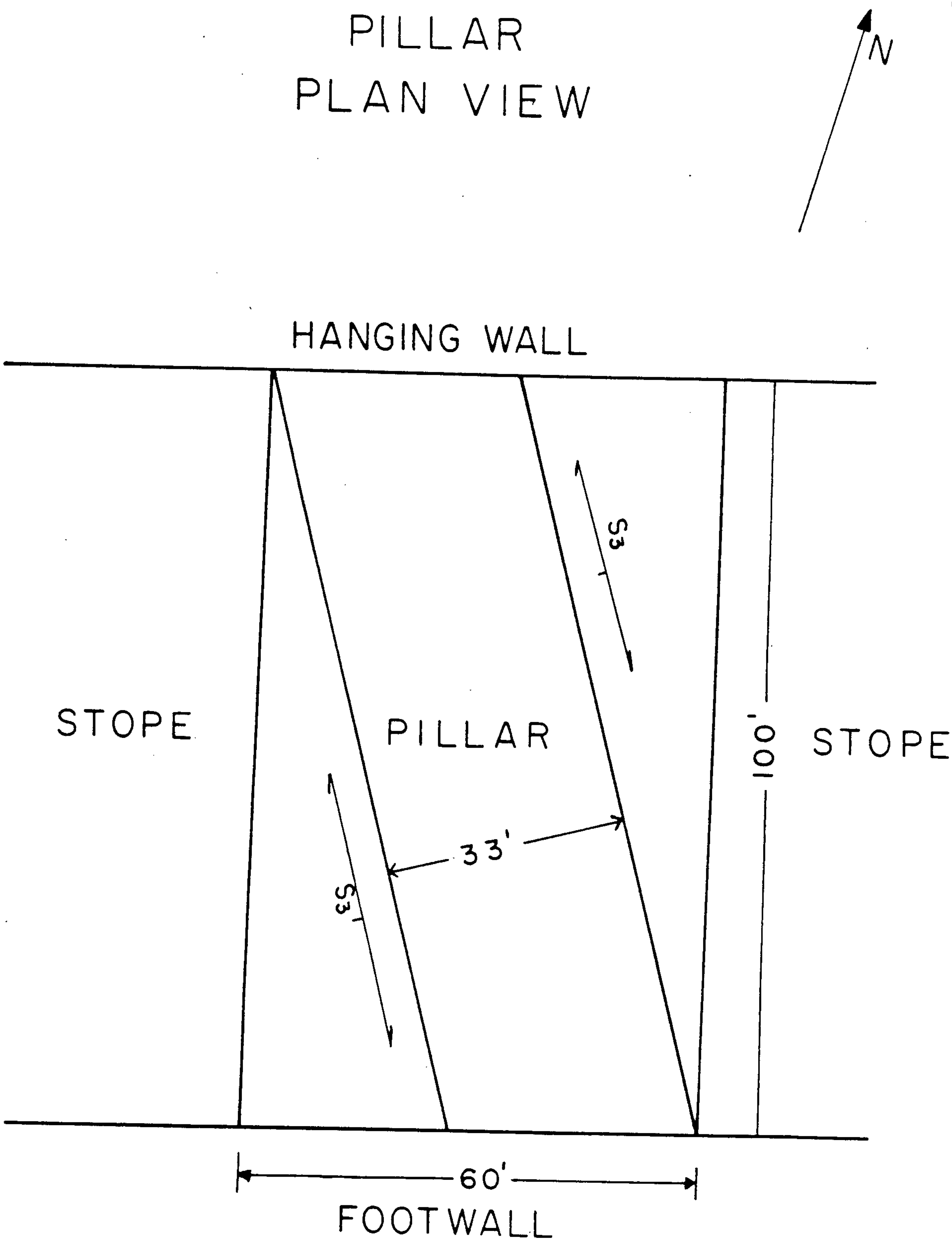

FIGURE 26 The Effect of S_3 Fractures on 30 m. (100 ft.) Wide Rib Pillars. (After Allcott & Archibald) [11]

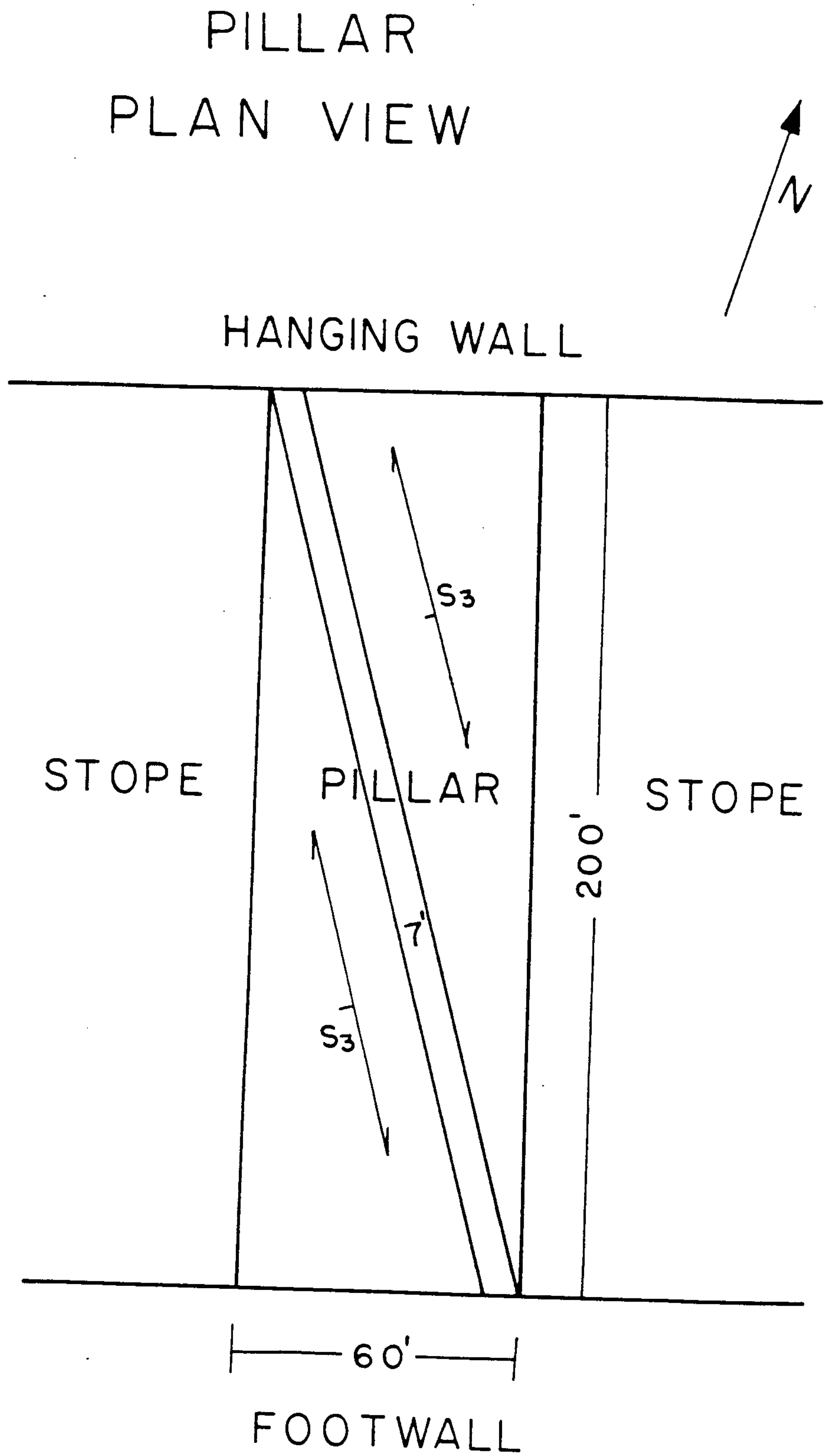

FIGURE 27 The Effect of S_3 Fractures on 60 m. (200 ft.) Wide Rib Pillars (After Allcott & Archibald)[11]

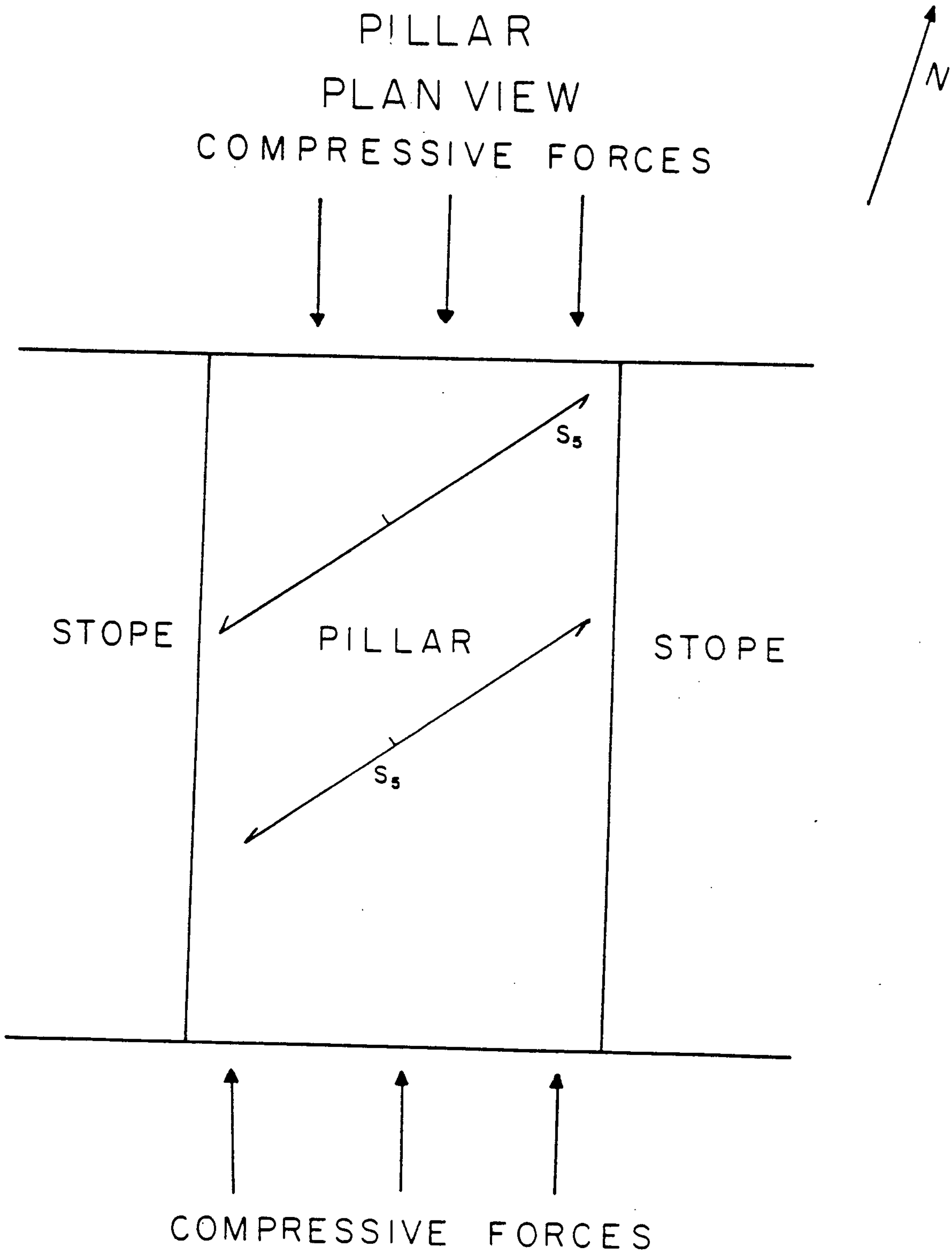

FIGURE 28. S_5 Fracture System

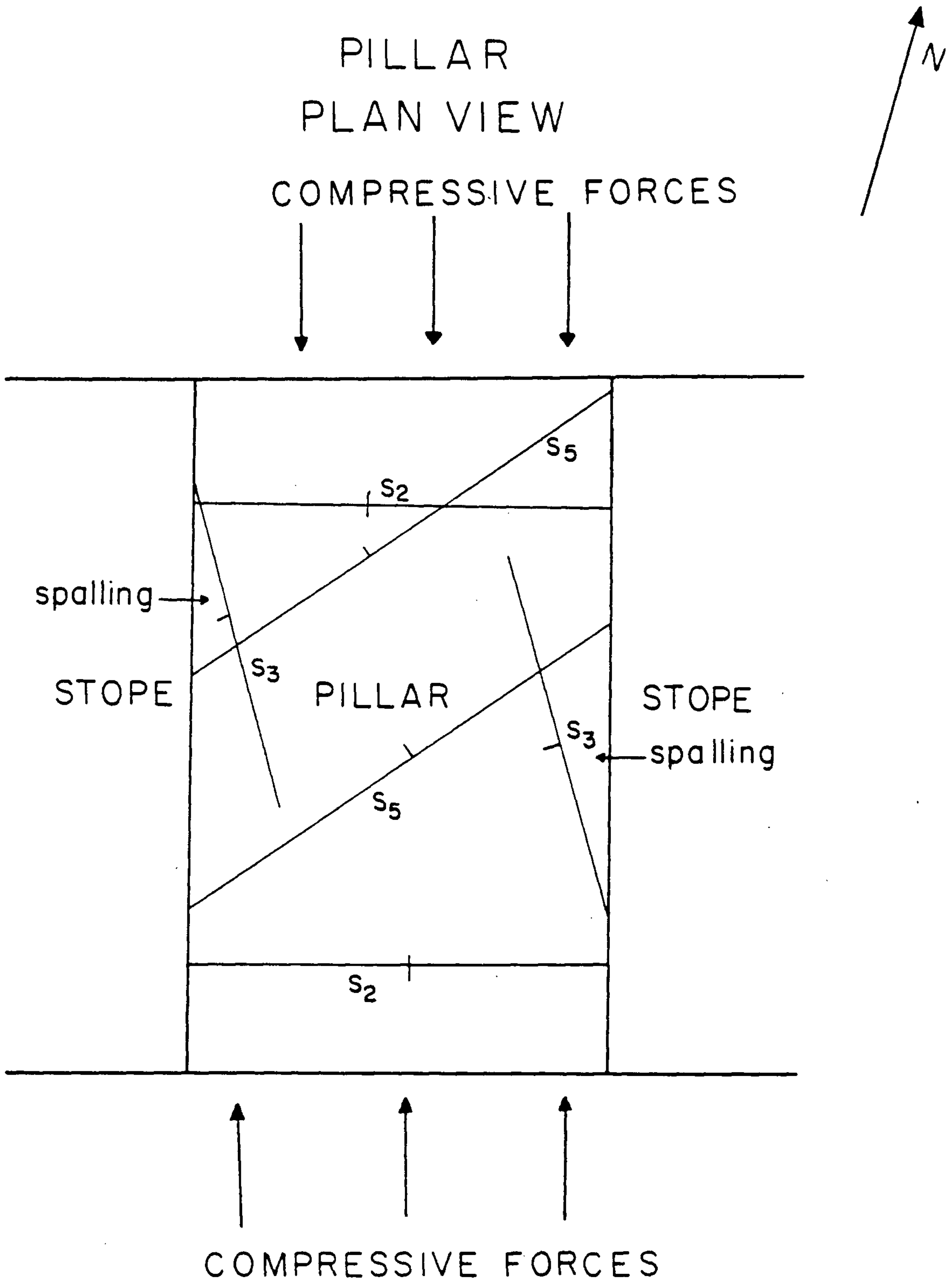

FIGURE 29 Combined Effect of S_3 and S_5 Fractures

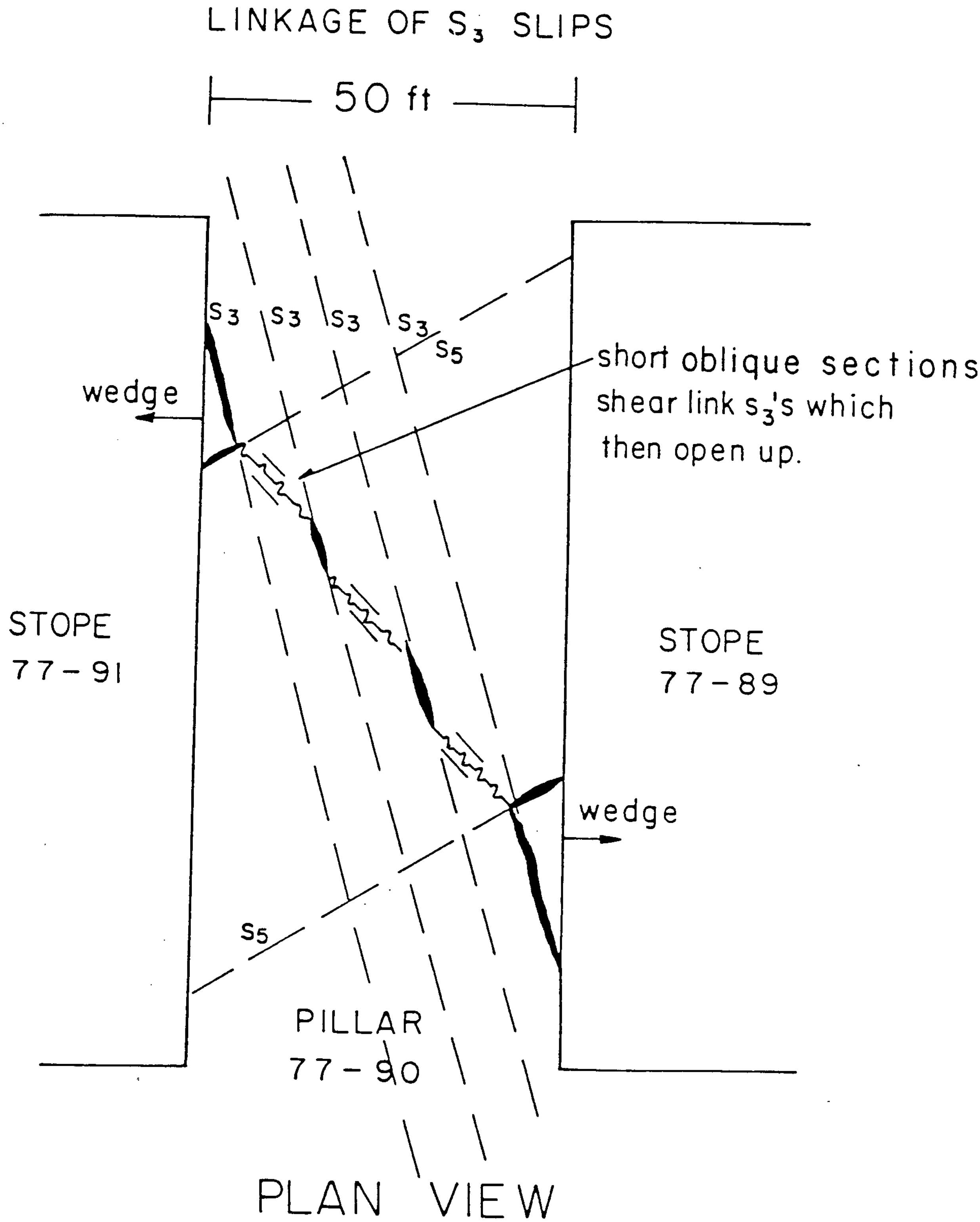

FIGURE 30 77-90 Rib Pillar Sliding. (After Allcott & Archibald)[11]

FIGURE 31 (After Allcott & Archibald)[11]

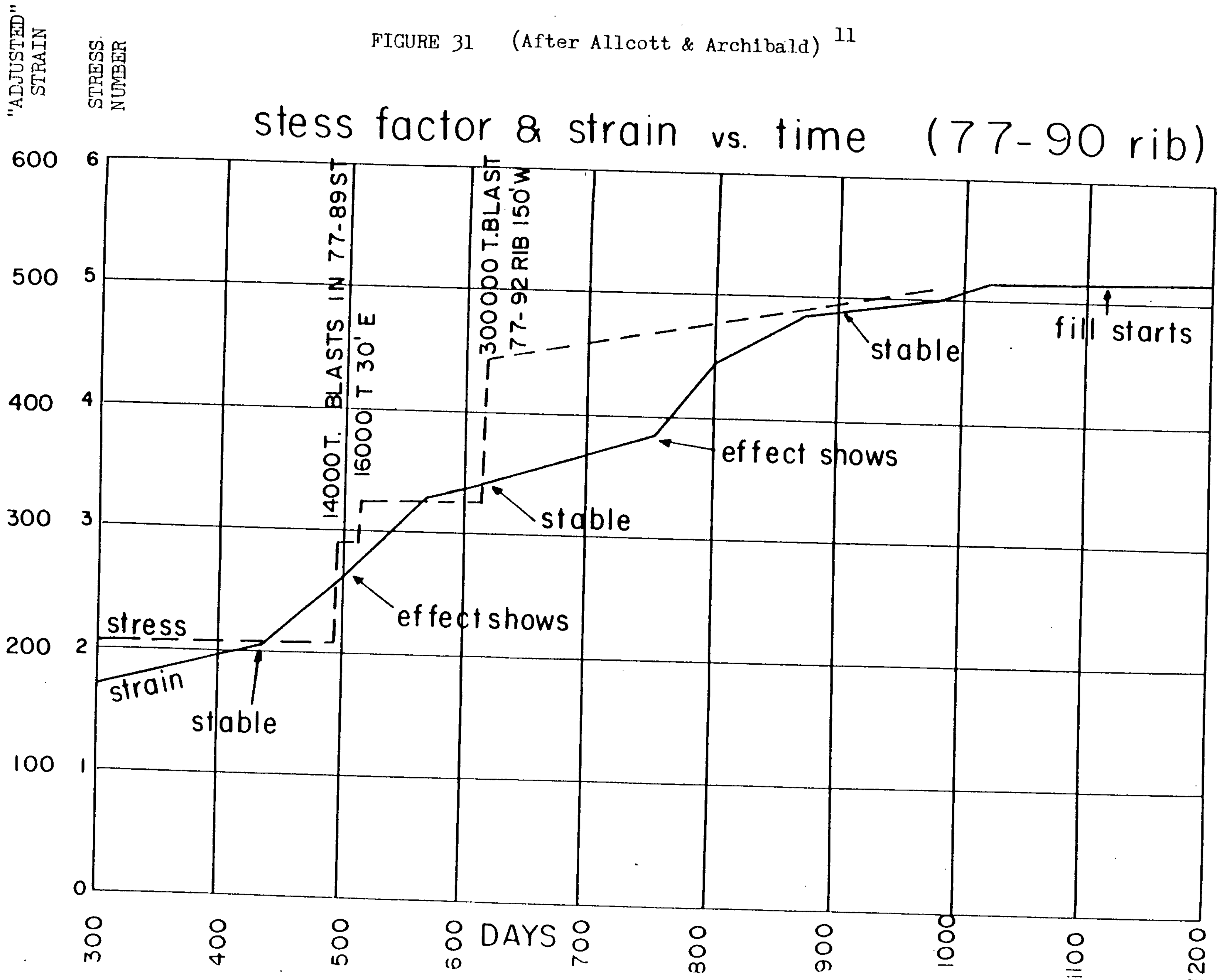

Because the 77-90 pillar is only 15m. (50 ft) wide (east-west axis), these wedge failures may induce major stability problems, and provoke pillar sliding (Figure 30).

The deformation of the 77-90 rib pillar was monitored and Figure 31 clearly shows that the pillar sliding described previously, occurred.

5.7.3 Phase 3: Empirical Methods

Empirical methods may be used to estimate the load acting on a pillar, and its ultimate strength at failure. Since a) 77-92 and b) 77-94 pillars were reported failed (Section 5.6), and c) 77-90 suffered structural failure (Section 5.7.2), the empirical methods will be applied to these three cases.

5.7.3.1 Estimation of Pillar Load by the Extraction Ratio Formula

The stress can be calculated for each pillar, using the following relationship:

$$\sigma_p = \sigma_1 . N$$

where:

N = Extraction number (Figures 32, 33, 34)

σ_p = Average pillar stress

$$N = \frac{\text{Sum of 1/2 strike length of each Adjacent stopes + strike length of pillar}}{\text{Strike Length of Pillar}}$$

σ_1 = 17.24 MPa (360 KPSF) (Section 5.3.4)

A) <u>77-90 Pillar Failure Geometry</u> (Figure 32)

Pillar	N	σ_1 (MPa)	σ_p (MPa)
77-90	3.4	17.24	58.48
77-92	2.1	17.24	36.20
77-94	1.9	17.24	32.76

B) 77-92 Pillar Failure Geometry (Figure 33)

Pillar	N	σ_1 (MPa)	σ_p (MPa)
77-90	--------F A I L E D -----------		
77-92	3.1	17.24	53.44
77-94	1.9	17.24	32.76

C) 77-94 Pillar Failure Geometry (Figure 34)

Pillar	N	σ_1 (MPa)	σ_p (MPa)
77-90	--------F A I L E D ------------		
77-92	-- Failed and Recovered -------		
77-94	6.3	17.24	108.61

5.7.3.2 Estimation of Pillar Strength; Hoek's Method

The pillar strength may be estimated using the curves developed by Hoek & Brown (1980)[3] (Figure 35). The pillar material was classified by Golder Associates (1981)[12] as a good quality rock mass ($Q \simeq 20$), and the uniaxial compressive strength is:

$$\sigma_c = 176.5 \text{ MPa } (25598 \text{ psi})$$

A) 77-90 Pillar Failure Geometry

Pillar	W/H	Pillar Strength/σ_c	Pillar Strength (MPa)
77-90	1.0	0.3	52.95
77-92	0.75	0.25	44.13
77-94	0.75	0.25	44.13

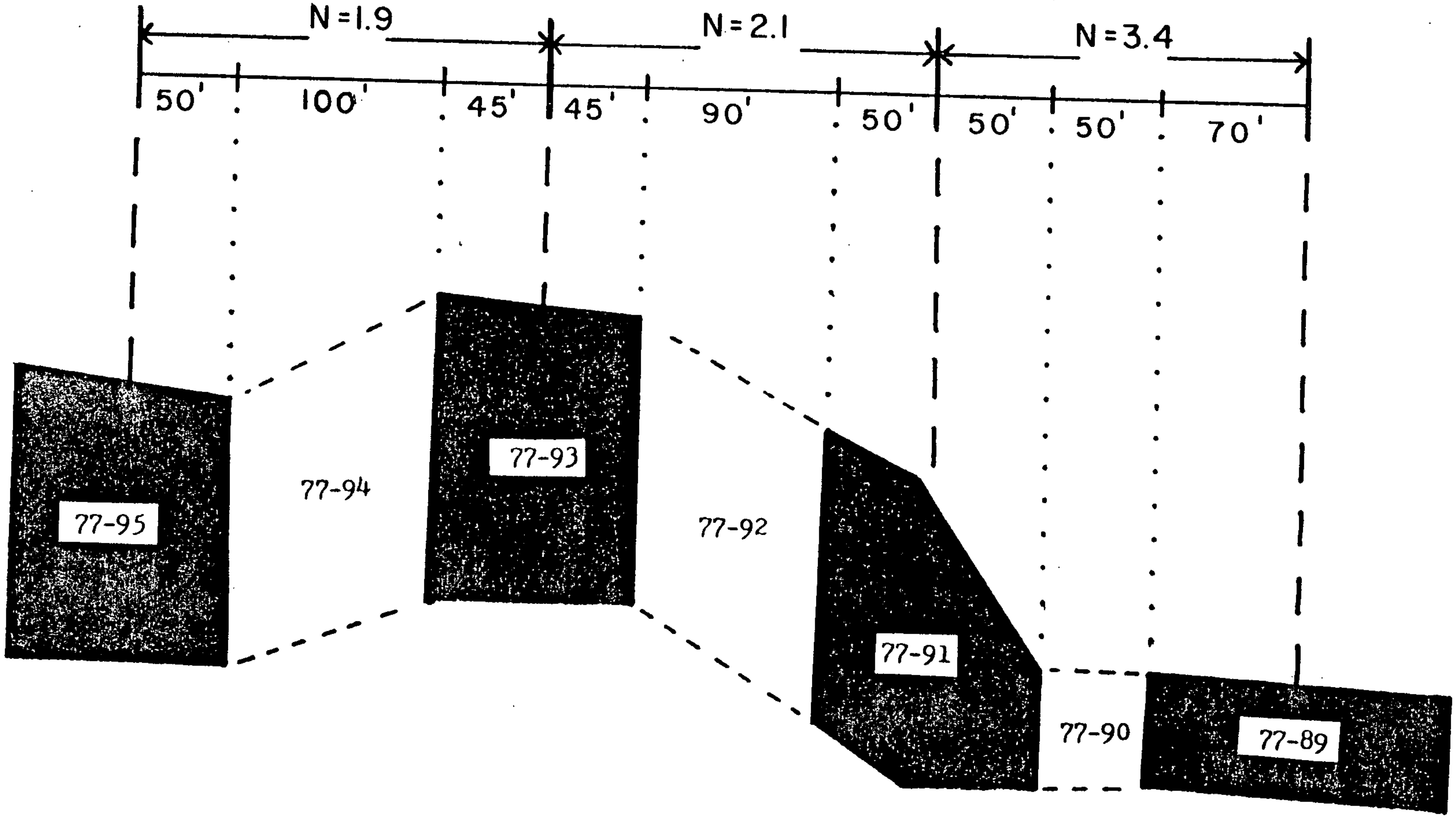

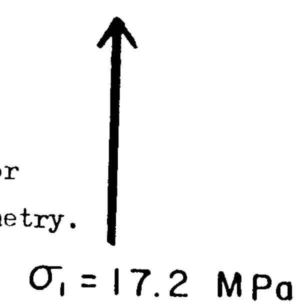

FIGURE 32 Pillars Extraction Numbers for the 77-90 Pillar Failure Geometry.

PLAN VIEW

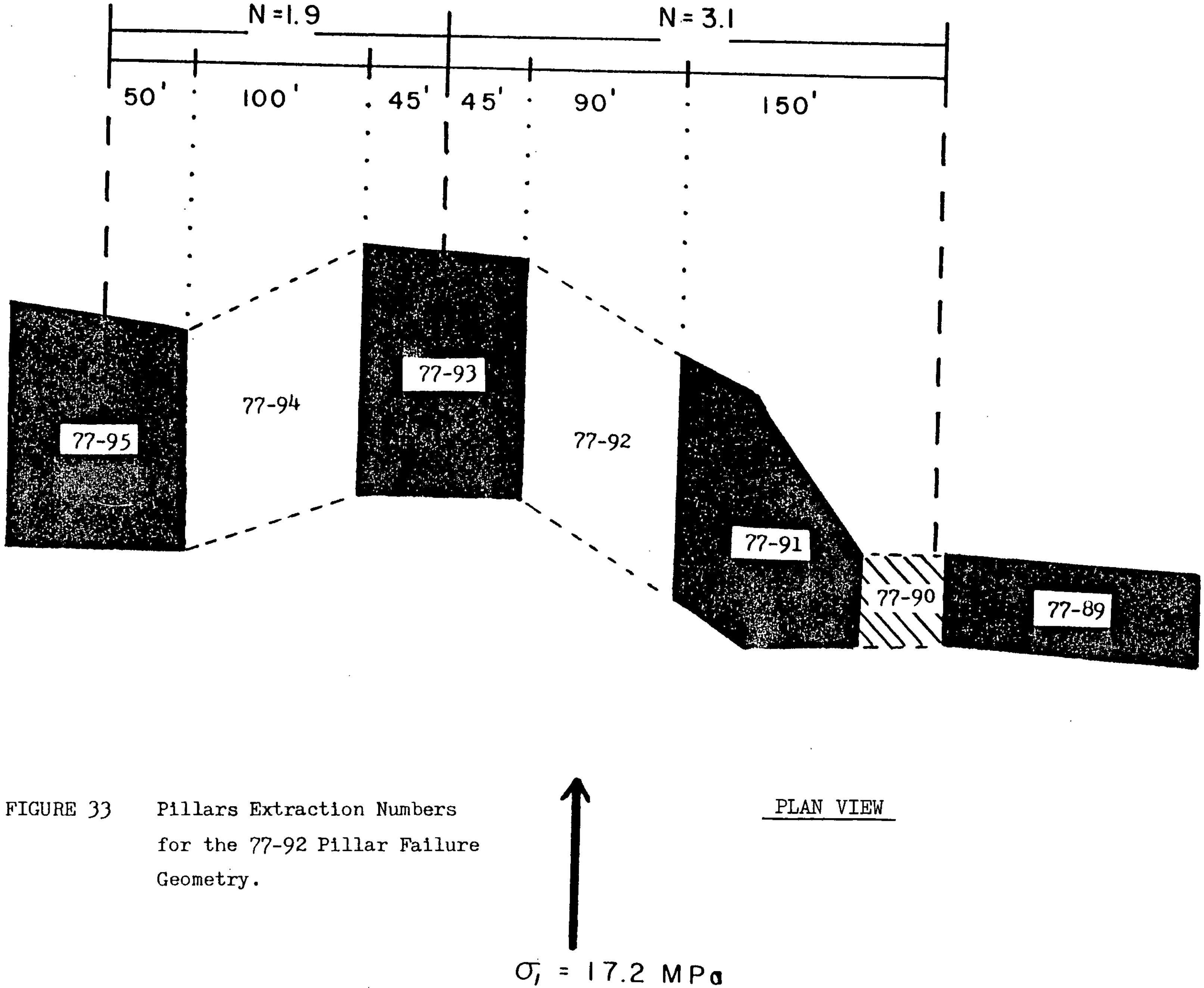

FIGURE 33 Pillars Extraction Numbers for the 77-92 Pillar Failure Geometry.

PLAN VIEW

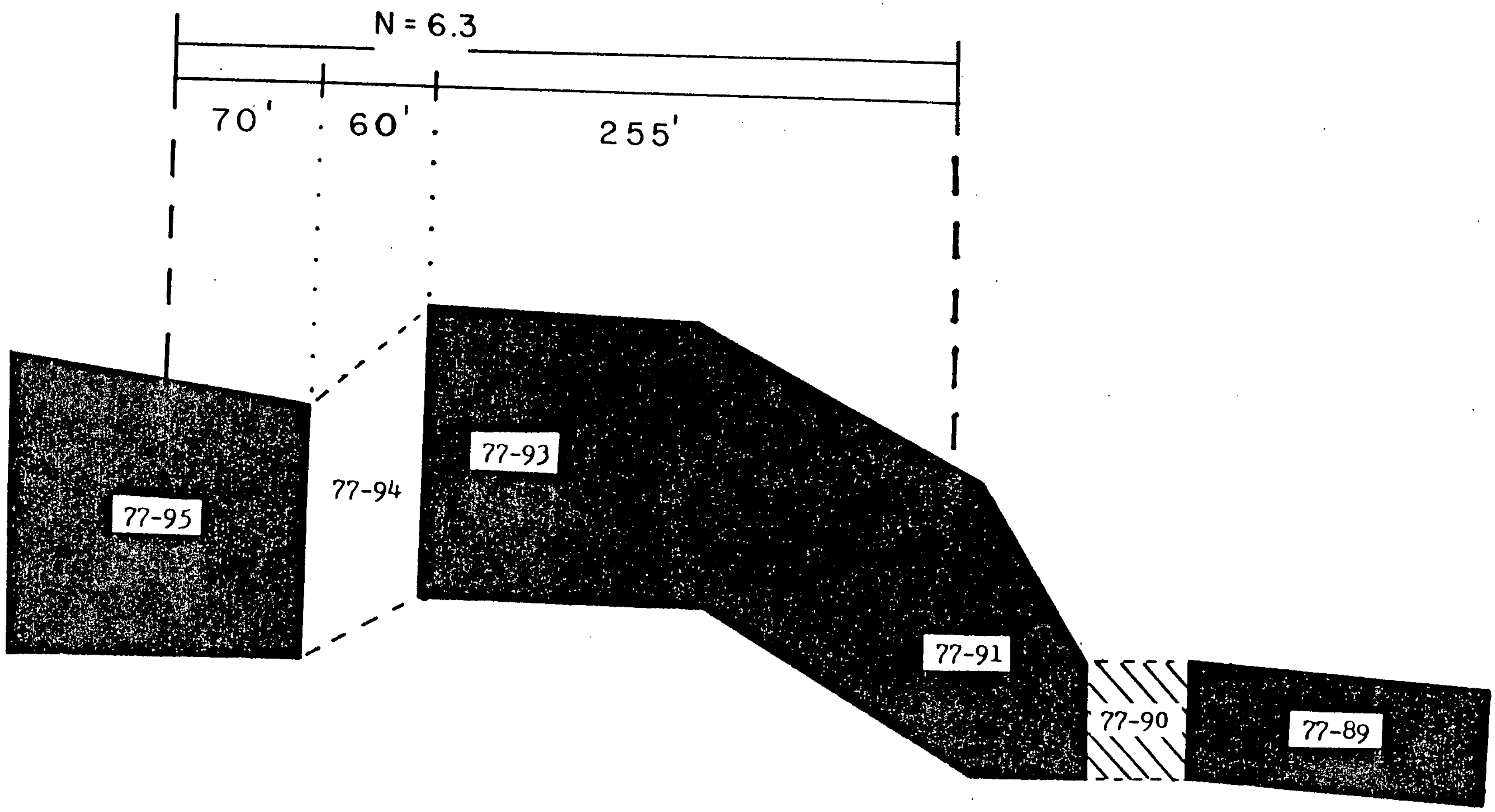

FIGURE 34 Pillars Extraction Numbers for the 77-94 Pillar Failure Geometry.

PLAN VIEW

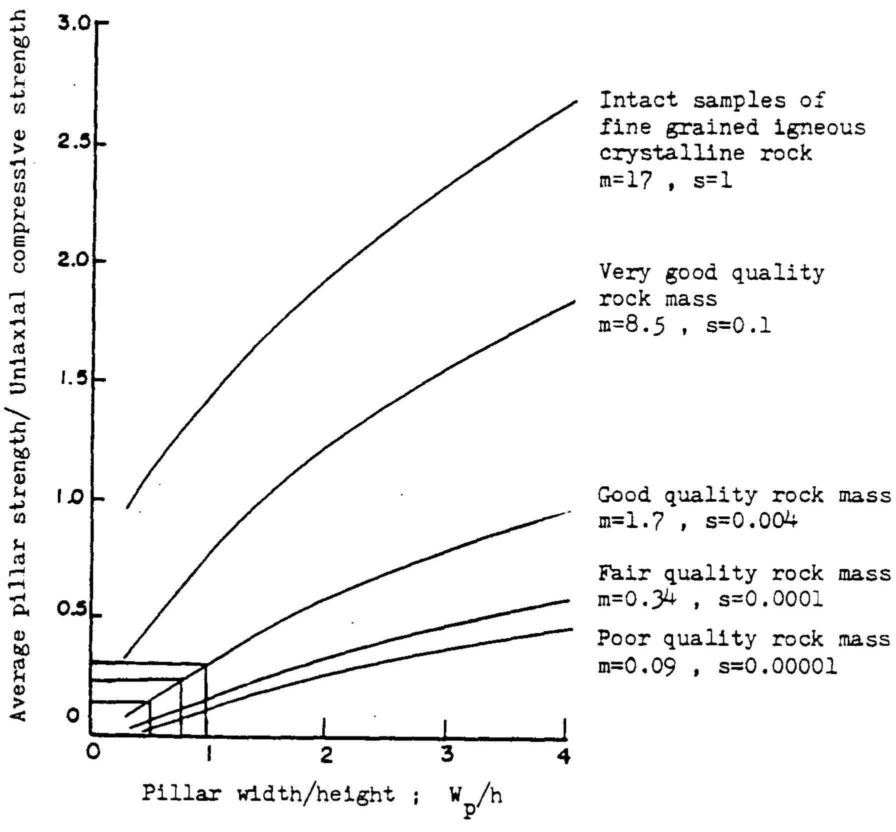

FIGURE 35 The Effect of the Width to Height Ratio on Average Pillar Strength.

B) 77-92 Pillar Failure Geometry

Pillar	W/H	Pillar Strength/σ_c	Pillar Strength (MPa)
77-90	------------F A I L E D ---------------------		
77-92	0.75	0.25	44.13
77-94	0.75	0.25	44.13

C) 77-94 Pillar Failure Geometry

Pillar	W/H	Pillar Strength/σ_c	Pillar Strength (MPa)
77-90	------------F A I L E D ----------------------		
77-92	-----FAILED AND RECOVERED --------------------		
77-94	0.5	0.15	26.48

5.7.4 Theoretical Methods

It was stated in Chapter 3 that the theoretical methods are useful for better understanding the mechanism involved in pillar design.

However, the complexity and the great amount of data required make them impractical, difficult to apply, and inaccurate. Thus, no theoretical methods have been used for the Heath Steele case history analysis.

5.7.5 Phase 5. Computer Methods

The computer stress analysis program used was "BITEM", a two-dimensional boundary element program developed by the C.S.I.R.O. This program has been modified and adapted to the U.B.C. main frame I.B.M. computer by R. Pakalnis. Again, the three situations modelled were the pillar failure geometries of 77-90, 77-92 and 77-94. The pillar stress is taken as the average value of 30 nodal stresses distributed within each pillar.

N.B. The stress units of the computer output are in kilo pounds per square foot (KPSF). Figures 36, 37, 38.

A) 77-90 Pillar Failure Geometry (Figure 36)

Pillar	σ_p Average Pillar Stress	
77-90	43.09 MPa	900 (KPSF)
77-92	27.77 MPa	580 (KPSF)
77-94	28.73 MPa	600 (KPSF)

B) 77-92 Pillar Failure Geometry (Figure 37)

Pillar	σ_p Average Pillar Stress	
77-90	----Failed -----------	
77-92	38.30 MPa	800 (KPSF)
77-94	32.85 MPa	687 (KPSF)

C) 77-94 Pillar Failure Geometry (Figure 38)

Pillar	σ_p Average Pillar Stress	
77-90	----Failed -----------	
77-92	----Recovered---------	
77-94	57.46 MPa	1200 (KPSF)

PLAN VIEW

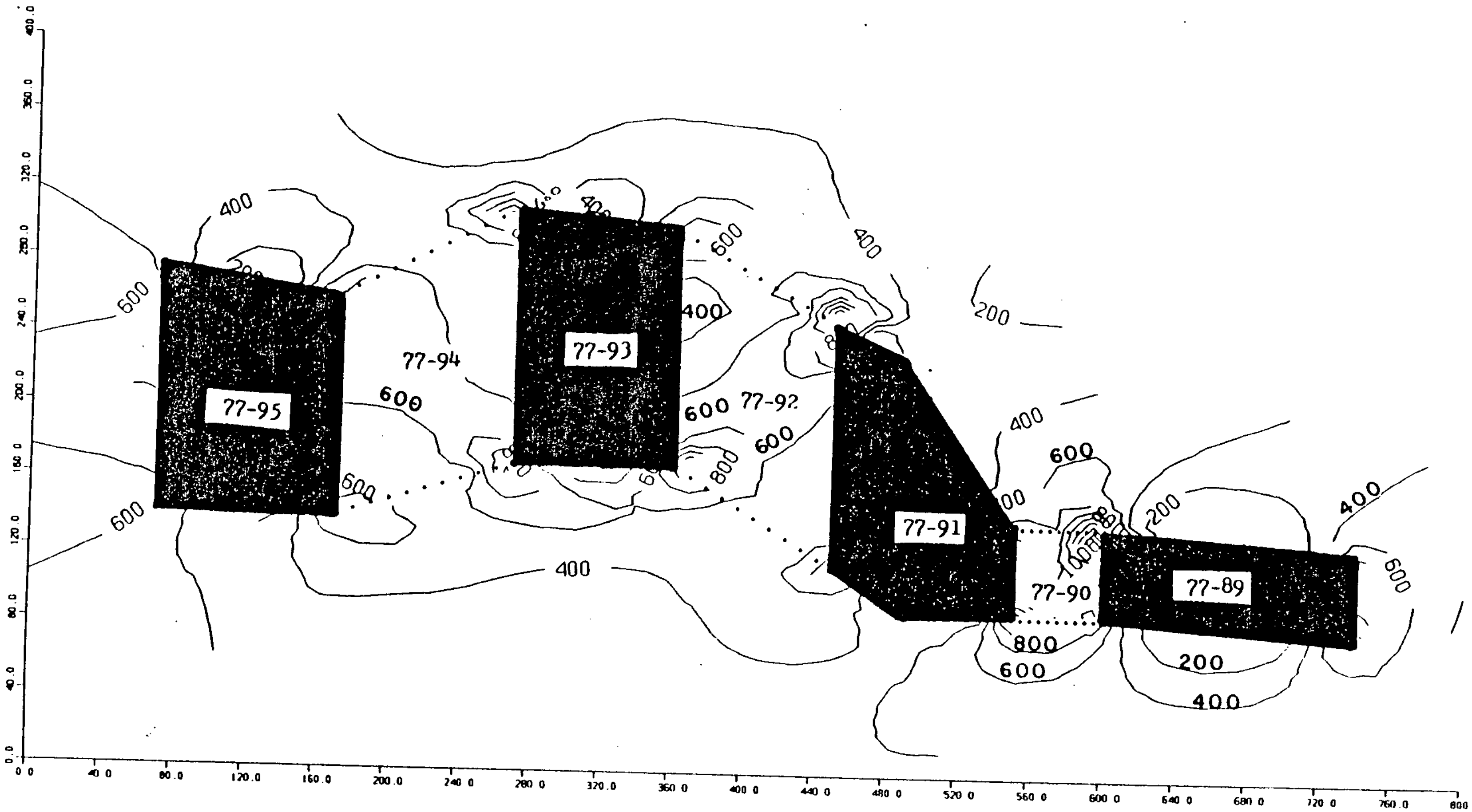

FIGURE 36 Computer Output of the 77-90 Pillar Failure Geometry. Principal Major Stress Contour.

PLAN VIEW

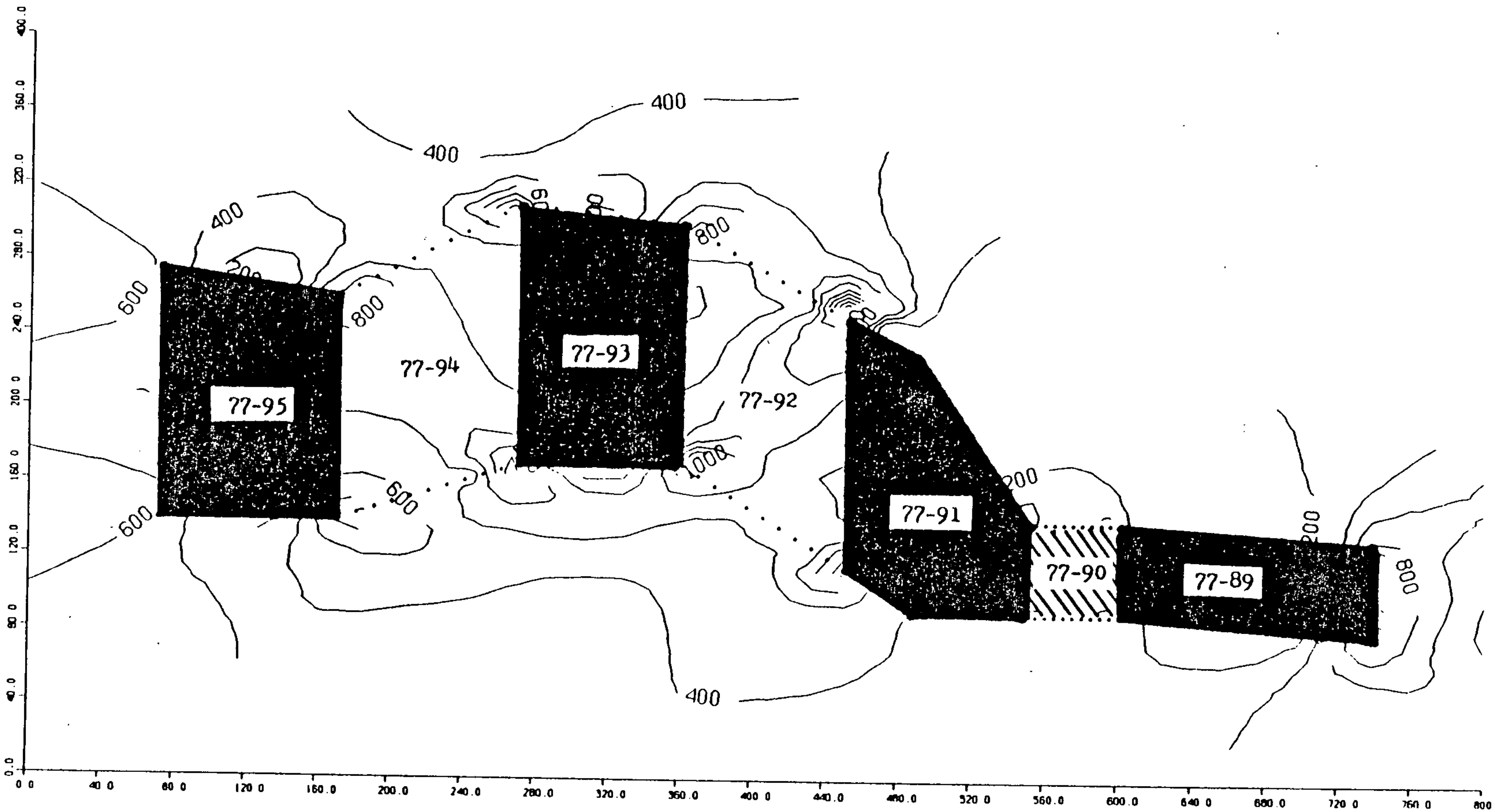

FIGURE 37 Computer Output of the 77-92 Pillar Failure Geometry. Principal Major Stress Contour.

PLAN VIEW

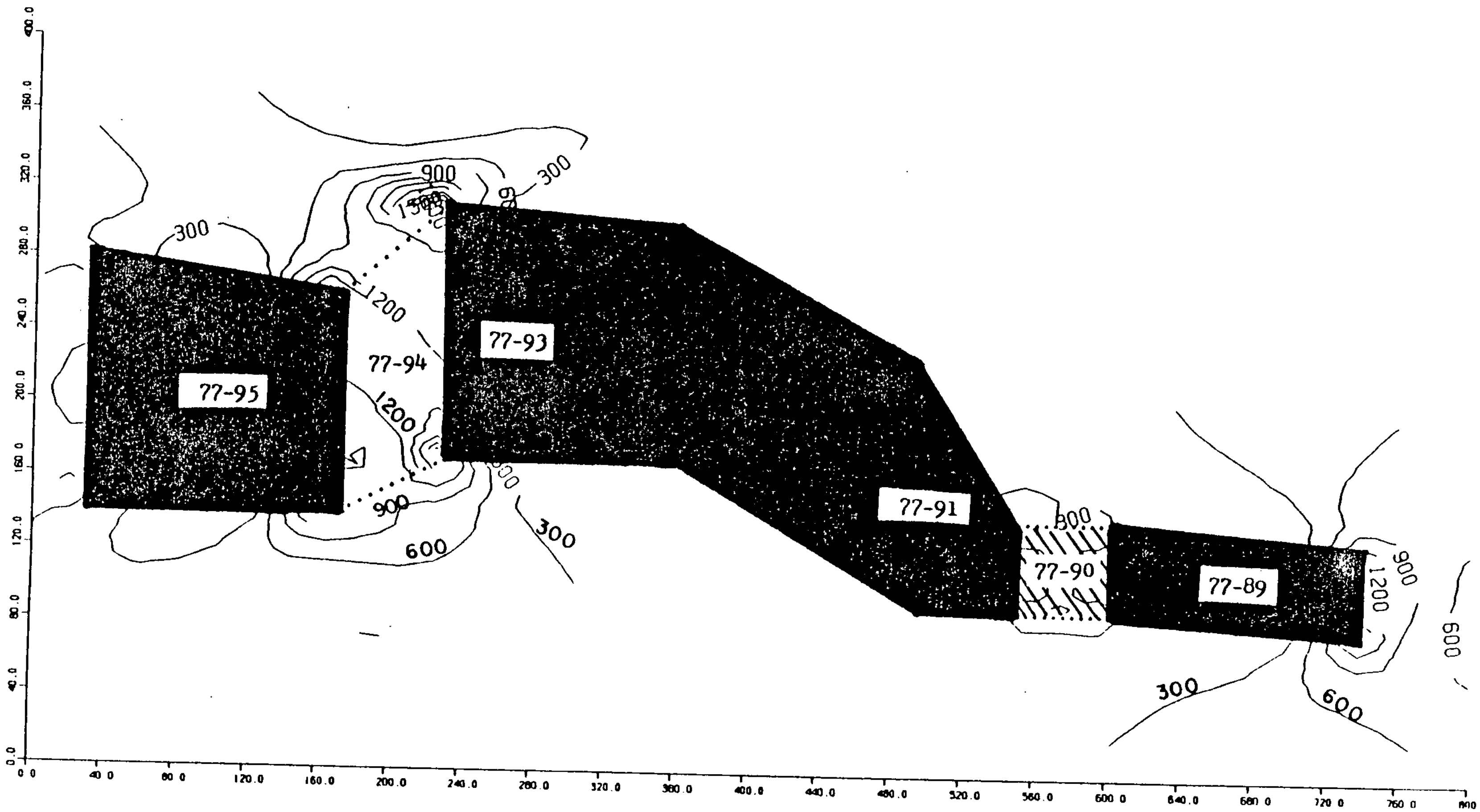

FIGURE 38 Computer Output of the 77-94 Pillar Failure Geometry. Principal Major Stress Contour.

5.8 Discussion of the Results

Before discussing the rock mechanics results of A) 77-90, B) 77-92 and C) 77-94 pillar failures, the required assumptions must be reviewed.

1. The virgin stress was estimated from measurements at Brunswick Mining and Smelting.
2. For every pillar failure case reported, stopes and pillars' dimensions were assessed.

For each situation the pillar loads were calculated using two different methods, tributary area and computer simulation. The results of both methods corroborate very well (Table 11). The pillar strengths were estimated using Hoek and Brown (1980)[3] curves. A so-called "safety factor" which is the ratio of the pillar strength over the pillar load at a given time was also calculated. A safety factor of 1 means that the load acting on the pillar equals its ultimate strength and failure is imminent.

The failure history can then be reconstructed using Table 11:

A) <u>77-90 Pillar Failure Geometry</u> (Nov. 1977)

The first pillar to collapse was 77-90 (S.F. = 1.04) (November, 1977). The failure was not documented, probably because it was progressive, non-violent, and caused by sliding along the S_3 fracture (Figures 30, 31).

B) <u>77-92 Pillar Failure Geometry</u> (Nov. 1977)

After the 77-90 pillar partially lost its bearing capability, a part of the load was redistributed causing the 77-92 pillar to fail. (S.F. = 0.96).

C) <u>77-94 Pillar Failure Geometry</u> (Sept. 1978)

According to the actual geometry of the panel, Table 11 shows that the 77-94 pillar had previously failed. (S.F. = 0.46).

TABLE 11

HEATH STEELE PILLAR ANALYSIS RESULTS

Pillar	Extraction Number	Tributary Area (MPa)	Computer Stress (MPa)	Mean (1) Stress (MPa)	W/H (Plan View)	Pillar Strength (MPa)	Safety Factor	Extraction Ratio %	Remarks
A) 77-90 Pillar Failure Geometry, November 1977									
77-90	3.4	58.48	43.09	50.79	1	52.95	1.04	71	Pillar Slide
77-92	2.1	36.20	27.77	31.99	0.75	44.13	1.38	51	Stable
77-94	1.9	32.76	28.73	30.75	0.75	44.13	1.44	49	Stable
B) 77-92 Pillar Failure Geometry, November 1977									
77-90	----------	----------	----------	----------	F A I L E D	----------	----------	----------	----------
77-92	3.1	53.44	38.30	45.87	0.75	44.13	0.96	68	Pillar Failed
77-94	1.9	32.76	32.85	32.80	0.75	44.13	1.35	49	Stable
C) Actual Geometry (77-94 Failed) September 1978									
77-90	----------	----------	----------	----------	F A I L E D	----------	----------	----------	----------
77-92	----------	----------	----------	----------	F A I L E D and R E C O V E R E D	----------	----------	----------	----------
77-94	6.3	108.61 (2)	57.46	57.46	0.5	26.48	0.46	84	Pillar Failed

(1) The mean stress is assumed to be the average value of computer and tributary area methods. Only the computer stress was considered in C) Actual Geometry 77-94, the tributary area value was judged irrelevant.

(2) Irrelevant value.

These conclusions from the results of computational design methods (Table 11) are in agreement with the instability events experienced at Heath Steele (according to the documentation) which suggest that the dimensions and stress values assumed were correct.

Furthermore, Allcott and Archibald (1981)[11] attempted to elaborate an empirical design curve for Heath Steele pillars, using bore-hole extensometers' deformation records. From the observations of failing pillars, four stages of deterioration have been defined.

Stage 1: Intact Pillar

No visible or audible evidence of movement, although extensometers may register convergence.

Stage 2: Pillar Failure

Sound and movement are observed. It is still possible to drill, blast and muck the pillar material, but at times continuous movement will prevent this. After stabilization recovery can begin again.

Stage 3: Post Failure

Manageable recovery is no longer possible, but stabilization will allow retention of fill or through access.

Stage 4:

No reliable use remains in the pillar.

Combining these qualitative observations with the deformation versus extraction number curve (Figure 39), Allcott and Archibald notices that pillars failed at Stage 2 of deterioration corresponding to an extraction number (N) of 3.3. Table 11 results confirm Allcott and Archibald's observations.

Figure 40 depicts a plot of the extraction number versus safety factor, showing that pillar failure (S.F. = 1) effectively occurred around an extraction number N = 3.3.

FIGURE 39 Pillar Deformation Versus Extraction Number. (After Allcott & Archibald) 11

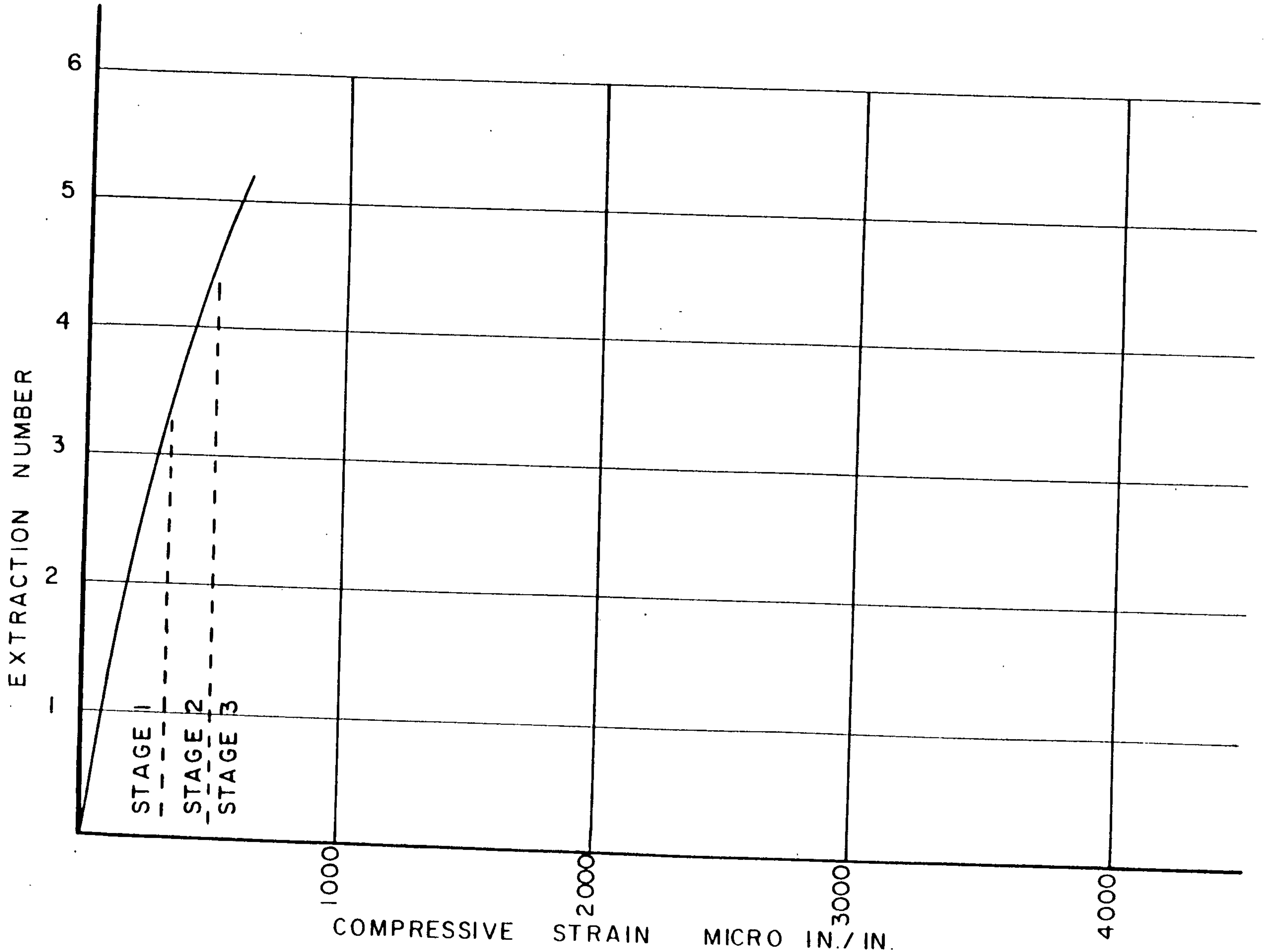

FIGURE 40 EXTRACTION NUMBER VS SAFETY FACTOR

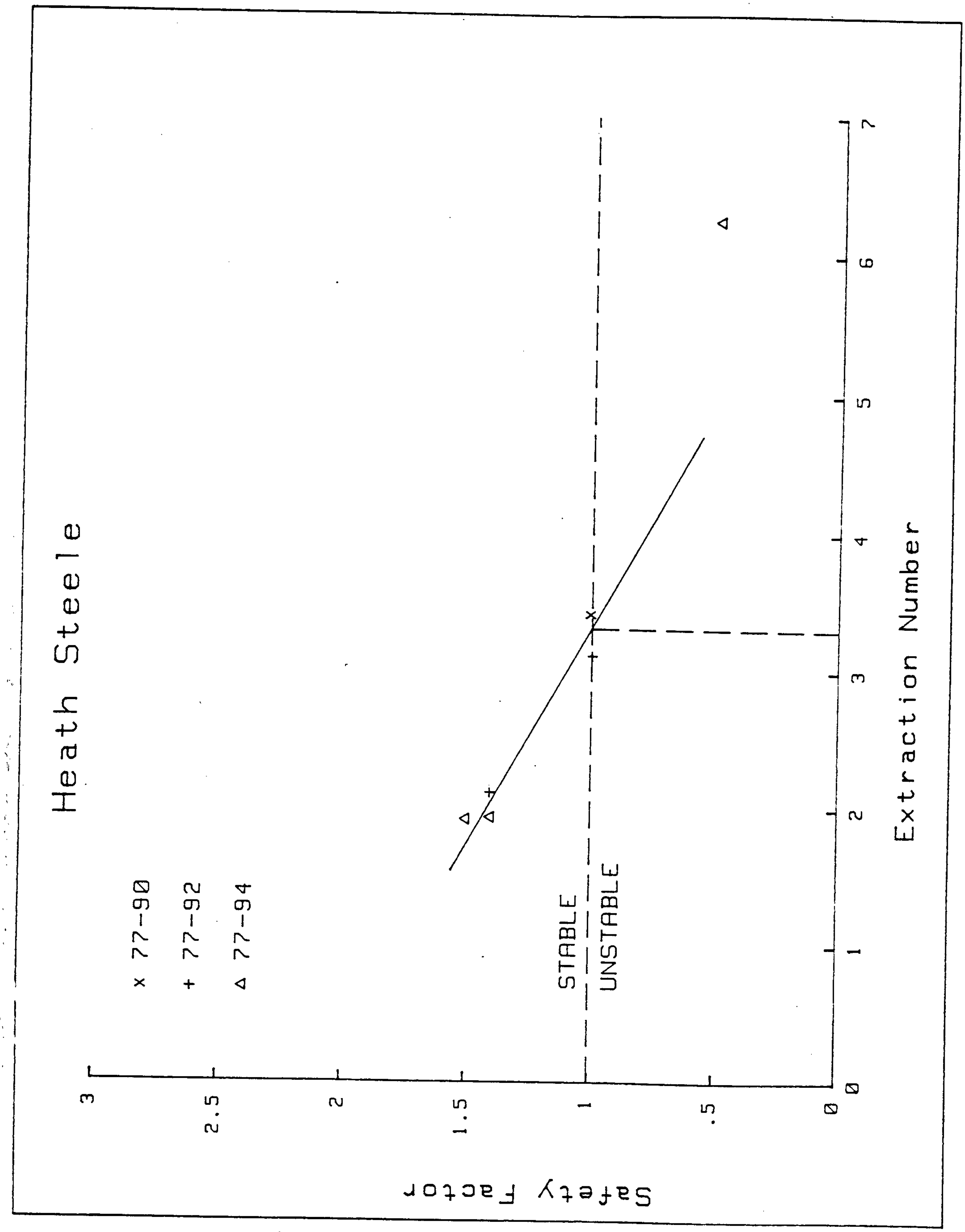

Because several methods have been employed which give substantially the same result as the Allcott and Archibald experiments, the pillar design procedure and imput parameters can be considered calibrated at Heath Steele.

Finally, Figure 41 represents a plot of the local extraction ratio "e" versus the safety factor of each pillar at different stages of extraction. Note:

$$e = 100 \times \frac{(\text{sum of 1/2 width of each adjacent stope})}{\text{sum of 1/2 width of each adjacent stope} + \text{the width of pillar}}$$

Figure 41 indicates that at 300 m (1000 ft.) depth, instability is initiated when the extraction ratio exceeds 65 - 70%. Thus it is suggested to limit primary extraction to 65% at this depth. This will minimize stability problems that have caused extra support costs, mining delay, loss of ore reserves as well as making pillars recovery very difficult.

Curves similar to Figure 41 should be developed in order to determine the optimum percentage of extraction at different depths (600 m, 900 m,1200 m) at Heath Steele.

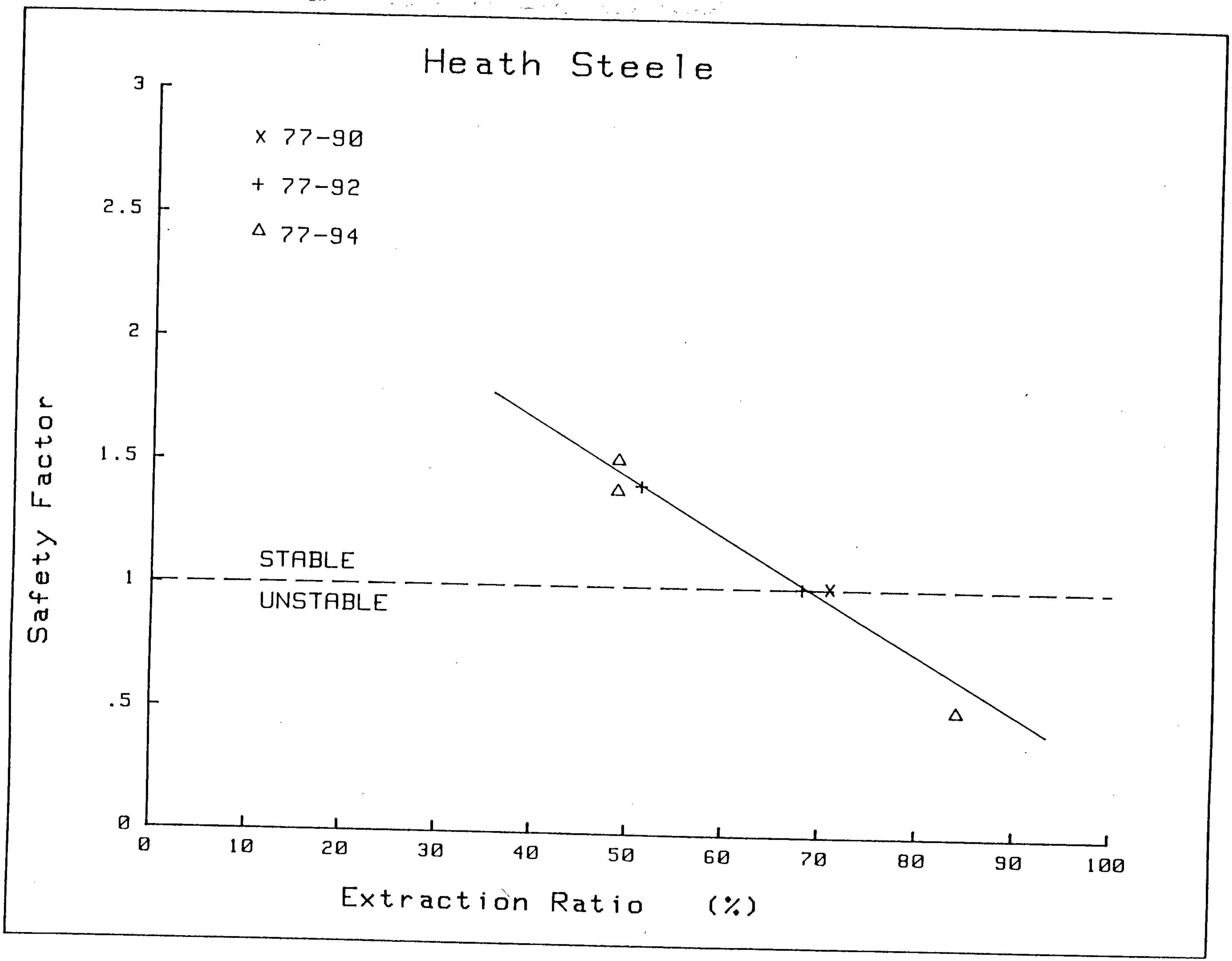

FIGURE 41 EXTRACTION RATIO VS SAFETY FACTOR

CHAPTER 6

GECO CASE HISTORY ANALYSIS

6.1 Geology (after Bray (1967)[10]

6.1.1 Regional Geology

The Manitouwadge Syncline is a broad easterly plunging syncline of metasediments and metavolcanics. The surrounding country rocks are mainly granite and trondjemite, showing evidence of granitization near the syncline in the form of gneissic granite and migmatite.

The metasediments consist of quartz feldspar biotite gneiss, quartzites with varying amounts of biotite, iron formation and the quartz muscovite group which is host rock for the Geco orebody.

The metavolcanics are older than the metasediments and contain hornblende schist and amphibolite.

6.1.2 Mine Geology

The Geco orebody is located in the sericite schist group of rocks on the south limb of the Manitouwadge syncline. A large open drag fold approximately 760 m. (2500 ft) long and plunging 35° to the east is the host structure for the orebody.

The orebody is large and steeply dipping with a core of massive sulphides and a surrounding envelope of disseminated sulphides. The major economic minerals mined are chalcopyrite, sphalerite and galena.

A cross-Section from south to north across the Geco orebody shows the following sequence of formations:

- grey gneiss (including biotitic quartzite)
- sericite schist (containing the orebody)
- biotite amphibole garnet gneiss.

Intrusive into these formations are basic dykes, granite, pegmatite dykes and diabase dykes. Table 12 and Figure 42 summarize the Geco geology.

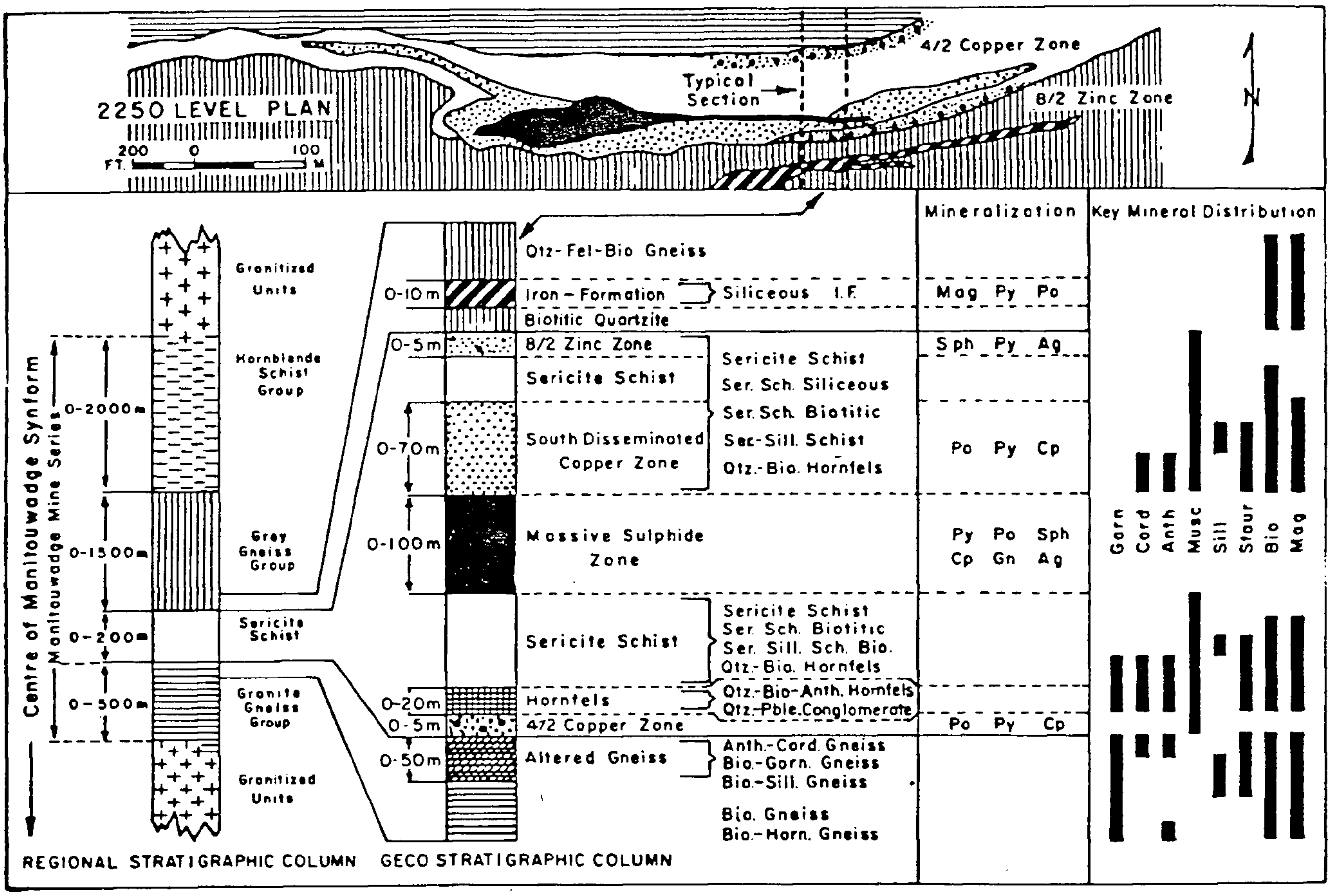

FIGURE 42 Schematic Stratigraphic Columns Illustrating Generalized Relationships of Sulphide Zones, Geco Mine

The orebody forms a tabular mass lying more or less vertical, and raking eastward at from 20 degrees to 30 degrees. In cross-section, the orebody has the shape of an onion, with the bulbous bottom portions conforming to the curvature of the dragfold.

The massive sulphide core (orebody) varies in thickness from a few inches to about 45 m. (150 ft) with an average thickness of 12 m. (40 ft).

The grade of the ore averages better than 2 percent copper, 4 percent zinc and 2 oz/ton of silver.

TABLE 12

SUMMARY OF THE GEOLOGY AT GECO

Rock Types

GRANITE GROUP

1) Granite
2) Biotite garnet gneiss
3) Biotite sillimanite gneiss

SERICITE SCHIST GROUP

4) Quartz biotite anthophyllite hornfels
5) Sericite schist
6) Chalcopyrite
7) Sphalerite
8) Pyrite, pyrrhotite, sphalerite, chalcopyrite

GREY GNEISS GROUP

9) Quartz feldspar biotite gneiss
10) Biotitic quartzite
11) Iron formation

INTRUSIVES

12) Diabase
13) Pegmatite
14) Quartz diorite

6.1.3 Structural Geology

Multiple folding in the ore bearing schist, transverse to the main dragfolding, aggravates the ground weaknesses induced by faulting and fracturing, and in some places increases the tendency to slough.

As a rule, the pegmatite dykes are not mineralized, except where in contact with the massive sulphide core. They are, therefore, rarely included in a stope, but may form a stope wall. Since the large dykes (over 1 m. (3 ft) are extensively fractured, they tend to slab and break off when exposed over a wide surface. By contrast, the massive sulphide core of the orebody is relatively free from joints and fractures and has been observed standing solidly over horizontal lengths of 21 m. (70 ft) and vertical heights of over 90 m. (300 ft).

Ground control in the mine is also adversely affected, especially when we have folding in the area of the top of the stope. Because the folded schist is not standing vertically, it will not support the same vertical load as steeply dipping schists. This problem will increase with depth and more intense folding.

Thus, the structural weaknesses of the ore-bearing formation consists of:

(a) foliation and some faulting in an east-west direction.

(b) jointing and minor faulting in a north-south direction.

(c) weak contacts along diabase dykes and along quartz diorite/quartz muscovite schist contacts.

(d) regional, drag and cross folding.

(e) irregular fractures and joints in broad pegmatites.

- Jointing. After Golder Associates (1981)[12]

There are two steeply dipping joint sets. The first one has an east-west strike, the other strikes roughly north-south. No persistent near horizontal joint sets were found at Geco.

6.2 Mining Method and Underground Structure Dimension

The principal mining method at Geco is blasthole mining, but where the ore narrows to 8 m (25 ft) or less it is necessary to use a cut and fill method.

The rocks at Geco are not the best suited to open stoping as they will slough readily when exposed in the large areas of a stope wall. Geco have overcome the problem by modifying the mining method by introducing fill as the ore is drawn; thus keeping the stopes full at all times. To prevent instability in the backs, they are cable bolted using tensioned 9.1 m long cable bolts.

The orebody is divided into blocks for convenience of identification. Mining started in 1957 at the west extremity of the orebody (Block A) and progressed eastward.

A typical block is about 150 to 180 m. (500 ft) high, consisting of three 21 m (70 ft) wide primary stopes separated by two 37 m (120 ft) pillars and flanked by two boundary pillars 46 m (150 ft) wide. The primary stopes are mined first and drawn under rock fill and then consolidated with the introduction of cemented hydraulic fill. The two 37 m (120 ft) pillars are then removed between the filled stopes. These pillars are usually mined in 60 to 90 m (200 to 300 ft) lifts to minimize dilution from the fill walls.

To date most of the primary stoping is completed and pillar mining contributes a large share of the production.

6.3 Rock Mechanics Data

6.3.1 Rock Strength Parameters

- Density Ore Massive Sulphide = 5334 kg/m^3 (333 lbs/ft^3)
  Disseminated ore = 3204 kg/m^3 (200 lbs/ft^3)

Waste: Hanging wall = 2666 kg/m^3 (166 lbs/ft^3)
and footwall

- Elastic Modulus and Poisson's Ratio

Ore: E = 103425 MPa (15M. psi)

ν = 0.31

Waste: E = 105340 MPa*

ν = 0.2*

6.3.2 Laboratory Test. After Golder Associates (1981)[12]

- Unconfined Compressive Strength

Ore: σ_c = 100 MPa

	(psi)	(MPa)
Quartz biotite schist	6,000	41
Quartzite	23,000	159
Sericite	4,000	27.5
Quartz biotite gneiss	7,500	52
Quartz biotite muscovite	15,500	107
Hornblende biotite qtz schist	7,000	48
Granite (gneiss)	9,000	62
Granite biotite	10,500	72
Quartz biotite	27,000	186
Quartz muscovite schists	13,500	93

- Tensile Strength Ore: σ_t = 8 MPa

- Triaxial Compressive Strength

Ore: σ_3 = 6.9 MPa σ_1 = 150 MPa

σ_3 = 13.8 MPa σ_1 = 232 MPa

σ_3 = 20.7 MPa σ_1 = 307 MPa

* Estimated from the typical value of Elastic Modulus and Poisson Ratio for gneiss rock. (Hoek and Brown (1980)[3], p. 262,267)

6.3.3 Rock Mass Classification

The footwall, hanging wall and orebody rocks were classified by Golder Associates (1980)[12].

2850 level 28-54.5 Cross-cut

Sericite Schist (Two Ratings)

	NGI	NGI
RQD	60	50
Jn	4	6
Jr	2	2
Ja	0.75	1.0
Jw	1.0	1.0
SRF	2	1.0
Q =	20	16.7

	CSIR
Intact Strength	7
RQD	13
Spacing of Joints	10
Condition of Joints	12
Ground Water	10
	52

Hangingwall Ramp Below 2850 L

Biotite Garnet Gneiss (Two Ratings)

	NGI	NGI
RQD	60	90
Jn	6	4
Jr	3	2
Ja	1	0.75
Jw	1	1
SRF	2.5	1
Q =	12	60

	CSIR
Intact Strength	7
RQD	13
Spacing of Joints	20
Condition of Joints	6
Ground Water	10
	56

1850 Level Hangingwall Drift off 18-36 Cross-Cut

Hangingwall Schist (Two Ratings)

	NGI	NGI
RQD	90	60
Jn	2	3
Jr	1	1.5
Ja	1	2
Jw	1	1
SRF	2.5	2.5
Q	18	6

	CSIR
Intact Strength	7
RQD	20
Spacing of Joints	20
Condition of Joints	6
Ground Water	10
	63

1850 Level in Footwall of 19-40 Pillar Stope

Footwall Sericite Schist (Two Ratings)

	NGI	NGI
RQD	75	60
Jn	4	3
Jr	1	2
Ja	4	2
Jw	1	1
SRF	2.5	2.5
Q =	1.9	8

	CSIR
Intact Strength	7
RQD	13
Spacing of Joints	20
Condition of Joints	6
Ground Water	10
	56

1850 Level 44 Pillar Sill

Massive Sulphides (Two Ratings)

	NGI	NGI
RQD	60	80
Jn	9	9
Jr	1	1.5
Ja	2.0	0.75
Jw	1.0	1
SRF	4.0	1
Q =	0.8	17.8

	CSIR
Intact Strength	7
RQD	13
Spacing of Joints	20
Condition of Joints	6
Ground Water	10
	56

2250 Level 27-61 Stope

Footwall Schist (Two Ratings)

	NGI	NGI
RQD	50	70
Jn	4	3
Jr	1	2
Ja	4	3
SRF	2.5	2.5
Q =	1.3	6.2

	CSIR
Intact Strength	7
RQD	13
Spacing of Joints	20
Condition of Joints	6
Ground Water	10
	56

Values obtained for the footwall schist varied from 1.3 to 20 (poor to good rock); 0.8 to 17 for the sulphides (poor to good rock); and from 6 to 60 for the hangingwall schist (poor to very good rock).

6.3.4 Virgin Stress

No stress measurements have been performed at Geco. However, the vertical stress is assumed to be equal to the weight of the overlying rock.

$$\sigma_V = \gamma h = \sigma_3$$

where: γ = density of the waste rock

h = depth below surface

The major principal stress σ_1 and intermediate principal stress σ_2, both horizontal, are estimated using two different sources, described in Appendix B. The mean values are:

$$\sigma_1 = 2.6\ \sigma_V$$

$$\sigma_2 = 2.1\ \sigma_V$$

(see Figure 43)

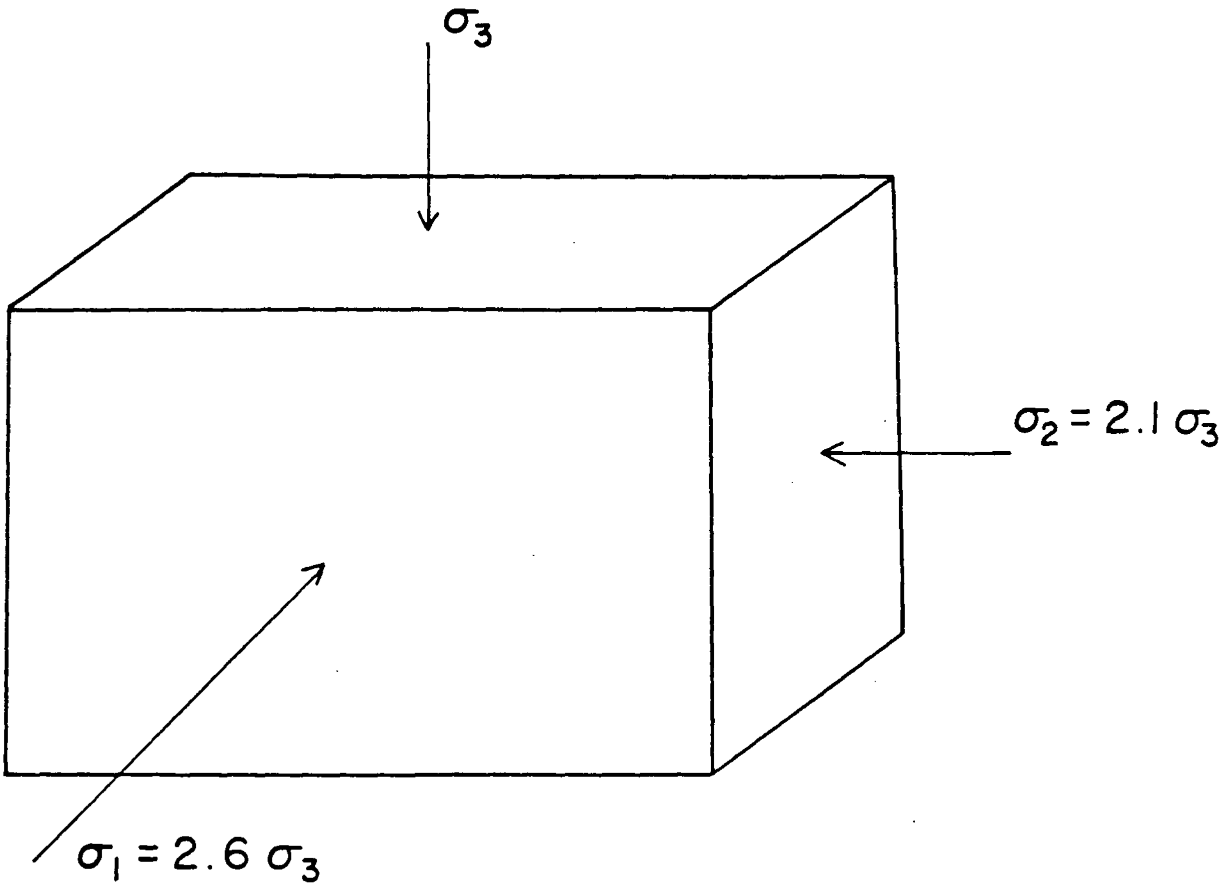

FIGURE 43 Assumed Stress Regime at Geco

At 215 metres (700 ft) depth, the stress regime is:

$$\sigma_3 = \gamma . h = 2660 \text{ kg/m}^3 \times 215 \text{ m} = 5.72 \times 10^5 \text{ kg/m}^2$$

$$\sigma_3 = 5.72 \times 10^5 \text{ kg/m}^2 = 5.66 \text{ MPa (116 KPSF)}$$

$$\sigma_1 = 2.6\sigma_3 = 14.73 \text{ MPa (302 KPSF)}$$

$$\sigma_2 = 2.1\sigma_3 = 11.89 \text{ MPa (244 KPSF)}$$

6.4 Pillar Characteristics

Six stopes with intervening pillars were used to mine the 'B' Block. The stopes' initial dimensions were 21m. (70 ft) long and up to 150 m. (500 ft) high (vertical).

The rib pillars, designed to be recovered at a subsequent stage, were 37 m. (12 ft) long.

The pillar material is a massive sulphide which is relatively strong (σ_C = 100 MPa).

6.5 Mining Sequence

The investigated area consists of four open stopes (10 - 19.5, 10 - 21, 10 - 22 and 10 - 23.5) separated by three rib pillars (10 - 20, 10 - 21.5, 10 - 23). The depth varies from 150 m. (500 ft) to 320 m. (1050 ft) below surface, and a 215 m (700 ft) depth was assumed for calculation purposes.

Figure 44 is a longitudinal view of the stope/pillar/panel layout and Tables 13 to 16 summarize the mining sequence.

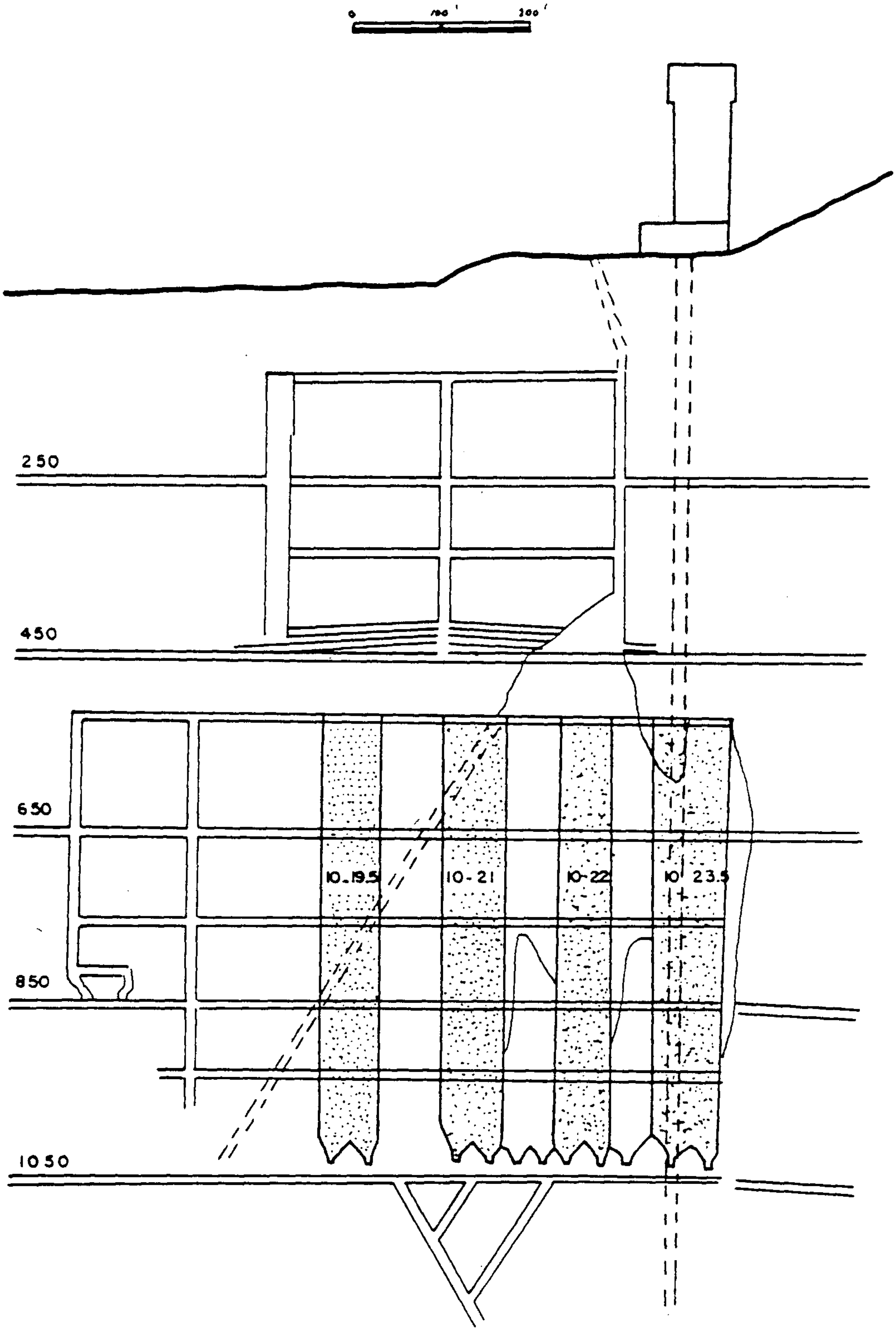

FIGURE 44 Longitudinal View of the Investigated Area at Geco.

TABLE 13

STOPE 10-19.5 MINING SEQUENCE

Date	Broken Ore	Total Tons	Remarks
Feb. 1960	8,050		
March 1960	20,150	28,200	
April 1960	60,030	88,230	
Sept. 1960	10,000	98,230	
Oct. 1960	105,630	203,860	
Dec. 1960	6,820	210,680	
Sept. 1961	?	?	Sloughing

TABLE 14

STOPE 10-21 MINING SEQUENCE

Date	Broken Ore	Total Tons	Remarks
Nov. 1959	3,890	3,890	
Dec. 1959	11,500	15,390	
Jan. 1960	19,903	35,293	
Feb. 1960	18,678	53,971	
Mar. 1960	67,027	120,998	
Sept. 1960	20,000	140,998	
Oct. 1960	5,000	145,998	Small amount of sloughing from north side
Nov. 1960	15,230	161,228	10-21.5 pillar cracked
Dec. 1960	32,390	193,618	10-21.5 pillar failed
10-21 SOUTH STOPE			
March 1961	27,677	221,295	
April 1961	3,100	224,395	
May 1961	9,400	233,795	
June 1961	24,640	258,435	

TABLE 15

STOPE 10-22 MINING SEQUENCE

Date	Broken Ore	Total Tons	Remarks
March 1960	1,930	1,930	
June 1960	3,250	5,180	
July 1960	7,500	12,680	
August 1960	15,000	27,680	
Sept. 1960	48,350	76,030	
Nov. 1960	15,000	91,030	
Dec. 1960	35,800	126,830	10-23 Pillar Failed
March 1961	3,074	129,904	'Caving'
10-22 SOUTH STOPE			
June 1961	6,990	136,894	
July, 1961	14,340	151,234	
August 1961	50,220	201,454	
10-21.5 PILLAR			
Dec. 1960	50,000	50,000	
April 1961	10,000	60,000	10-21.5 pillar recovery
June 1961	30,000	90,000	

TABLE 16

STOPE 10-23.5 MINING SEQUENCE

Date	Broken Ore	Total Tons	Remarks
May 1960	250	250	
June 1960	2,285	2,535	
Aug. 1960	10,600	13,135	
Sept. 1960	16,300	29,435	
Oct. 1960	38,945	68,380	
Dec. 1960	19,140	87,520	10-23 Pillar Failed
Jan. 1961	13,550	101,070	
March 1961	12,830	113,900	
May 1961	26,455	140,355	
July 1961	22,619	162,974	
Aug. 1961	407	163,381	Over Break
Sept. 1961	1,395	164,776	Over Break

10-23 PILLAR

Dec. 1960	5,000	5,000	
Feb. 1961	20,000	25,000	
March 1961	17,889	42,889	
April 1961	10,000	52,889	

6.6 Failure Histories and Pillar Geometries

(After Bray 1967)[10]

- October, 1960:	sloughing started in 10-21 stope.
- November, 1960:	extensive cracking of: . 10-21.5 pillar . 10-23 pillar
	850 level, major remedial work on: . 10-21.5 pillar
- December, 1960:	10-21.5 pillar collapsed from the 7A to 5A sublevel. (The upper half of the pillar).
	650 level, 10-23 pillar showed extensive sloughing.
- January, 1961:	A full raise was driven to surface to back-fill 10-22 stope.
- March, 1961:	10-22 stope cave to the elevation of the 450 level. The fill raise acted as a slot.
- September, 1961:	The west side of the 10-20.5 pillar suffered sloughing.
- April, 1962:	10-19.5 stope cave to the elevation of 450 level.
- October, 1963:	Caving reached the 250 level cross-cut.

From Figure 45 extraction flowchart, the stope and pillar geometries and dimensions were estimated:

a) when 10-21.5 rib pillar failed, in November, 1960 (Figure 46, Table 17).

b) when 10-23 rib pillar failed, in November, 1960 (Figure 47, Table 18).

c) when 10-20 rib pillar failed, in August, 1961 (Figure 48, Table 19).

This design study will concentrate on these three particular cases, and because the major principal stress is horizontal in the north-south direction, only the plan view needs to be considered.

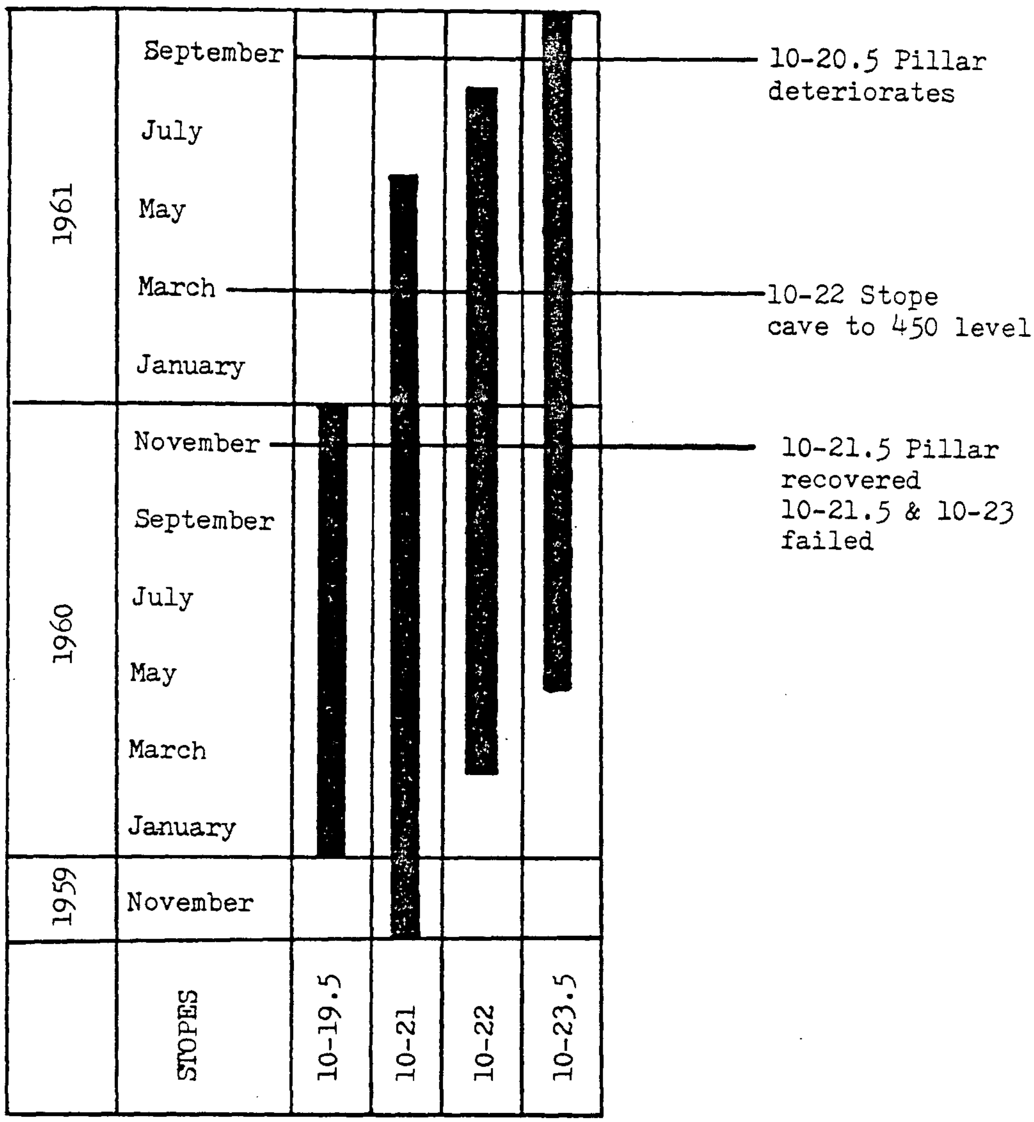

FIGURE 45 Extraction Flowchart of 10-19.5, 10-21, 10-22, and 10-23.5 Stopes

TABLE 17

APPROXIMATE STOPE AND PILLAR DIMENSIONS
WHEN 10-21.5 PILLAR FAILED

(November, 1960)

Stopes	Length	Width	Height
10-19.5	21 m. (70 ft.)	20 m. (65 ft.)	150 m. (500 ft.)
10-21	30 m. (100 ft.)	20 m. (65 ft.)	150 m. (500 ft.)
10-22	21 m. (70 ft.)	17 m. (55 ft.)	150 m. (500 ft.)
10-23.5	24 m. (80 ft.)	14 m. (45 ft.)	150 m. (500 ft.)
Pillars			
10-20	21 m. (70 ft.)	21 m. (70 ft.)	150 m. (500 ft.)
10-21.5	9 m. (30 ft.)	20 m. (65 ft.)	150 m. (500 ft.)
10-23	15 m. (50 ft.)	18 m. (60 ft.)	150 m. (500 ft.)

TABLE 18

APPROXIMATE STOPE AND PILLAR DIMENSIONS WHEN 10-23 PILLAR FAILED
(November, 1960)

Stopes	Length	Width	Height
10-19.5	21 m. (70 ft.)	20 m. (65 ft.)	150 m. (500 ft.)
10-21) 10-22)	61 m. (200 ft.)	18 m. (60 ft.)	150 m. (500 ft.)
10-23.5	24 m. (80 ft.)	14 m. (45 ft.)	150 m. (500 ft.)
Pillars			
10-20	21 m. (70 ft.)	21 m. (70 ft.)	150 m. (500 ft.)
10-21.5	--------------------	F a i l e d	-------------------------
10-23	15 m. (50 ft.)	18 m. (60 ft.)	150 m. (500 ft.)

TABLE 19

APPROXIMATE STOPE AND PILLAR DIMENSIONS WHEN 10-20 PILLAR FAILED
(August, 1961)

Pillars	Length	Width	Height
10-20	15 m. (50 ft.)	30 m. (100 ft.)	150 m. (500 ft.)
10-21.5	--------------------	F a i l e d	------------------------
10-23	--------------------	F a i l e d	-----------------------
Stopes			
10-19.5	24m. (80 ft.)	20 m. (65 ft.)	150 m. (500 ft.)
10-21 10-22 10-23.5	100 m. (333 ft.)	30 m. (100 ft.)	240 m. (80 ft.)

Scale: 1 in. = 100 ft.

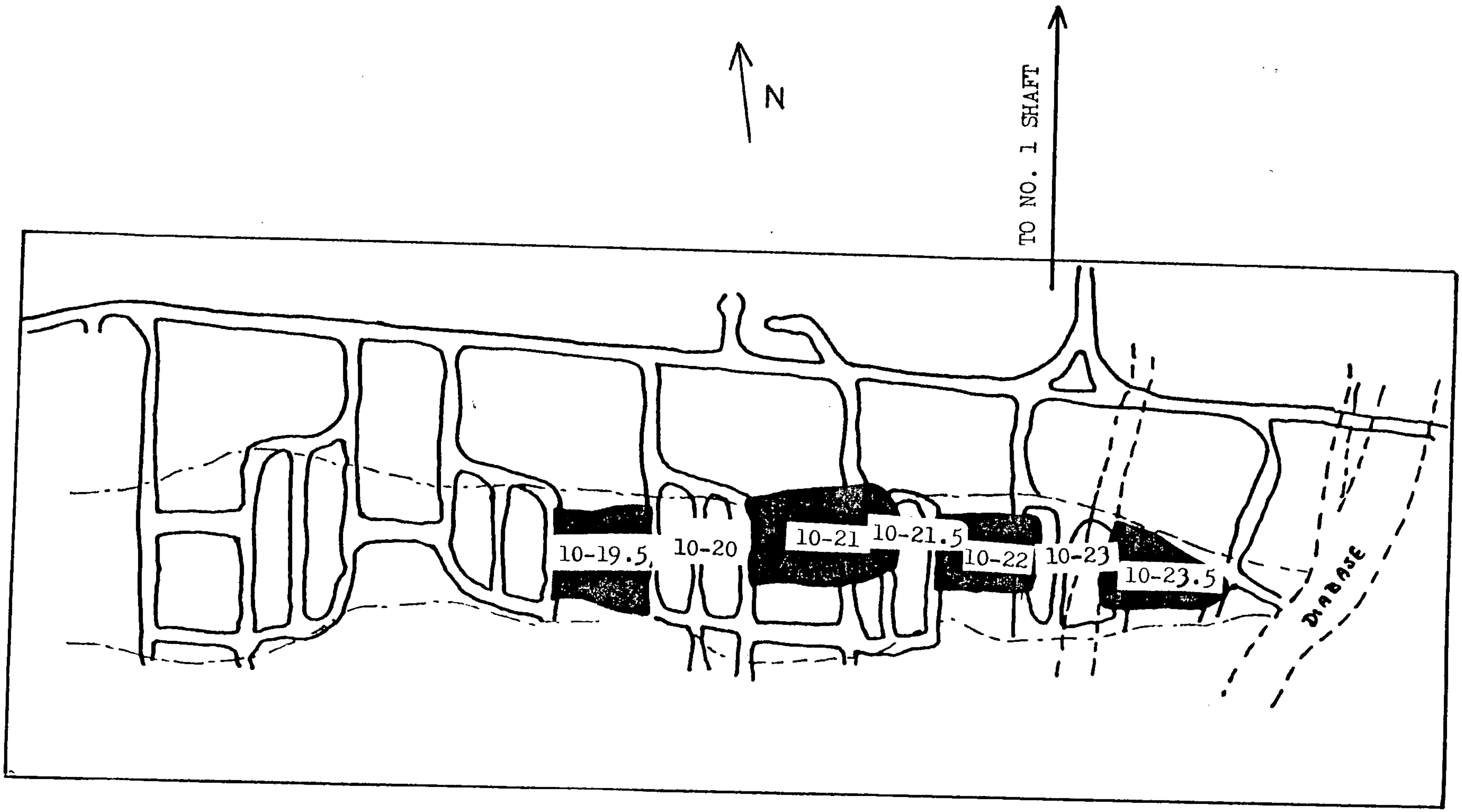

PLAN VIEW

FIGURE 46 Estimated Layout When 10-21.5 Pillar Failed.

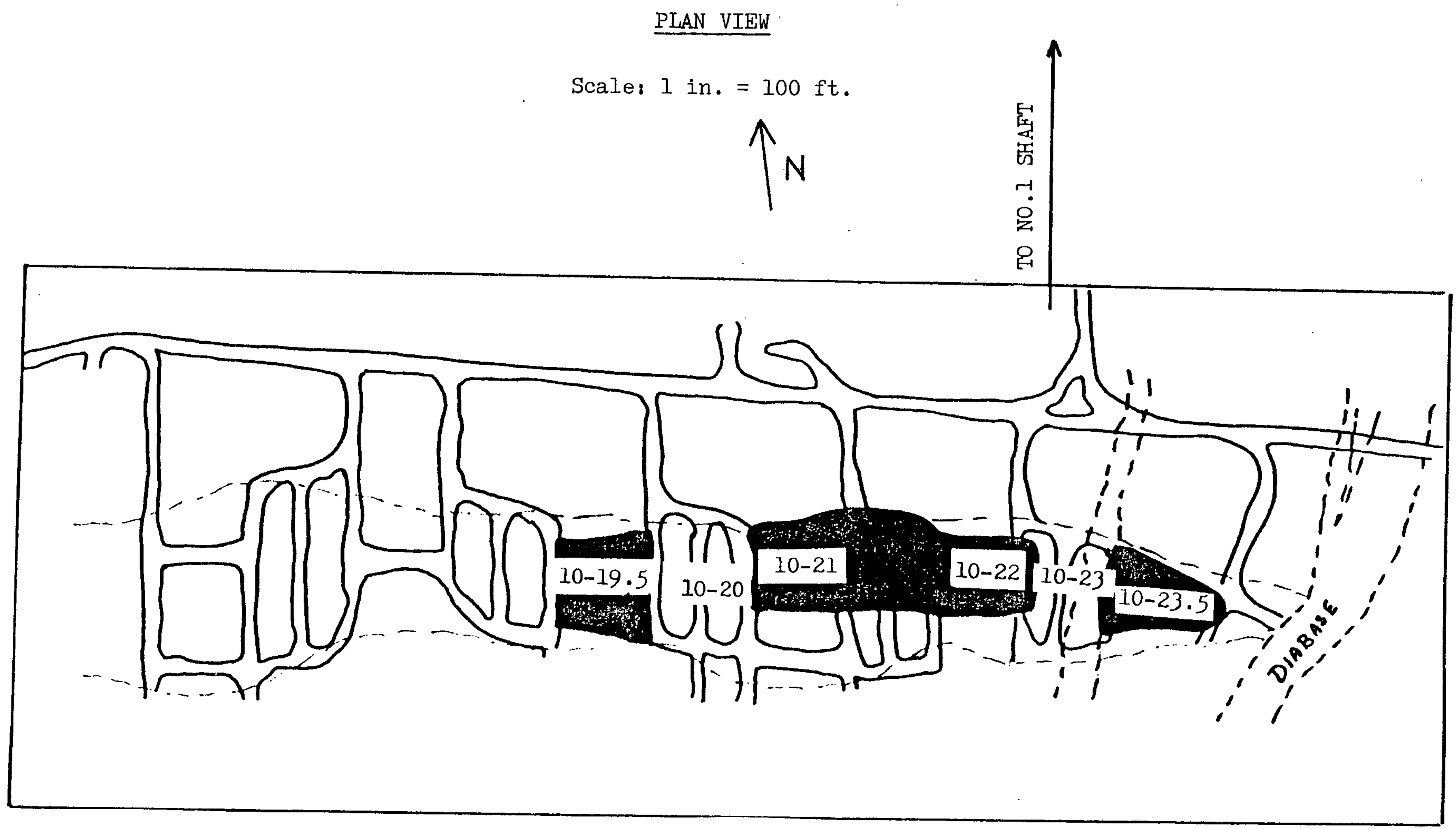

FIGURE 47 Estimated Layout When 10-23 Pillar Failed.

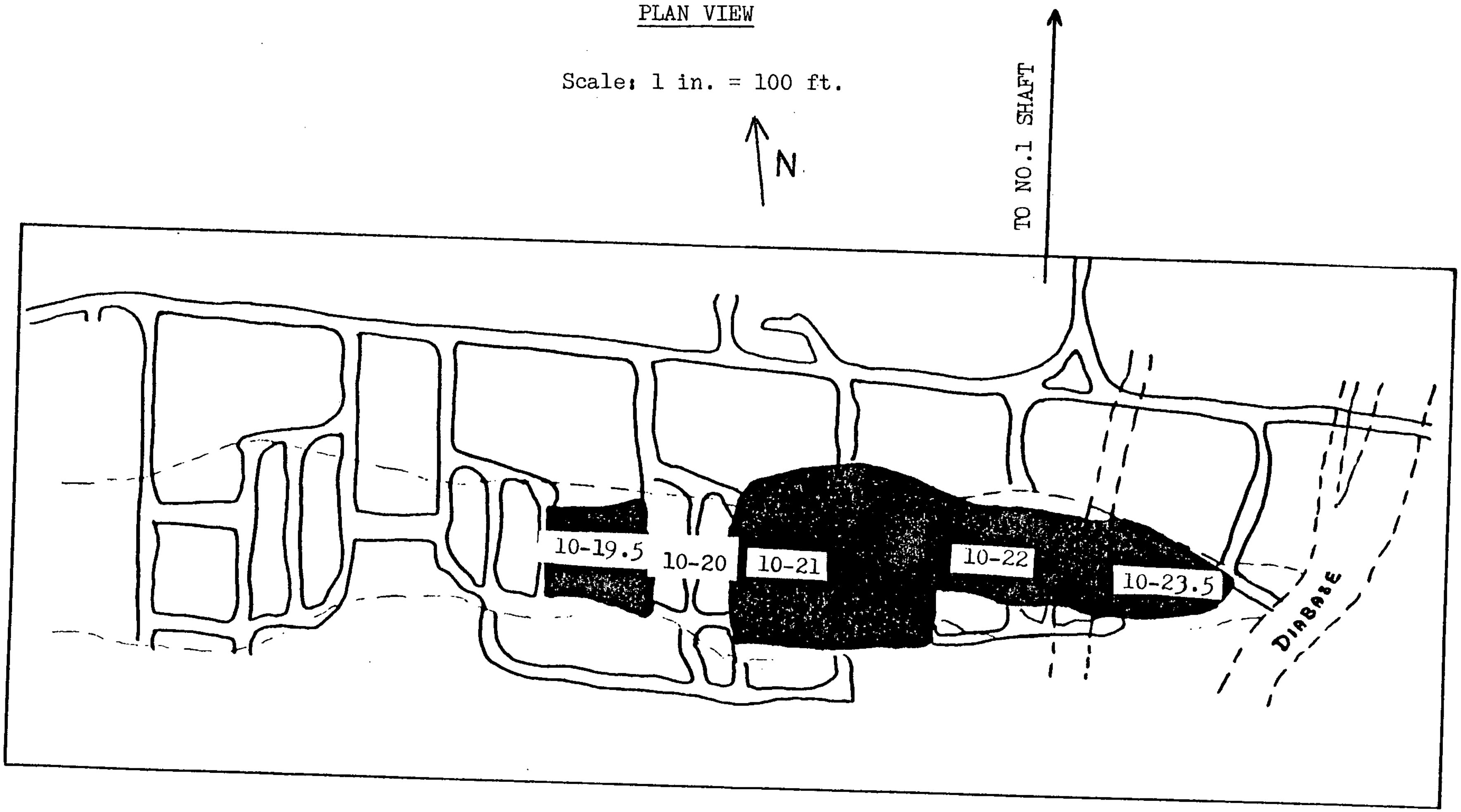

FIGURE 48 Estimated Layout When 10-20 Pillar Failed

6.7 Pillar Design Study

The three rib pillars involved in the present study (10-20, 10-21.5, 10-23) may be classified as "separation pillars' (Category two).

According to the design charts, the following design methods should be applied.

6.7.1 Phase 1. Experience Design

From the description of the mining method (Section 6.2) a typical "block" is mined using three 21 m. (70 ft.) wide primary stopes separated by 37 m. (120 ft.) pillars and flanked by two boundary pillars 46 m. (150 ft.) wide. The primary stopes are mined first and drawn under rock fill and then consolidated with the introduction of hydraulic fill. The two 37 m. (120 ft.) pillars are then removed between the filled stopes.

6.7.2 Phase 2. Pillar Structural Analysis

The rib pillars are located mostly in the massive sulphide core which is relatively free from joints and fractures (Section 6.1.3). Thus, it is believed that the structures (faults, joints and discontinuities) do not play an important role in pillar stability at Geco.

6.7.3 Phase 3. Empirical Methods.

Estimation of pillar load by the extraction ratio formula (Tributary area)

$$\sigma_p = \sigma_1 . N$$

where: N = extraction number

σ_p = average pillar stress

σ_1 = 14.74 MPa (302 KPSF) (Section 6.3.4)

A) 10-21.5 Pillar Failure Geometry (Figure 49)

Pillar	N	σ_1 (MPa)	σ_p (MPa)
10-20	2.4	14.74	35.38
10-21.5	3.8	14.74	56.01
10-23	2.5	14.74	36.85

B) 10-23 Pillar Failure Geometry (Figure 50)

Pillar	N	σ_1 (MPa)	σ_p (MPa)
10-20	2.9	14.74	42.75
10-21.5	-----Failed and Recovered------------		
10-23	3.8	14.74	56.01

C) 10-20 Pillar Failure Geometry (Figure 51)

Pillar	N	σ_1 (MPa)	σ_p (MPa)
10-20	5	14.74	73.70
10-21.5	------Failed and Recovered------------		
10-23	-----------Failed---------------------		

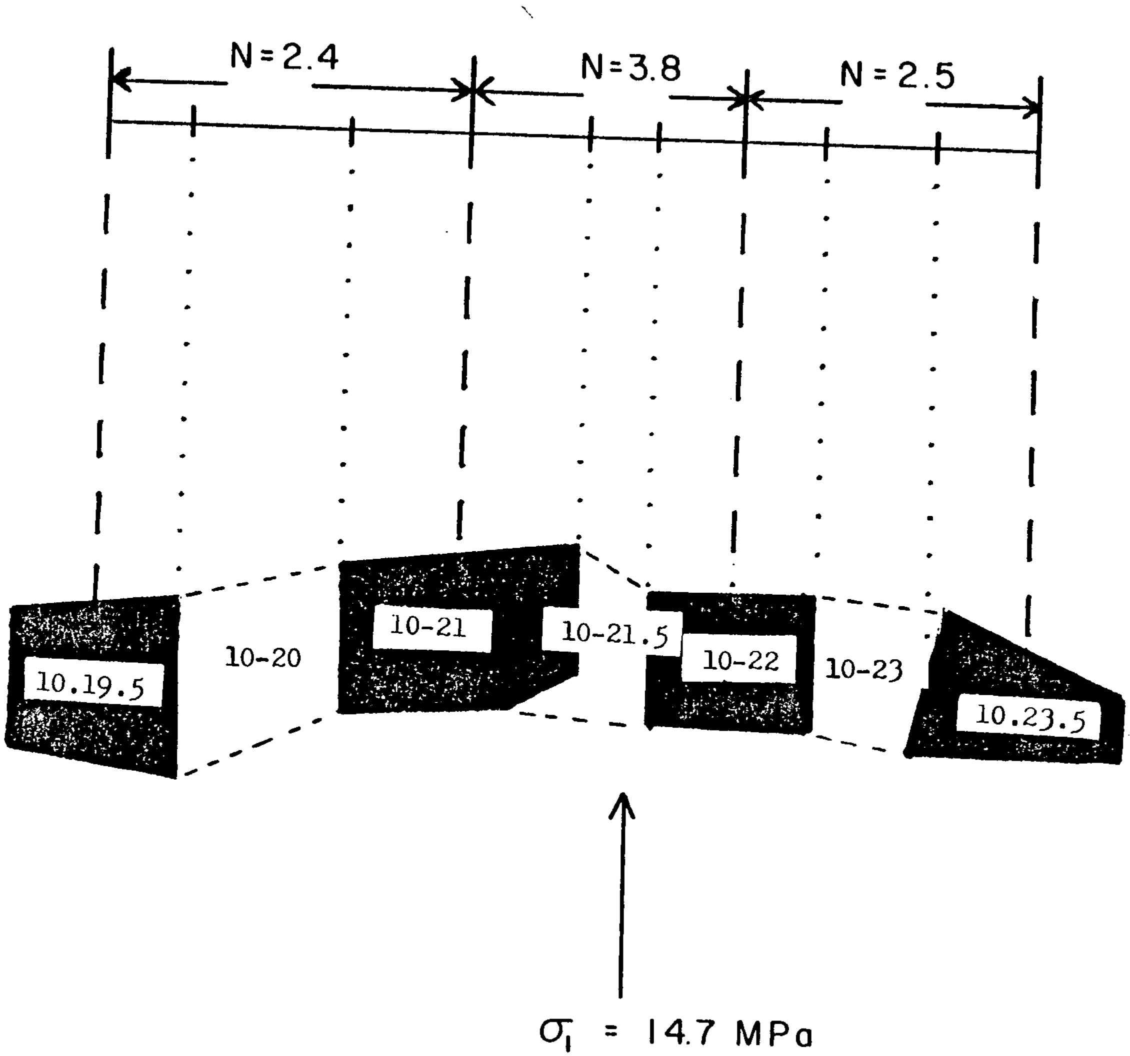

FIGURE 49 Pillars Extraction Numbers for the 10-21.5 Pillar Failure Geometry.

PLAN VIEW

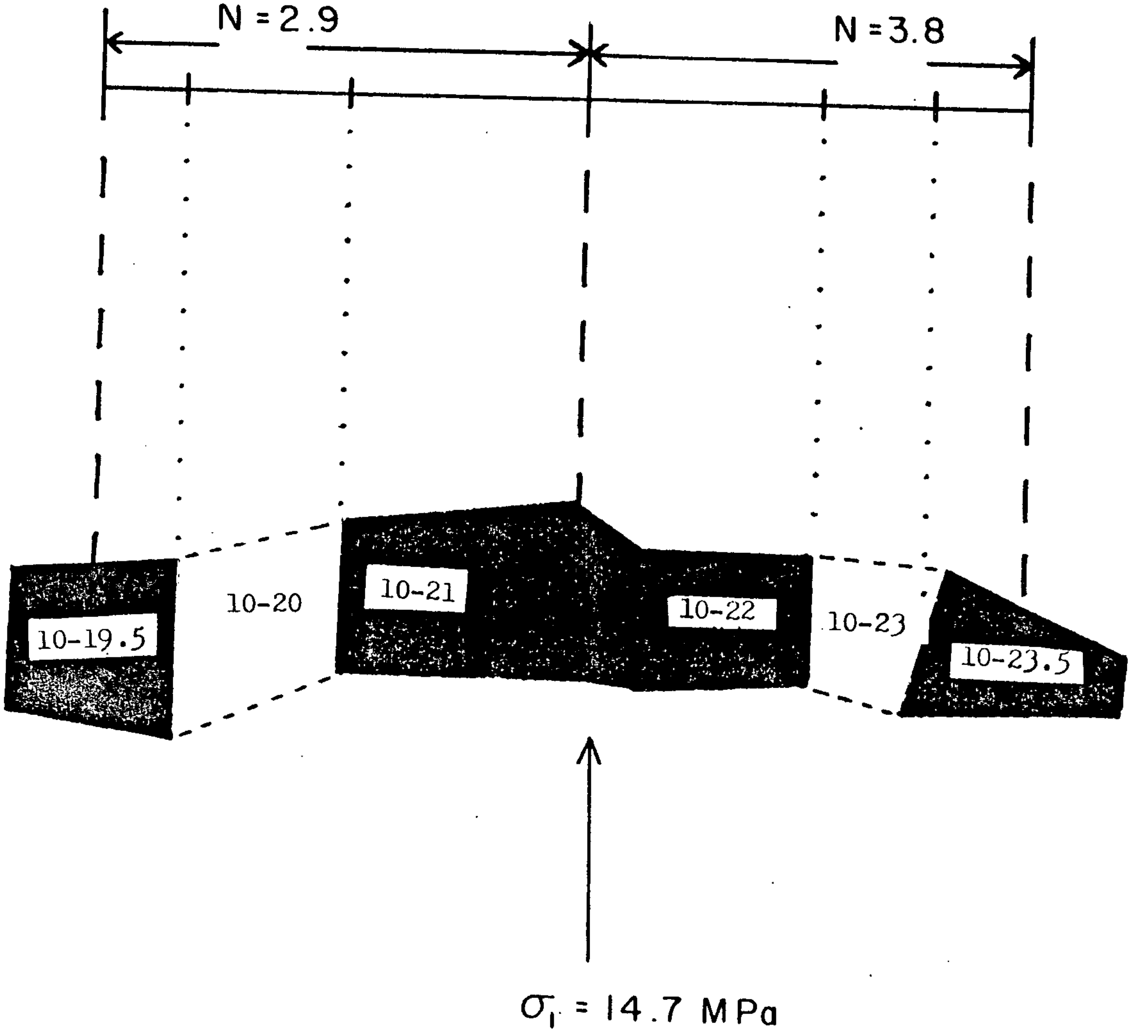

FIGURE 50 Pillars Extraction Numbers for the 10-23 Pillar Failure Geometry.

PLAN VIEW

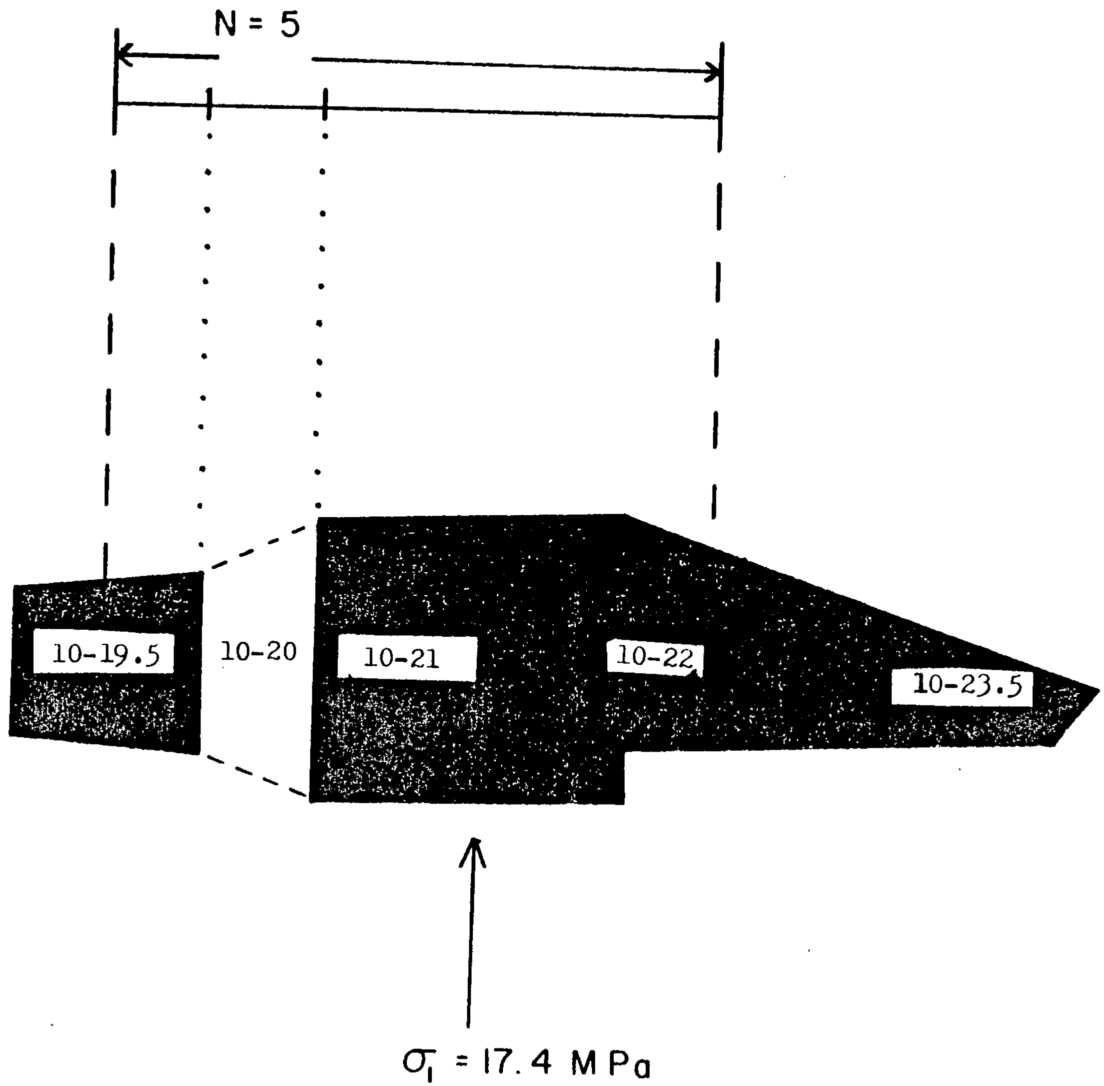

FIGURE 51 Pillars Extraction Numbers for the 10-20 Pillar Failure Geometry.

PLAN VIEW

6.7.3.2 Estimation of Pillar Strength; Hoek's Method

The pillars' strength can be estimated using Hoek and Brown (1980)[3] curves (Figure 8). The pillar material was classified (Section 6.3.3) and the Rock Quality Index varies from Q = 0.8 to Q = 17.8. A good quality rock mass is then assumed, and the uniaxial compressive strength is σ_c = 100 MPa (2105 KPSF).

A) 10-21.5 Pillar Failure Geometry

Pillar	W/H	Pillar Strength/σ_c	Pillar Strength (MPa)
10-20	1	0.3	30
10-21.5	0.5	0.2	20
10-23	0.8	0.25	25

B) 10-23 Pillar Failure Geometry

Pillar	W/H	Pillar Strength/σ_c	Pillar Strength (MPa)
10-20	1	0.3	30
10-21.5	----------Failed and Recovered -------------------		
10-23	0.8	0.25	25

C) 10-20 Pillar Failure Geometry

Pillar	W/H	Pillar Strength/σ_c	Pillar Strength (MPa)
10-20	0.5	0.2	20
10-21.5	-------------Failed and Recovered -----------------		
10-23	-----------------Failed ---------------------------		

6.7.4 Theoretical Methods

As in Heath Steele's case history, no theoretical methods have been used for the Geco pillar failure analysis.

6.7.5 Computer Methods

The two-dimensional boundary elements program "BITEM" was used again to model the three situations: (a) 10-21.5, (b) 10-23 and (c) 10-20 pillar failure geometry. (Figure 52,53,54).

A) 10-21.5 Pillar Failure Geometry (Figure 52)

Pillar	σ_p Pillar Load (MPa)
10-20	26.33 (550 KPSF)
10-21.5	38.30 (800 KPSF)
10-23	31.12 (650 KPSF)

B) 10-23 Pillar Failure Geometry (Figure 53)

Pillar	σ_p Pillar Load (MPa)
10-20	31.12 (650 KPSF)
10-21.5	-----Failed-------
10-23	39.84 (832 KPSF)

C) 10-20 Pillar Failure Geometry (Figure 54)

Pillar	σ_p Pillar Load (MPa)
10-20	38.30 (800 KPSF)
10-21.5	----Failed------
10-23	----Failed------

FIGURE 52 COMPUTER OUTPUT OF THE 10-21.5 PILLAR FAILURE GEOMETRY
MAJOR PRINCIPAL STRESS CONTOUR

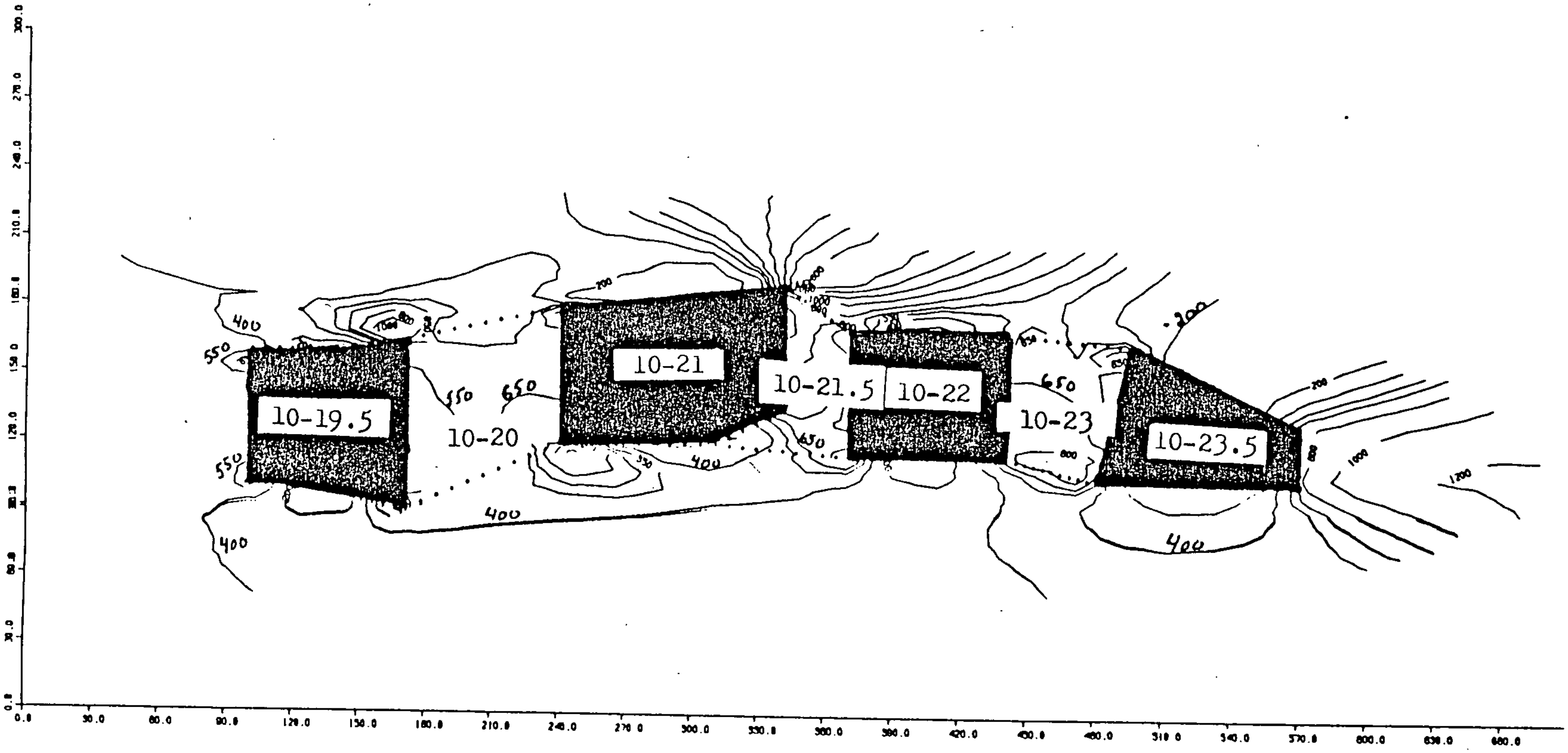

PLAN VIEW

FIGURE 53 COMPUTER OUTPUT OF THE 10-23 PILLAR FAILURE GEOMETRY MAJOR PRINCIPAL STRESS CONTOUR

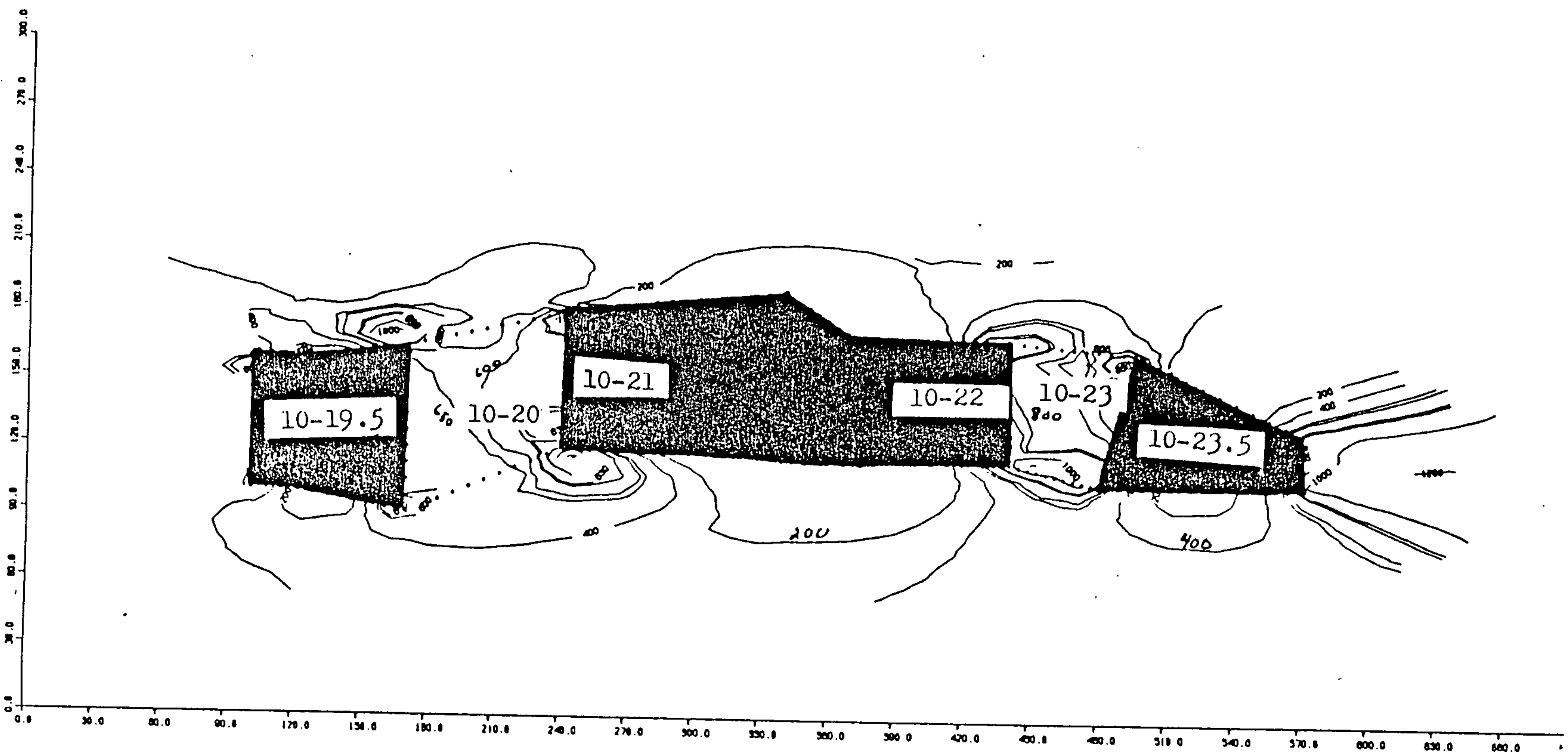

PLAN VIEW

FIGURE 54 COMPUTER OUTPUT OF THE 10-20 PILLAR FAILURE GEOMETRY
MAJOR PRINCIPAL STRESS CONTOUR

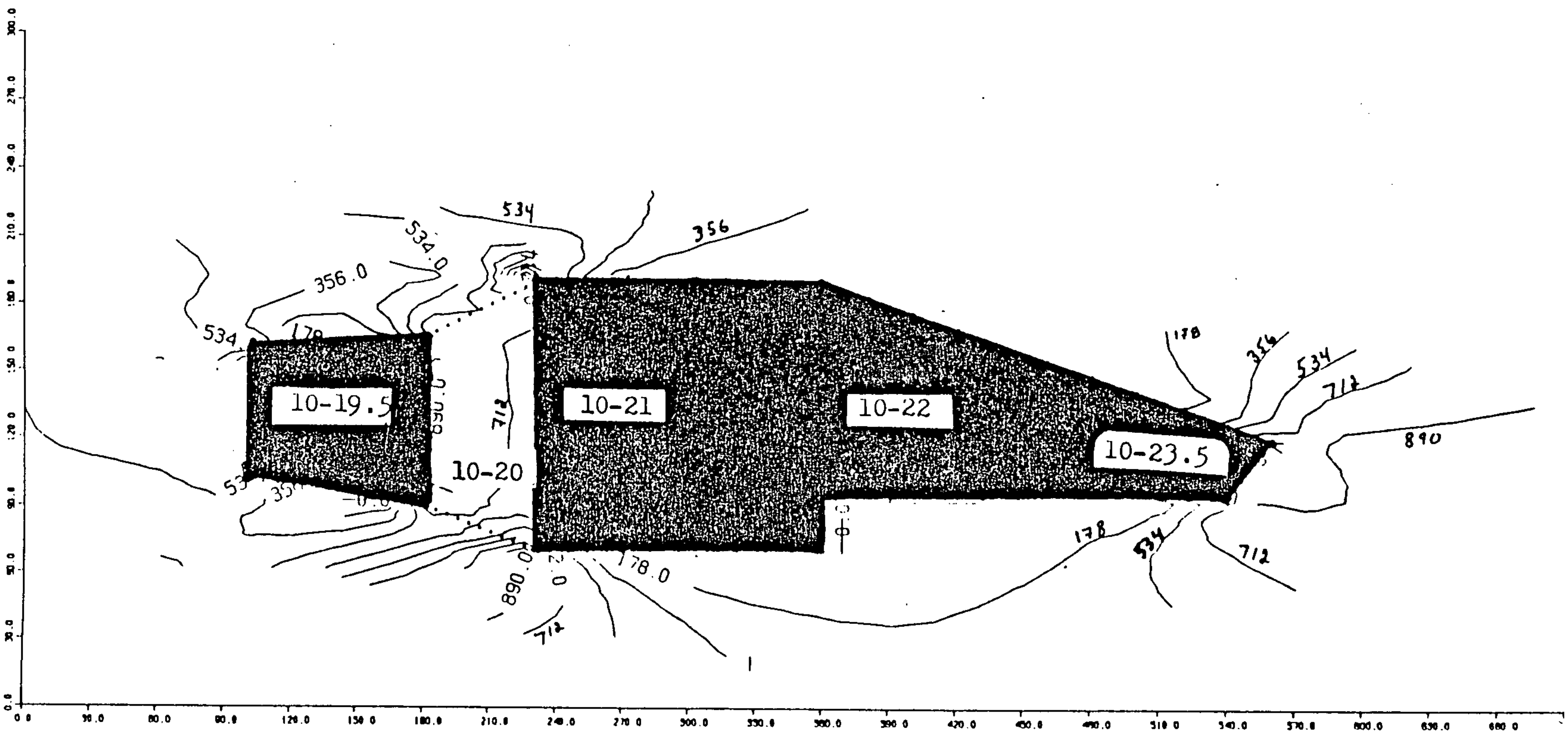

PLAN VIEW

6.8 Discussion of the Results

Before discussing the rock mechanics results of A) 10-20, B) 10-21.5 and C) 10-23 pillar failures, we must review the assumptions required.

- The virgin stress was estimated following the procedure described in Appendix B.
- Elastic Modulus and Poisson Ratio were selected using Hoek and Brown (1980)[3] typical values for gneiss rock in this area.
- Each time a pillar was reported failed, stope and pillar dimensions were assessed.

The pillar load was calculated using tributary area and computer simulation. The load values determined by the tributary area are about 30% higher than those from computer simulation. Since the tributary area oversimplifies the problem and represents the upper limit of the average pillar stress, the load values from computer simulation are judged more realistic and kept as mean values. The pillar strength was estimated using Hoek and Brown (1980)[3] curves, and each pillar's safety factor was determined.

The sequence of failure events, according to the computational methods summarized in Table 20 are as follows:

A) 10-21.5 Pillar Failure Geometry (November 1960)

According to the documentation (Bray (1967))[10], both 10-21.5 and 10-23 pillars failed in November, 1960. Table 20 shows that 10-21.5 was the first pillar to fail (S.F. = 0.53). This low safety factor indicates that the geometry assumed at failure was not exact (S.F. should be around 1). Nevertheless, the results are still capable of reconstructing the history of the failures.

TABLE 20

GECO PILLAR ANALYSIS RESULTS

Pillar	Extraction Number "N"	Tributary Area (MPa)	Computer Stress (MPa)	Mean Stress (MPa)	W/H (Plan View)	Pillar Strength (MPa)	Safety Factor	Extraction Ratio %	Remarks
A) 21.5 Pillar Failure Geometry, November 1960									
10-20	2.4	35.38	26.33	26.33	1	30	1.15	55	Stable
10-21.5	3.8	56.01	38.30	38.30	0.5	20	0.53	74	Pillar failed
10-23	2.5	36.85	31.12	31.12	0.8	25	0.81	60	Failure initiated
B) 23 Pillar Failure Geometry, November 1960									
10-20	2.9	42.75	31.12	31.12	1	30	0.97	66	Stable
10-21.5	Failed and Recovered								
10-23	3.8	56.01	39.84	39.84	0.8	25	0.63	74	Pillar failed
C) 10-20 Pillar Failure Geometry, August 1961									
10-20	5	73.70	38.30	38.30	0.5	20	0.53	80	Pillar failed

B) 10-23 Pillar Failure Geometry (November 1960)

Just after the 10-21.5 pillar collapsed, the stress redistribution caused the complete failure of 10-23 pillar (S.F. = 0.63), and the 10-20 pillar probably started to show some instability (S.F. = 0.97)

C) 10-20 Pillar Failure Geometry (August 1961)

The 10-20 pillar safety factor of 0.53 indicates that in August 1961, the load had already largely exceeded the bearing capability of the pillar. Although these results are not as precise as those of Heath Steele's case history, they are consistent with the failure events at Geco. While the accuracy of the design procedure and input data must still be improved, the results are valuable as a starting point for future designs.

Figure 55 is a plot of the local extraction ratio "e"* versus the safety factor of each pillar at different stages of extraction. It can be observed that at this depth (±300 m) stability problems begin when the extraction ratio exceeds 55%. Permissible extraction ratio can be determined at different depths using the same procedure. Geco actually limits primary mining to an extraction ratio of 37%.

It should be noticed that a lack of points in the upper part of the curve (Figure 55) is due to the inaccurate estimation of the stope and pillar dimensions in situation A: (10-21.5 Pillar Failure Geometry).

---

* Defined in Section 5.8

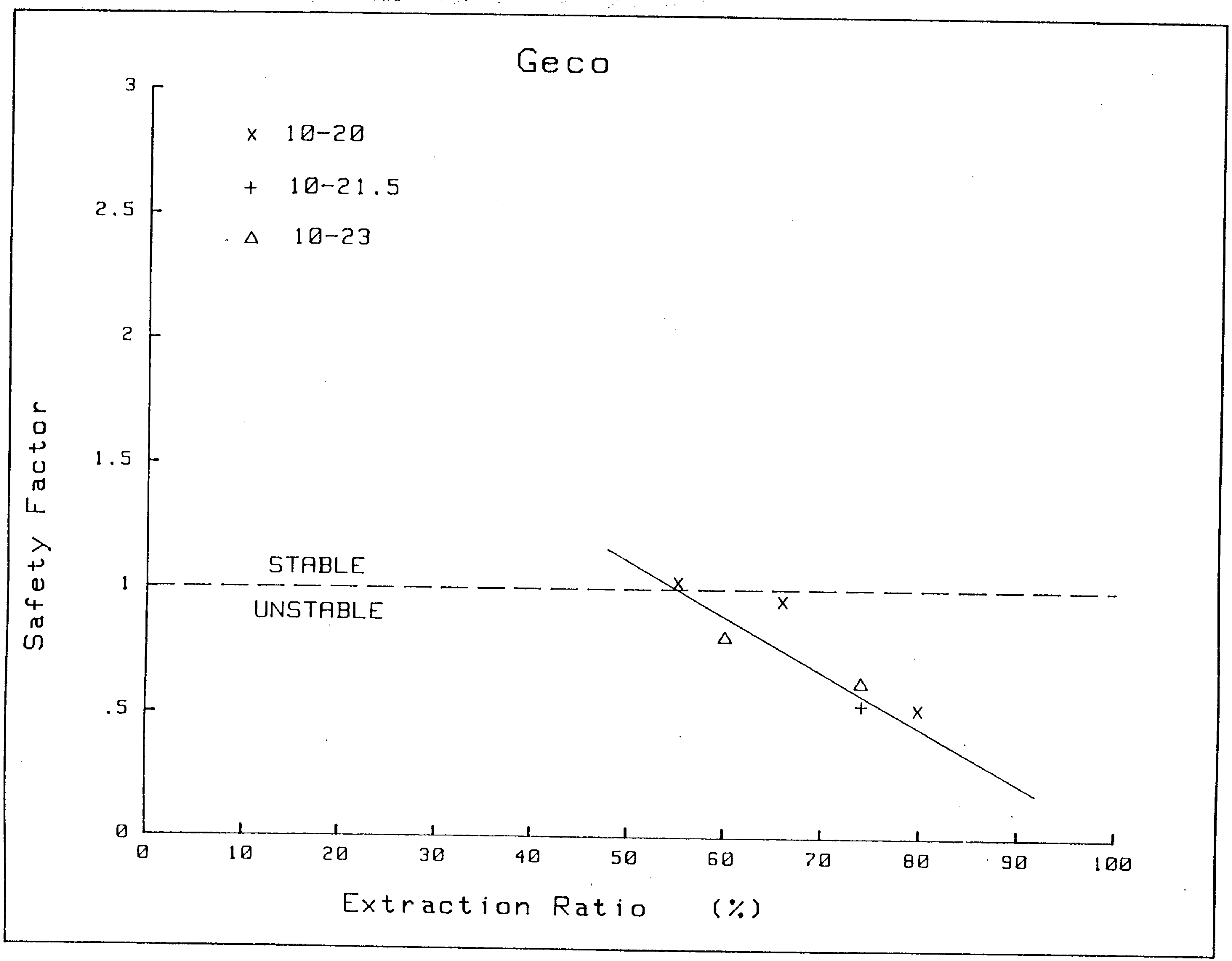

FIGURE 55 EXTRACTION RATIO VS SAFETY FACTOR

CHAPTER 7

SUMMARY AND CONCLUSIONS

7.1 Design Procedure

In the context of the North American mining industry, most underground pillars are still designed using a trial and error process.

Three major obstacles in designing pillars are responsible for this situation.

. Accurate estimation of pillar strength

. Evaluation of pillar load

. The multiplicity of pillars.

This study aims to improve the actual pillar design practices.

- A classification system was first proposed which divides pillars into four categories:

Category 1. Plate Pillars

Category 2. Separation Pillars

Category 3. Stub Pillars

Category 4. Inclined Pillars.

This classification resolves the problem of the multiplicity of pillars and allows standardization of the pillar design procedure.

- A five phase design procedure was developed. It suggests that every suitable designing method should be used, becoming more sophisticated as experience is gained with the rock material. Also, design charts provide a guideline for the selection of the pertinent methods. This procedure permits:

i) A standard design process for all pillar types.

ii) A more accurate estimation of pillar load and strength by using several methods which take into account different factors.

iii) An optimization of the rock mechanics data employed as a design tool.

Thus, the procedure helps to overcome the three major obstacles in designing pillars. Also, it is simple to apply and minimizes the possibility of misconstruing the results.

7.2 Case Histories

This pillar design procedure was applied in back-analysing pillar failure at Heath Steele and Geco Division. Because both case histories were well documented and involved simple geometry, the input parameters affecting the design of pillars could be understood, controlled and adjusted.

A plot depicting extraction ratio versus "safety factor" for each pillar at different stages of extraction appears to be an efficient manner of synthesizing the analysis results. As well, the curves indicate the limit of extraction permissible at a given depth.

Both mines--Heath Steele and Geco--had experienced costly pillar failures resulting in production delays, extra ground support and loss of ore reserves before they were able to determine a safe extraction ratio. Also, because it is based on experience only, there is no indication whether the pillars are overdesigned, or to which depth this extraction ratio (50% at Heath Steele and 37% at Geco) will remain safe for primary extraction.

Although further research is required in order to obtain a wider variety of pillars and rock mass qualities, the extraction ratio versus safety factor curves represent a method of optimizing primary extraction, avoiding major stability problems.

The curves take the following factors into account:

- virgin stress
- stress induced by mining
- strength of pillar material

- rock mass quality
- structural discontinuities
- percentage of extraction
- effect of adjacent openings
- overall geometry and orientation of the underground structures
- pillar width to height ratio
- depth below surface.

However, damage created by blasting, as well as groundwater effects were ignored because they are difficult to quantify. They may play an important part in pillar stability.

The use of rock mass classification allows results from different sites to be compared. Figure 56 combines the curves from both case histories. The rock mass quality is indicated for each case.

7.3 Design Methods

A review of the principal pillar design methods is given in Chapter 3. They are subdivided into four groups according to their level of sophistication, and this study makes the following conclusions:

Group 1. Experience Methods

- Most mines still rely principally upon experience design.
- Keeping detailed files on all information concerning the mine stability such as failure, slabbing, squeezing, caving, convergence will improve the experience design.

Group 2. Empirical Methods

- Because empirical methods ignore many factors influencing pillar stability, the knowledge of the conditions in which they were developed is essential.

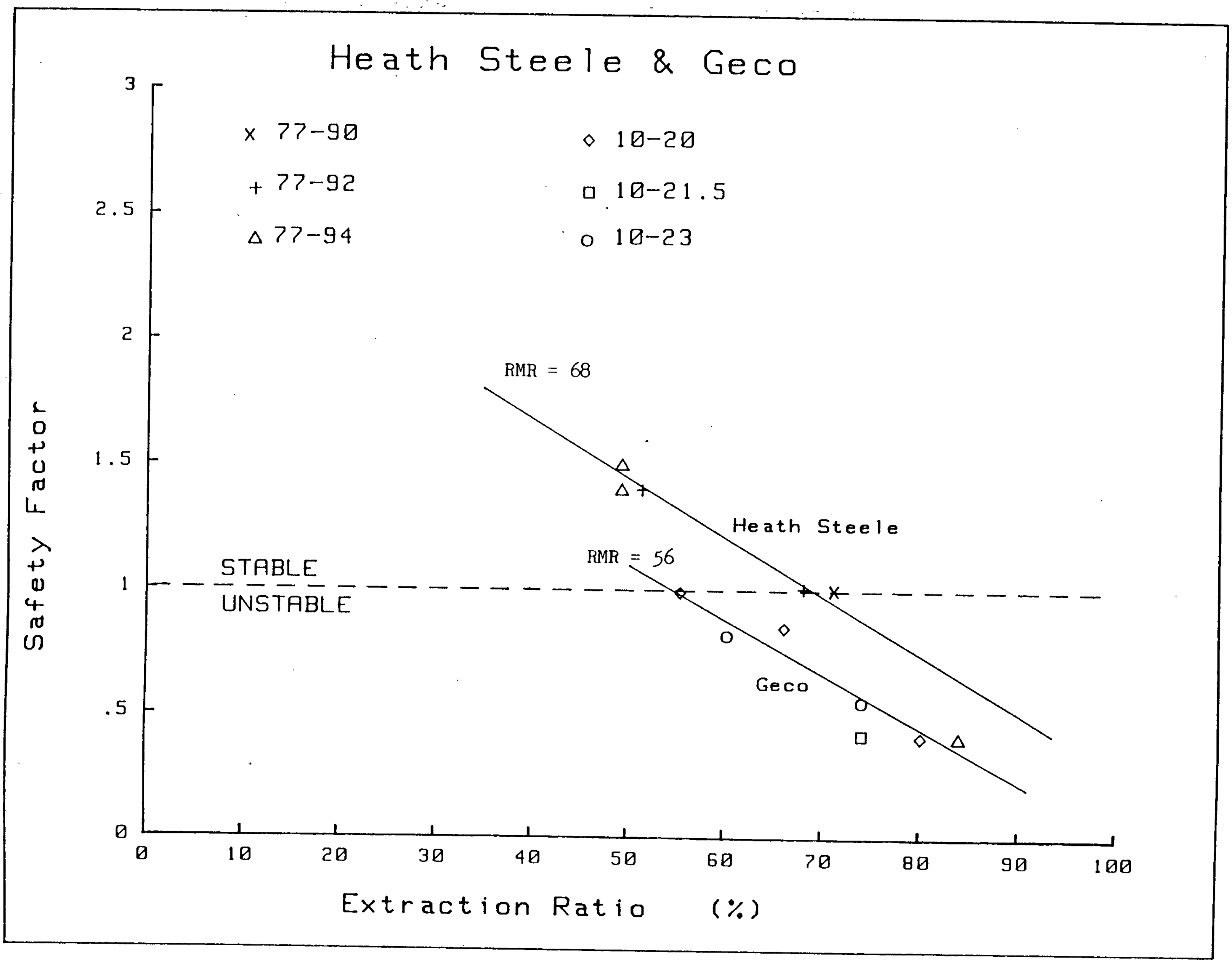

FIGURE 56 COMPARISON OF HEATH STEELE AND GECO PILLAR ANALYSIS

Group 3. Theoretical Methods

- The theoretical and analytical methods are complex and difficult to apply, and their results are often not reliable. They are useful in further comprehending the mechanism involved in pillar design.
- To determine theoretically pillar strengths; only Wilson's formula has been widely used.
- The Coates' wall deflection formula and the photoelastic technique to determine pillar load were relatively popular in the past but are no longer employed.
- If the pillar's structure can be realistically represented by the beam or plate theory, it is a well-accepted method of designing pillars.

Group 4. Computer Methods

- The computer methods are versatile and may be adapted to every category of pillar.
- Although they are mathematically precise, the accuracy of the results is related to the quality of the input data and designer's skills.

Finally, it is important to remember that designing underground pillars is a progressive task. The accuracy and the designer's confidence in the results will improve concurrently with the continuing application of the design procedure. Careful underground observations, monitoring and measurements should provide feedback on each design.

REFERENCES

1. Roche Mines Associés ltée (1984) ; Etat de la Question sur le Dimensionnement et la Stabilité des Pilliers de surface, Energy Mines and Resources Canada, Fevrier 1984

2. WAGNER, H. (1974) ; Determination of the Complete Load-Deformation Charactiristics of Coal Pillars , Advances in Rock Mech., Vol. 11B., International Society of Rock Mech., pp. 1076-1081, 1974

3. HOEK, E., BROWN, E.T. (1980) ; Underground Excavation in Rock , Institute of Mining and Metallurgy, London, 527 p.

4. BIENIAWSKI , Z.T. (1983) ; Improve Design of Room and Pillar Coal Mines for U.S. Conditions , Stability in Underground Mining, Society of Mining Eng. of AIME, 1983

5. SZWILSKI, T.B. (1983) ; Sizing of Chain Pillar, Stability in Under-Mining, Chapt. 25, Society of Mining Eng. of AIME, 1983, pp. 539-557

6. WITTAKER, B.N., SINGH, R.N. (1981) ; Stability of Longwall Mining Gate Roadways in Relation to Rib Pillar Size , Int. Journal Rock Mech., Min. Sci. and Geomech. abstr., Vol. 18, pp. 331-334

7. ASHLEY, G.H. (1930) ; Barrier Pillar Legislation in Pennsylvania Trans. AIME, Coal Div., 1930, pp. 76-96

8. BELINSKI, A., BORECKI, M. (1964) ; Results of Investigation on Rock Pressure by the Longwall System of Coal Mining in the Upper Silesian Coal Field , Proceeding 4th. Int. Conference on Strata Control and Rock Mech., Columbia University, 1964, pp.85-88

9. TOUSEULL, J.A., ; Stereographic Method of Determining Wether Planes of Weakness Transect Pillars , U.S. Bureau of Mines, Denver, Colorado.

10. BRAY, R.C.E. (1967) ; Control of Ground Movement at the Geco Mine , Annual General Meeting, Noranda Mines, Geco Div. Geology Dept., Ottawa 1967

11. ALLCOTT, G.A., ARCHIBALD, D.E. (1981) ; Description of Pillar Behaviour at Heath Steele Mines, CIM Bulletin, Oct. 1981, pp. 80-87

12. Golder Associates (1981) ; Prediction of Stable Excavation Spans for Mining at Depth Below 1000 Meters in Hard Rock, Canada Center for Mineral and Energy Technology, Canmet Contract no. 80-00081, April 1981, 134 p.

13. COATES, D.F. (1966) ; Pillar Loading: II Model Studies, Mines Branch Research Report R-170, Queen's Printer, Ottawa 1966

APPENDIX A

REVIEW OF LITERATURE

(See "LITERATURE RESEARCH REPORT" June 1984)

APPENDIX B

Determination of the Geco Stress Regime at 700 ft. Depth

No stress investigations have been performed at Geco. Both horizontal stresses are estimated using the following methods:

1. From Herget (1983)

Results from groundstress determinations in the Canadian Shield are analyzed in regard to change with depth of the ratio of maximum horizontal stress to measured vertical stress ($\sigma_{h\ max}/\sigma_v$) and minimum horizontal stress to measured vertical stress ($\sigma_{h\ min}/\sigma_v$).

$$(\sigma_{h\ max}/\sigma_v) = \frac{253.87}{\text{depth (m)}} + 1.45$$

$$(\sigma_{h\ min}/\sigma_v) = \frac{279.82}{\text{depth (m)}} + 0.88$$

- at 215 m. (700 ft.) depth

$$\frac{\sigma_1}{\sigma_3} = \frac{\sigma_{H(max)}}{\sigma_v} = \frac{253.87}{\text{depth}} + 1.45 = 2.64$$

$$\frac{\sigma_2}{\sigma_3} = \frac{\sigma_{H(min)}}{\sigma_v} = \frac{279.82}{\text{depth}} + 0.88 = 2.20$$

2. From Hoek and Brown (1980)

In situ stress measurements have been done at Wawa Mine, not far from Geco, and the shallow depth results (∿300 m.) tend to confirm stress values determined by Herget's formulas.

		Depth (m.)	σ_h	σ_h/σ_v	ref.
G.W. MacLeod Mine, Wawa, Ontario	Siderite	370	16.1	1.29	81
G.W. MacLeod Mine, Wawa, Ontario	Tuff	370	15.1	2.54	81
G.W. MacLeod Mine, Wawa, Ontario	Tuff	575	21.5	1.23	81
G.W. MacLeod Mine, Wawa, Ontario	Tuff	575	14.6	1.25	81
G.W. MacLeod Mine, Wawa, Ontario	Meta-diorite	480	18.7	1.54	81
G.W. MacLeod Mine, Wawa, Ontario	Chert	575	26.6	1.52	81
Wawa, Ontario	Granite	345	20.0	2.50	82
Elliot Lake, Ontario	Sandstone	310	(11.0)*	2.56	83
Elliot Lake, Ontario	Quartzite	705	(17.2)	1.70	83
Elliot Lake, Ontario	Diabase dyke	400	17.2	1.90	84

APPENDIX C

ILLUSTRATION OF PILLARS

(after Roche Mines Associates (1984)[1])

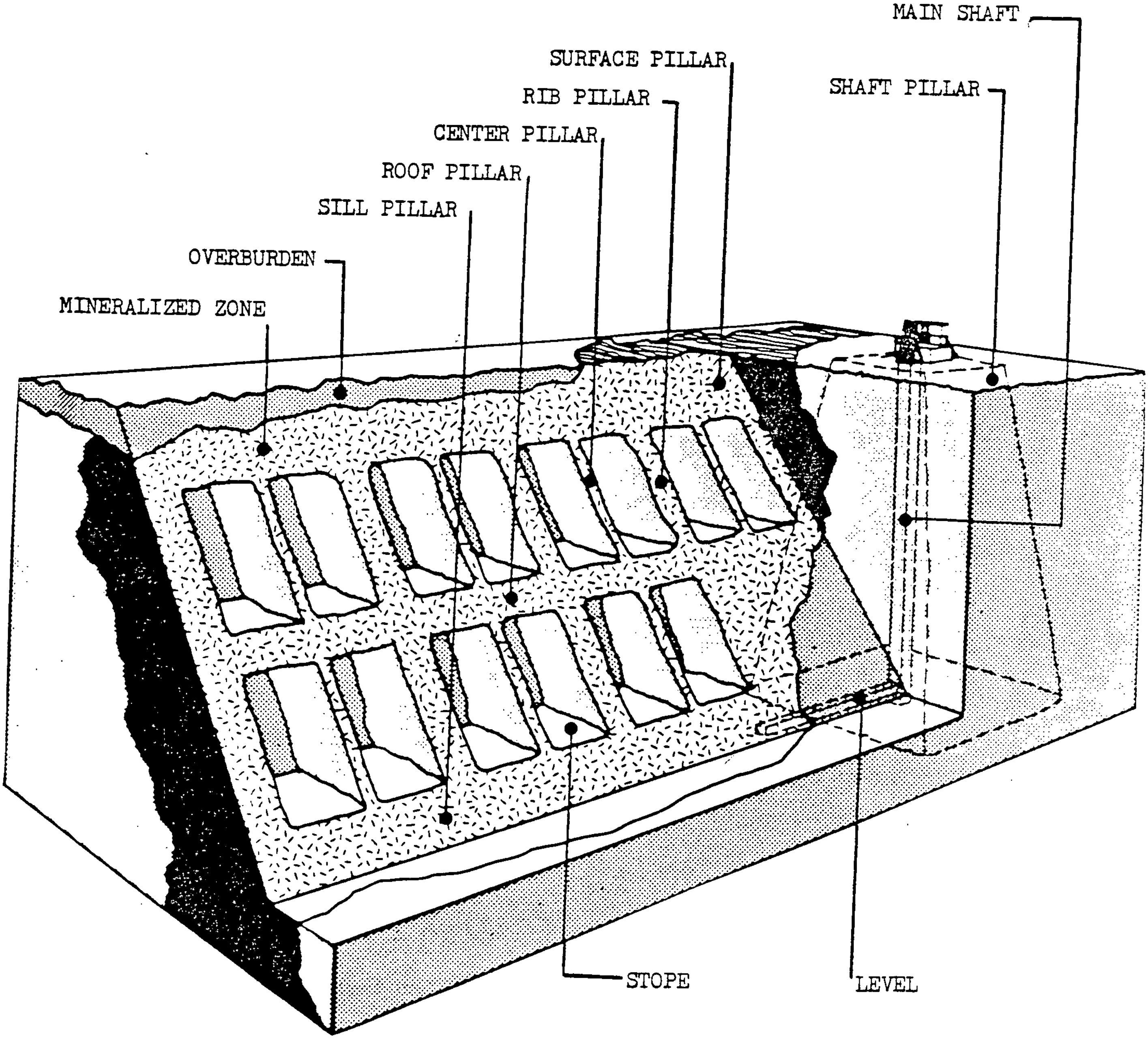

FIGURE 5 HARD ROCK PILLAR

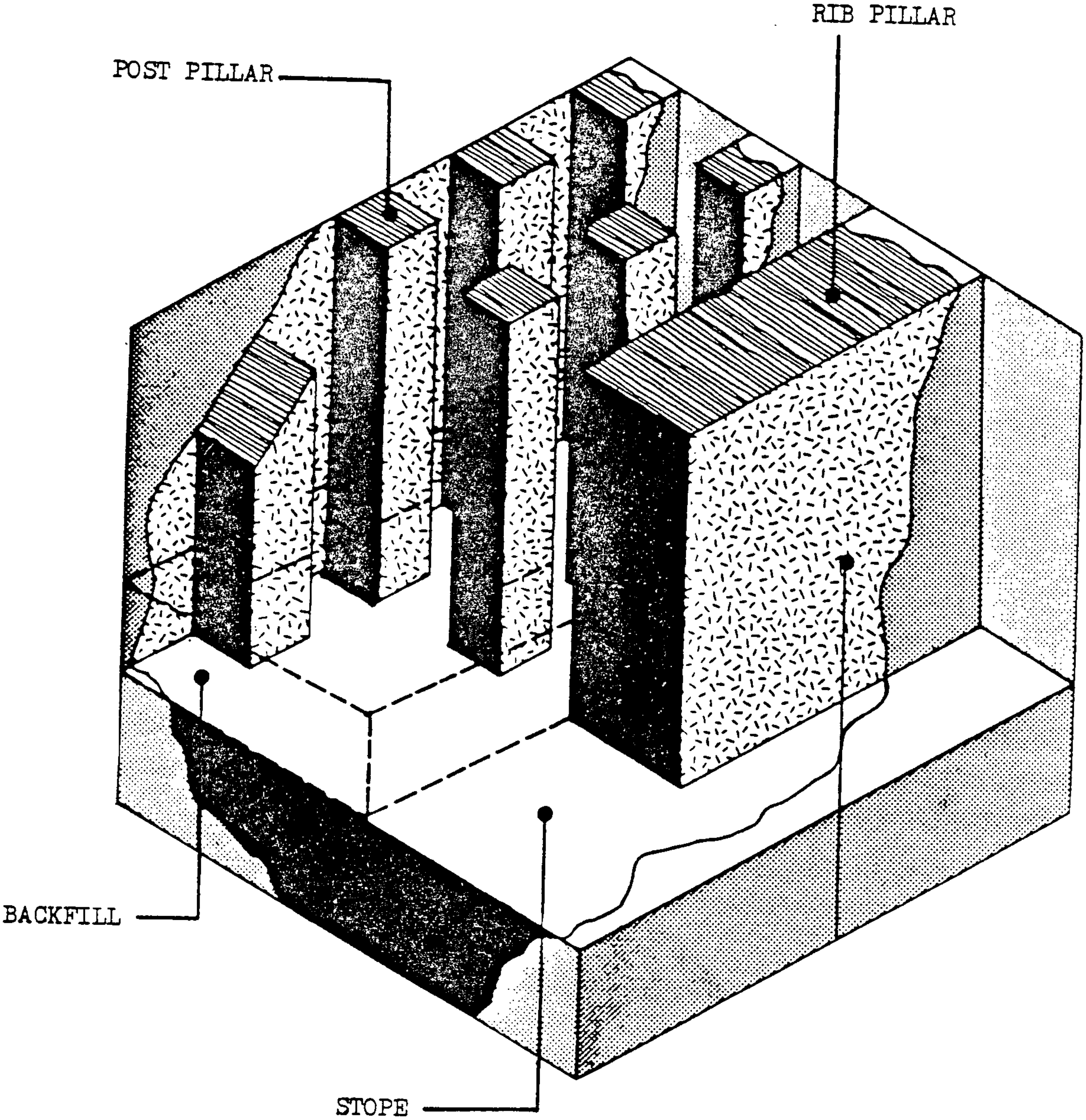

FIGURE 6 · HARD ROCK PILLARS

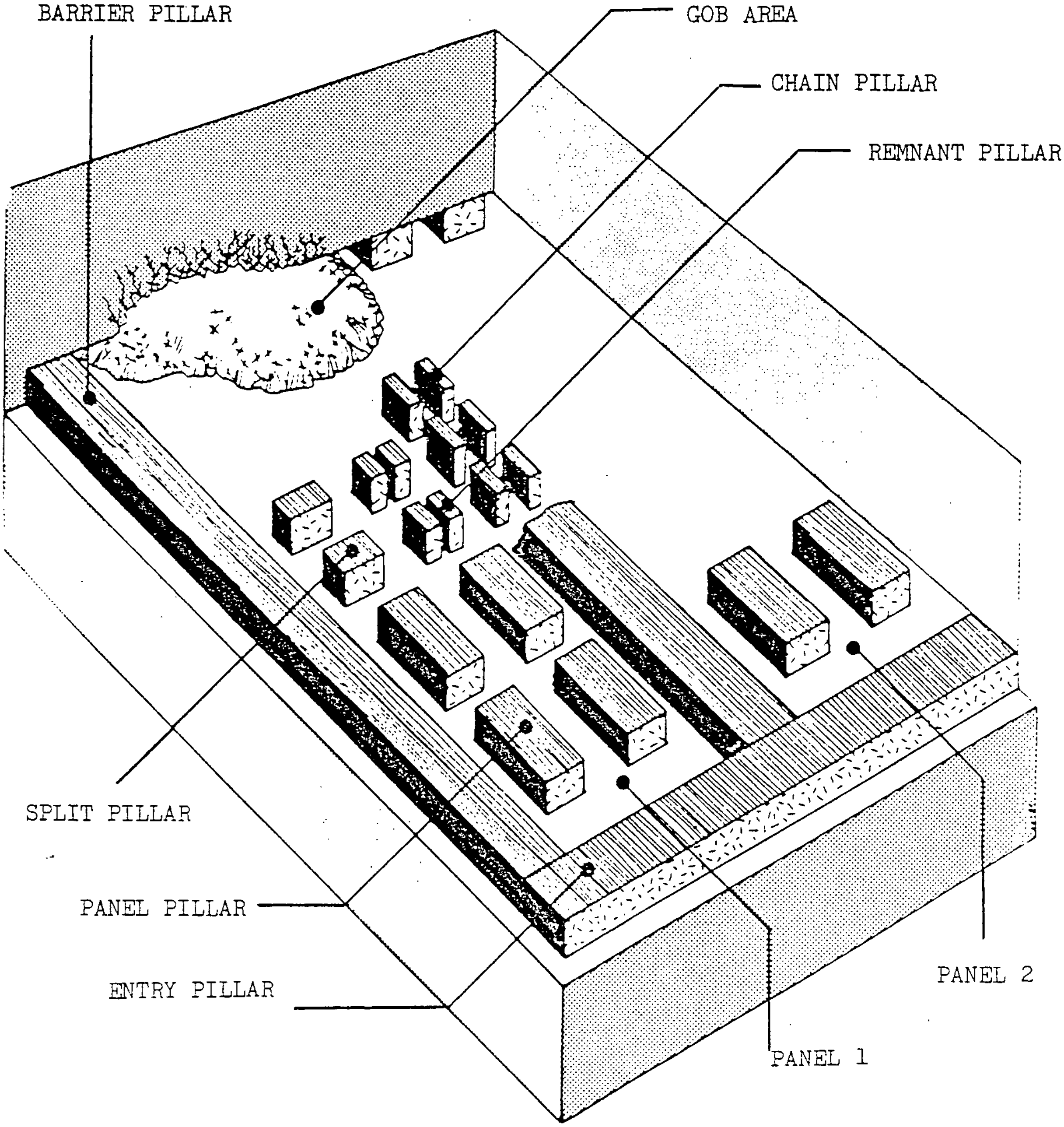

FIGURE 7 SOFT ROCK PILLARS

APPENDIX D

"BITEM", 2-D Boundary Element Program

DESCRIPTION OF BITEM

Program BITEM is based on program BITE, which was developed by P.C. Riccardella during PhD studies at Carnegie-Mellon University and has been released through CSIRO. BITE performs elasticity analyses for homogeneous solids only; BITEM has been developed at CSIRO to analyse systems consisting of a number of regions with different material properties.

The boundary integral technique uses only information relating to the **boundary surface** to enable an analysis of the whole solid. The net effect is a reduction in the dimension of the problem posed. As applied in BITEM the boundary integral equation technique enables a two-dimensional analysis of plane strain (or stress) linear elasticity problems given only a description of the (one-dimensional)boundary surfaces of the solid. Advantages of this technique over other available stress analysis methods, which require as input data a specification of the whole body, are as follows:

1. Reduction in volume of input data, and thus greater ease modelling problems
2. Savings in computer time and storage

PROGRAM CAPABILITY

Program BITEM solves two-dimensional elasticity problems for a piece-wise homogeneous isotropic linearly elastic material, using the boundary integral equation technique. Data required by the program include the elastic properties of each individual homogeneous domain, a description of the geometry of the boundary surface of each such domain, and some of the displacement and traction boundary conditions along these boundaries. Such boundary condition specifications need only be made on those surfaces which do not interfaces between adjoining regions, e.g. on excavation boundaries in mining applications. The program is capable of generating the remaining traction and displacement unknowns on all boundaries of the solid, interface or otherwise, together with stress calculations on the boundaries and stress and displacement solutions for specified locations within the solid. Linearly varying (rather than constant value) displacements and tractions are assumed over the discretized segments of the boundaries. This linear boundary value approach is more accurate than the constant boundary value approach, while requiring little or no increase in computer running times and storage requirements.

In addition to its applicability in normal geomechanics problems, BITEM is able to solve several inclusion-type problems; for example, the problem of an inclusion which has been stressed prior to its insertion in a solid.